DESIGN, OPTIMIZATION AND IMPLEMENTATION OF BILINEAR LOW-PASS SWITCHED-CAPACITOR LEAPFROG FILTERS

by

Yeck K. Co

A thesis
presented to the University of Manitoba
in partial fulfillment of the
requirements for the degree of
Master of Science
in
Electrical Engineering

Winnipeg, Manitoba, 1983

DESIGN, OPTIMIZATION AND IMPLEMENTATION

OF

BILINEAR LOW-PASS SWITCHED-CAPACITOR LEAPFROG FILTERS

BY

YECK K. CO

A thesis submitted to the Faculty of Graduate Studies of the University of Manitoba in partial fulfillment of the requirements of the degree of

MASTER OF SCIENCE

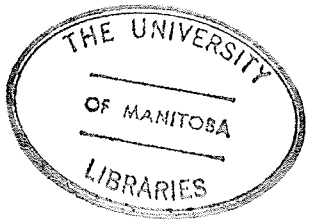

I hereby declare that I am the sole author of this thesis.

I authorize the University of Manitoba to lend this thesis to other institutions or individuals for the purpose of scholarly research.

Yeck K. Co

I further authorize the University of Manitoba to reproduce this thesis by photocopying or by other means, in total or in part, at the request of other institutions or individuals for the purpose of scholarly research.

Yeck K. Co

ABSTRACT

The design of a switched-capacitor leapfrog filter is based on the transformation of an analog network into a switched-capacitor network. The two common transformations used are the lossless-discrete-integrator transformation (LDI) and the bilinear transformation. In this thesis, Davis and Trick's method of designing an LDI switched-capacitor filter, and Eriksson's method of designing a bilinearly-transformed switched-capacitor filter are reviewed. Two new methods of designing a bilinearly-transformed switched-capacitor leapfrog filter are then presented : one is an extension to Davis and Trick's method, and the other is an equivalent circuit approach based on the results of Eriksson's method. These methods and Eriksson's method use the parasitic-insensitive LDI integrators as building blocks because the bilinear integrators are either parasitic-sensitive or inefficient in hardware. Eriksson's method and the equivalent circuit method are found to be preferable because they provide explicit design formulae and it is easy to extend these formulae to higher-order filters.

The thesis also proposes the optimization of a switched-capacitor leapfrog filter so that the resulting network will have the canonic number of op amps, an optimum dynamic

range, the minimum total capacitance, and preferably a small passband/stopband ripple. The computer-aided optimization uses the simplex direct search method.

A fifth-order elliptic low-pass filter has been designed and optimized. The optimization results in a 30% saving of the total capacitance of the filter. This filter has been implemented using discrete switches, capacitors and op amps. The magnitude response satisfies the specifications and is insensitive to variations in capacitor ratios.

ACKNOWLEDGEMENTS

The author wishes to express his sincere gratitude to Professor G.O. Martens for the guidance and encouragement given during the course of his study. The author also wishes to thank M. Ismail for many useful discussions, and A. Gole for providing a simplex computer subroutine program which was used in the optimization work of this thesis. Advice and assistance from colleagues E.D. De Luca, M. Jarmasz, P. Soble, and V.N. Shkawrytko are greatly appreciated.

Financial support from the University of Manitoba is also greatly appreciated.

TABLE OF CONTENTS

Chapter I

INTRODUCTION

Over the past three decades, considerable research has been conducted on the design and manufacture of low-cost, compact-sized and high-precision voice- and audio-frequency filters. The most promising method is to realize these filters in monolithic integrated circuit (IC) form [1,2,3].

Traditionally, RLC circuits are the most widely used filters in communication industries. However, they are usually expensive and large in size due to the presence of inductors. As communication systems get smaller, these classical RLC filters become impractical. With the development of inexpensive operational amplifiers (op amps), it has become practical to realize voice- and audio-band filters with op amps, resistors and capacitors only. However, it is difficult to fully integrate these active-RC filters without external trimming operations [1]. The reasons are : 1) the bandwidth defined by the RC products cannot be determined very accurately because the absolute values of R and C cannot be easily controlled in current IC technology; and 2) integrated resistors require a large area and have poor temperature and linearity characteristics [4].

With the advent of digital technology, the digital filter has become a viable alternative. However, in order to interface with external systems, they require extra hardware such as analog-to-digital and digital-to-analog converters. Moreover, they suffer from finite-word-length effects [5]. Research has been and is still being conducted towards solving these problems [6,7].

The recent advances in metal-oxide-semiconductor (MOS) technology allow filters to be realized on a single semiconductor chip by using the switched-capacitor (SC) approach [1]. The basic elements in an MOS SC filter are op amps, capacitors and switches. The advantages of using the SC approach are as follows:

1. The frequency characteristics of an SC filter depend only on the capacitance ratios (in contrast to active-RC filters for which absolute vaules of R and C are the factors). Since these ratios can be realized accurately [8], the frequency response of the filter will not deviate greatly from the nominal design. This reproducibility of the desired frequency response is a very important aspect in mass production.
2. The high-density MOS technology allows several circuits to be realized on a single chip [9,10,11].
3. The bandwidth of an SC filter can be varied by simply adjusting the frequency of the clock used to operate the switches. This property is common to all discrete-time filters.

A primitive method of designing an SC filter is to choose a passive- or active-RC filter as a prototype, and then replace each resistor by a corresponding switched capacitor [12,13,14]. As will be shown later, this method provides satisfactory results only when the clock frequency is much higher than the signal frequencies. Other methods of realization have been proposed, including the leapfrog simulation which is the most popular technique [15]. The main reason for the popularity of the leapfrog realization is that it can be used to simulate the operation of a doubly-terminated LC ladder network which has a frequency response very insensitive to changes in element values [16].

In this thesis, we will show how to derive an SC leapfrog filter based on either the lossless-discrete-integrator (LDI) [17] or bilinear [18] analog-to-digital transformation techniques. Since a bilinearly-transformed SC leapfrog filter requires integrators that are sensitive to parasitic capacitances, we will modify the flowgraph of this kind of filter so that parasitic-insensitive LDI integrators can be used as building blocks in the realization. Next, we will optimize the design so that the final circuit will have the canonic number of op amps, an optimum dynamic range, the smallest total capacitance, and a large passband/stopband tolerance. The sensitivity property of the SC filter will be studied : deterministically for the single-parameter case and statistically for the multi-parameter case. Finally, we

will design a fifth-order elliptic filter, optimize its parameters, and implement the filter with discrete components to verify the optimized design. Throughout this thesis, third- and fifth-order lowpass filters will frequently be used for explanatory purposes. However, it is easy to generalize the concepts to higher-order filters.

Chapter II will introduce the fundamental concepts required for an understanding of SC filters. Chapter III will describe the standard design procedure for an LDI-transformed or a bilinearly-transformed SC leapfrog filter. Chapter IV will discuss some practical considerations for the design and implementation of an SC filter, and will identify those aspects that should be optimized. Chapter V will provide an example to illustrate the complete design procedure.

Chapter II

BASIC THEORY OF SWITCHED-CAPACITOR FILTERS

This chapter will present the basic concepts related to SC filters. An SC filter exhibits some properties of analog filters and also some properties of discrete-time (also called sampled-data) filters. For a more in-depth description of discrete-time systems, the reader is referred to [18].

2.1 A SAMPLED-DATA SYSTEM

An analog filter processes continuous-time, continuous-amplitude signals. A digital filter processes discrete-time, discrete-amplitude signals; these signals are represented as sequences of numbers. An SC filter is an analog sampled-data system since its signals are continuous both in time and amplitude but change values only at discrete time instants.

In a sampled-data system, the input signal should be sampled according to the sampling theorem, i.e., the signal should be bandlimited to one half of the sampling frequency in order that it can be reconstructed from the samples without distortion. Thus, a system employing SC filters should generally have an anti-aliasing (or bandlimiting) filter,

two sample-and-hold devices and a reconstruction filter connected as shown in Fig. 2.1.

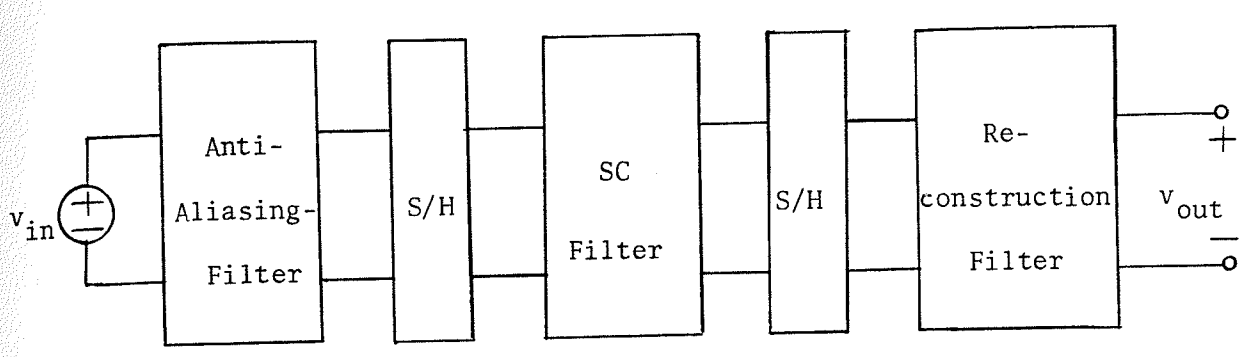

S/H : sample-and-hold device

Fig. 2.1 A sampled-data system employing a switched-capacitor filter.

The anti-aliasing filter is a low-pass filter used to bandlimit the input signal to one half of the sampling rate. The first sample-and-hold device is required because the SC filter operates on discrete-time samples. The second sample-and-hold device is required to convert the output samples into a continuous staircase-shaped output signal. Usually, the SC filter performs the functions of these devices inherently. The reconstruction filter is usually a low-pass filter used to retain only the baseband spectrum of the output signal — essentially it smoothes the output waveform by removing the high-frequency components.

Since an SC filter is basically a sampled-data system, the analysis and design are conveniently carried out in the z-domain. In the next section, a brief description of the z-transform will be presented.

2.2 Z-TRANSFORM

Consider a continuous-time signal $x(t)$ whose doubled-sided Laplace transform is defined as

$$X(p) = L\,[x(t)] = \int_{-\infty}^{\infty} x(t)\, e^{-pt}\, dt \tag{2.1}$$

where p is the Laplace transform variable.

Assume $x(t)$ is now sampled by an impulse train represented as

$$\Delta(t) = \sum_{n=-\infty}^{\infty} \delta(t - nT) \tag{2.2}$$

where $\delta(t)$ is an impulse function, and T is the sampling period (or time interval between two consecutive impulses). The impulse-sampled signal $x'(t)$ is then

$$x'(t) = x(t)\,\Delta(t) = \sum_{n=-\infty}^{\infty} x(nT)\delta(t-nT) \tag{2.3}$$

Taking the Laplace transform of $x'(t)$, we obtain

$$X'(p) = L\,[x'(t)] = \sum_{n=-\infty}^{\infty} x(nT)e^{-npT} \tag{2.4}$$

With a substitution of variable

$$z = e^{pT} \tag{2.5}$$

(2.4) defines a transform known as the z-transform :

$$X(z) = Z\,[\,x(nT)\,] = L\,[\,x'(t)\,]\Big|_{e^{pT}=z} = \sum_{n=-\infty}^{\infty} x(nT)\, z^{-n} \tag{2.6}$$

One of the most useful properties of the z-transform is the time-shifting property : if $X(z) = Z\,[x(nT)]$, then

$$Z\,[\,x(nT - kT)\,] = z^{-k}\, X(z) \tag{2.7}$$

where k is any integer number.

The output sequence y(nT) and input sequence x(nT) of a discrete-time (either digital or SC) filter are related in their z-transforms Y(z) and X(z) by the filter transfer function $H(z)=Y(z)/X(z)$. For an M-th order filter, the degree of the denominator polynomial of H(z) must be equal to M. Moreover, for the filter to be stable, all the poles of H(z) must lie inside the unit circle of the z-plane [18]. The frequency response of the discrete-time filter is determined by evaluating H(z) along the unit circle $z=e^{j\omega T}$ and is denoted by $H(e^{j\omega T})$. The corresponding attenuation in dB is defined as

$$A(e^{j\omega T}) = -\,20\,\log_{10}\,|H(e^{j\omega T})| \tag{2.8}$$

If the design of a discrete-time filter is based on a transformation from an analog transfer function or network, then it is necessary to introduce a new analog frequency variable s so that both analog and discrete-time transfer functions will be rational functions. The relationship between s and z (known as an s-to-z or analog-to-digital[1] frequency transformation) is not unique and we will discuss some common s-to-z transformations in the next section.

2.3 ANALOG-TO-DIGITAL FREQUENCY TRANSFORMATIONS

There are four commonly known analog-to-digital transformations [19] :

Backward difference (BD) :
$$\frac{1}{s} = T\,\frac{z}{z-1} \tag{2.9}$$

Forward difference (FD) :
$$\frac{1}{s} = T\,\frac{1}{z-1} \tag{2.10}$$

Lossless-discrete-integrator (LDI) :
$$\frac{1}{s} = T\,\frac{z^{\frac{1}{2}}}{z-1} \tag{2.11}$$

Bilinear transformation (BT) :
$$\frac{1}{s} = \frac{T}{2}\,\frac{z+1}{z-1} \tag{2.12}$$

---

[1] Strictly speaking, we should use the word sampled-data or discrete-time instead of digital. Nevertheless, in the current context, the word 'digital' will include SC filters too.

Note that LDI is the geometric mean of BD and FD, whereas BT is the arithmetic mean [20].

There are two requirements that an s-to-z transformation applied to a filter must satisfy [18] :

1. The left half of the s-plane should map into the inside of the unit circle of the z-plane so that stable analog filters will map into stable discrete-time filters.
2. The imaginary axis of the s-plane should map onto the unit circle of the z-plane so that the frequency characteristic of the analog filter will be preserved in the z-domain.

Of the four given s-to-z transformations, only LDI and BT satisfy the above two requirements. Hence, we will describe these two transformations in more detail.

2.3.1 LDI Transformation

The formulae relating s, p and z under the LDI are

$$s = \frac{1}{T}\frac{z - 1}{z^{\frac{1}{2}}} = \frac{1}{T}\left(z^{\frac{1}{2}} - z^{-\frac{1}{2}}\right) \tag{2.13}$$

$$s = \frac{2}{T}\sinh\frac{pT}{2} \tag{2.14}$$

$$z = e^{pT} \tag{2.5}$$

These mappings are illustrated in Fig. 2.2(a).

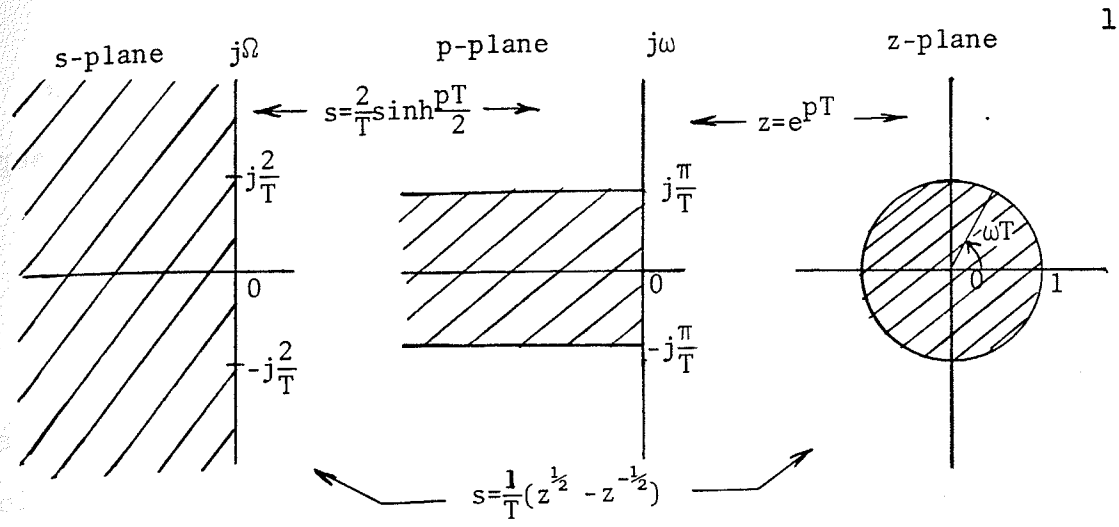

(a)

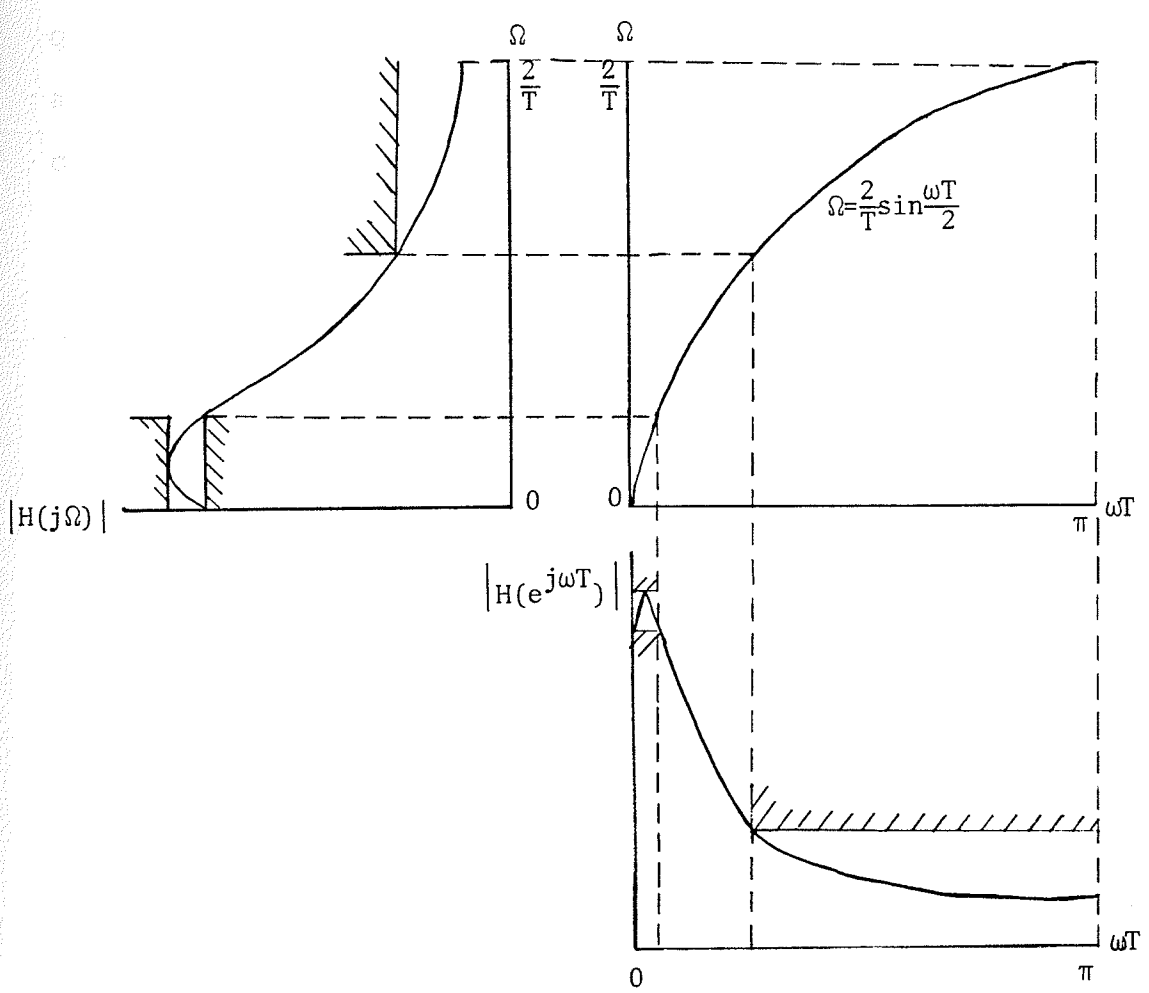

(b)

Fig. 2.2 (a) The mappings associated with the LDI.
(b) The transformation of an analog frequency response into a digital frequency response under the LDI.

We can show that the analog and digital steady-state frequencies (i.e., $s=j\Omega$, $p=j\omega$ and $z=e^{j\omega T}$) are related by

$$\Omega = \frac{2}{T} \sin \frac{\omega T}{2} \tag{2.15}$$

The normalized frequency variable ωT is represented as an angle in the z-plane. Since ωT is limited to the range of $-\pi \leq \omega T \leq \pi$, the corresponding analog frequency variable Ω is confined to the range of $-2/T \leq \Omega \leq 2/T$. Thus, the frequency characteristic outside the above region will be lost after the transformation. The LDI mapping of an analog frequency response into a discrete-time response is illustrated in Fig. 2.2(b).

2.3.2 Bilinear Transformation

The formulae relating s, p and z under the BT are

$$s = \frac{2}{T} \frac{z - 1}{z + 1} \tag{2.16}$$

$$s = \frac{2}{T} \tanh \frac{pT}{2} \tag{2.17}$$

$$z = e^{pT} \tag{2.5}$$

These mappings are illustrated in Fig. 2.3(a). Analogous to the LDI, we can show that the analog steady-state frequency Ω and its digital counterpart ωT are related by

$$\Omega = \frac{2}{T} \tan \frac{\omega T}{2} \tag{2.18}$$

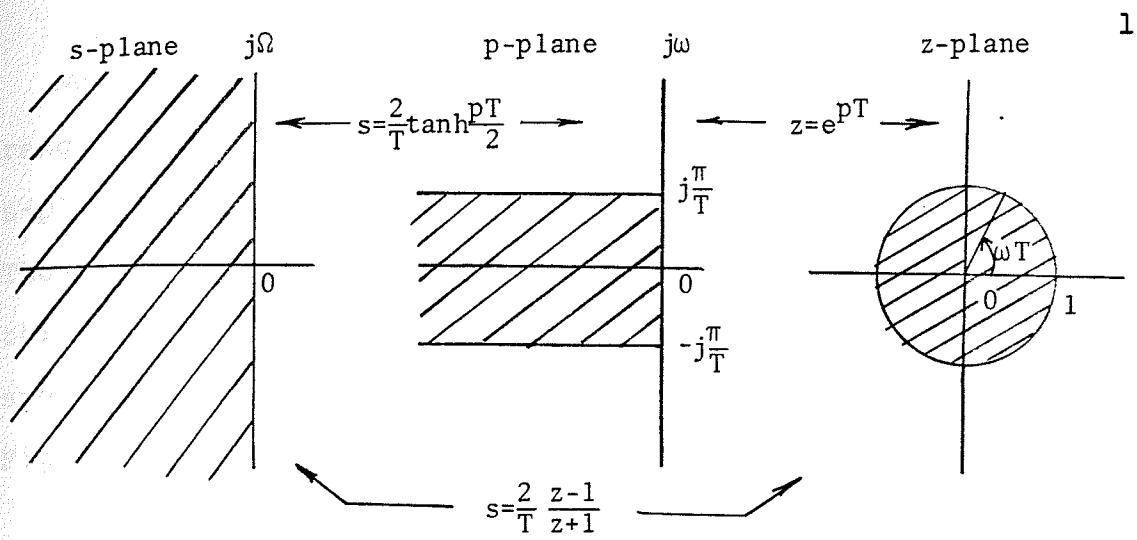

(a)

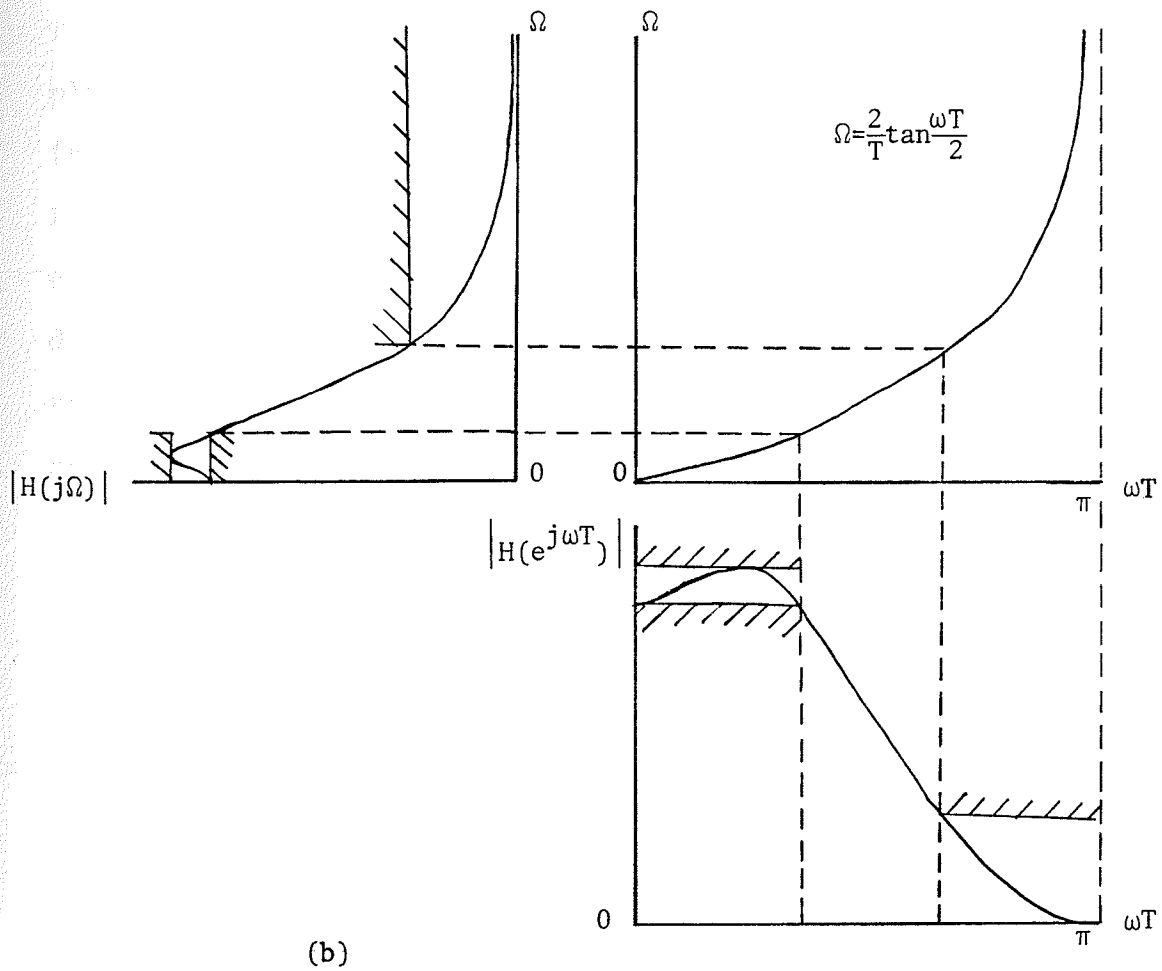

(b)

Fig. 2.3 (a) The mappings associated with the bilinear transformation.
(b) The transformation of an analog frequency response into a digital frequency response under the bilinear transformation.

Note that as ωT varies from $-\pi$ to π, Ω lies in the range of $-\infty < \Omega < \infty$, i.e., the entire imaginary axis of the s-plane is mapped onto the unit circle of the z-plane. Thus, the basic frequency characteristic is preserved under this transformation. The mapping of an analog frequency response into a discrete-time one is illustrated in Fig. 2.3(b).

2.3.3 Sampling Rate

The independent variable of the frequency response of a sampled-data filter is the normalized frequency $\omega T = 2\pi f/f_s$ (normalized with respect to the sampling frequency $f_s = 1/T$). If the cutoff frequency is set in advance at a certain value, say f_c, then the normalized cutoff frequency f_c/f_s will depend on the choice of f_s. Therefore, choosing a higher sampling rate implies a smaller normalized cutoff frequency and the filter becomes a narrower-band filter.

Once a filter has been designed for a specific f_c and f_s, the normalized cutoff frequency f_c/f_s is fixed. A subsequent increase in f_s will result in a higher f_c and the frequency response will be expanded. For example, suppose a filter is designed to be operated at $f_s = 100$ kHz, and to have a cutoff frequency of $f_c = 10$ kHz. The normalized cutoff frequency of the filter is then fixed at $f_c/f_s = 0.1$. If f_s is now doubled to 200 kHz, then f_c will be doubled to 20 kHz too.

A high sampling-rate SC filter will ease the requirement on the anti-aliasing filter (a first- or second-order filter is often adequate), but unfortunately, the capacitance spread and the total capacitance value of the filter will increase too [4,21].

2.4 SIMULATION OF A RESISTOR BY A SWITCHED CAPACITOR

The SC filter concept originated from the idea that a resistor could be simulated by a capacitor switched back and forth between two nodes of a circuit [12]. Although this model is not exact, it will be used to demonstrate the basic operation of an SC filter.

Consider the circuit in Fig. 2.4(a) where V_1 and V_2 are ideal voltage sources.

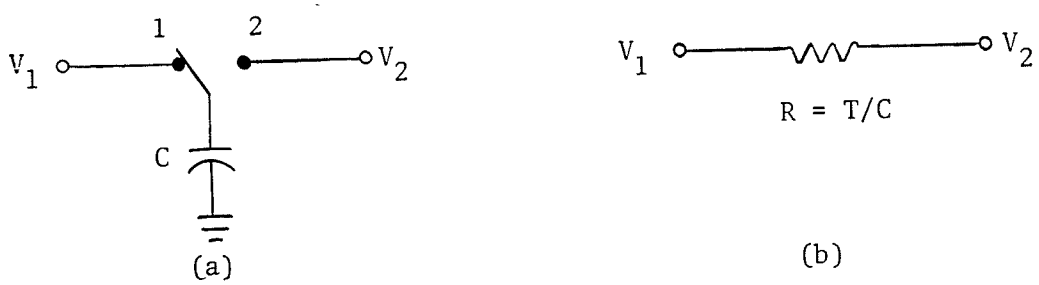

Fig. 2.4 (a) A switched capacitor.
(b) The simulated resistor.

Assume the switch is initially at position 1 so that the capacitor C is charged to V_1 volts. Suppose the switch is now thrown to position 2, then C will take on the new voltage V_2. The amount of charge that flows into V_2 is thus

$\Delta q = C(V_1 - V_2)$. If the switch is thrown back and forth every T seconds (or at a sampling rate of $f_s = 1/T$ Hz), then the average current flowing from V_1 into V_2 is

$$i = \frac{\Delta q}{\Delta t} = \frac{C(V_1 - V_2)}{T} \qquad (2.19)$$

A resistor of value R = T/C ohms will give the same average current. If f_s is much larger than the signal frequency of interest, then the sampling time of the signal can be ignored, and the switched capacitor can be considered as a direct replacement for the resistor shown in Fig. 2.4(b). If the above condition is not met, then the sampled-data z-transform technique is required for analysis; this will be discussed further in Section 2.6 .

The reason that the SC approach is useful can be seen by examining the time constant of an integrator shown in Fig. 2.5(a).

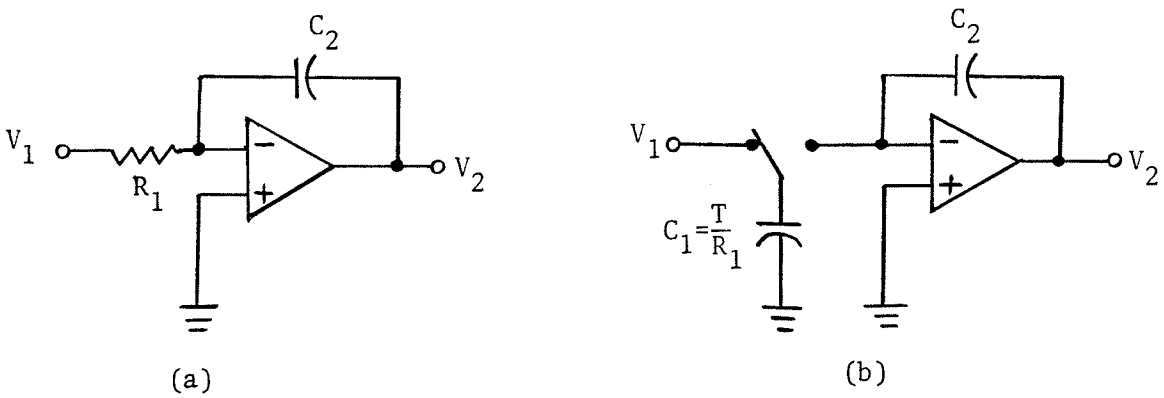

Fig. 2.5 (a) An active-RC integrator.
(b) An SC integrator.

The transfer function of the active-RC integrator is

$$\frac{V_2(s)}{V_1(s)} = -\frac{1}{s\,R_1\,C_2} \tag{2.20}$$

If R_1 is replaced by a switched capacitor of value $C_1 = T/R_1 = 1/(R_1 f_s)$, then the transfer function becomes

$$\frac{V_2(s)}{V_1(s)} = -\frac{1}{s\left(\frac{1}{f_s}\frac{C_2}{C_1}\right)} \tag{2.21}$$

Consequently, the integrator time constant is

$$\tau = \frac{1}{f_s}\frac{C_2}{C_1} \tag{2.22}$$

Since f_s can be very stable and accurate with a crystal oscillator, and capacitor ratios can be achieved with a very high precision in MOS technology, the integrator time constants are well controlled with the SC technique. Thus, these integrators can be used as building blocks in precision filters integrated by MOS processes.

2.5 BASIC ELEMENTS OF A SWITCHED-CAPACITOR FILTER

The basic elements of an SC filter are switches, capacitors and op amps. In addition, a clock is required to operate the switches properly. Each of these basic components will be discussed below.

2.5.1 MOS Switches

In MOS technology, switches are realized by MOSFET transistors. Two equivalent circuit representations [1] of an MOS switch are shown in Fig. 2.6.

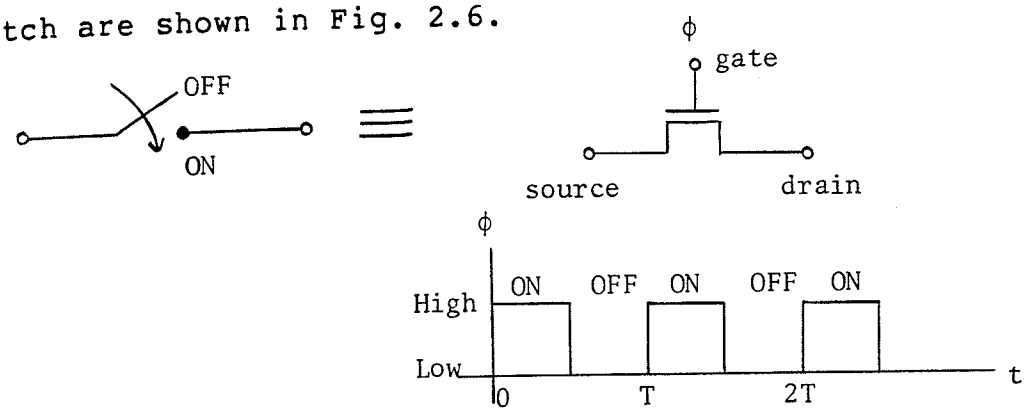

Fig. 2.6 Two equivalent models for an MOS switch, and the clock used to operate the switch.

The gate voltage ϕ acts as a clock which controls the operation of the switch : when ϕ is high, the switch is closed (or on), otherwise the switch is open (or off).

A toggle-switched capacitor (which employs a single-pole-double-throw switch) is represented by three equivalent models in Fig. 2.7. These models will be used interchangably throughout this thesis.

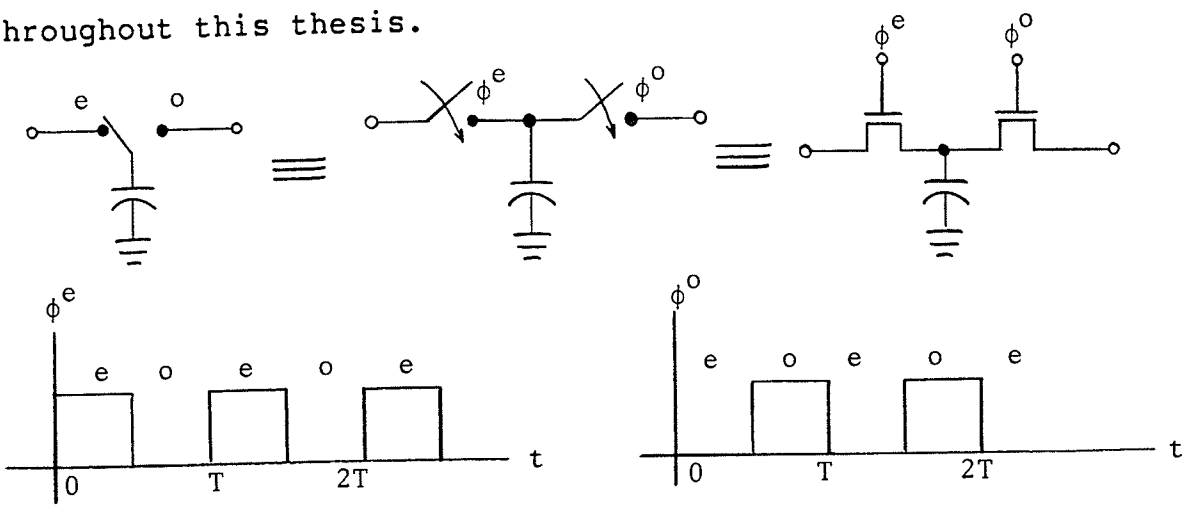

Fig. 2.7 Three equivalent models for a toggle-switched capacitor, and the two-phase clock required.

Note that the two control voltages, namely ϕ^e and ϕ^o, constitute a two-phase clock. The voltage ϕ^e, corresponding to the even clock phase, is high during the even time intervals 'e', and is low during the odd time intervals 'o' (see Fig. 2.7). On the other hand, the voltage ϕ^o, corresponding to the odd clock phase, is high during the odd time intervals, and is low during the even time intervals. It can be seen that ϕ^e and ϕ^o are non-overlapping; thus, only one transistor (or switch) can be turned on at one time.

An ideal switch is assumed to have zero impedance in the closed position, and infinite impedance in the open position. A practical switch exhibits such non-idealities as finite on-resistance, off-leakage currents, clock feedthrough and parasitic capacitances [1]. Parasitic capacitances (about 0.02 pF each) exist from the source and drain to the substrate [1]; they are represented in Fig. 2.8 as C_{p_1} and C_{p_2}, respectively.

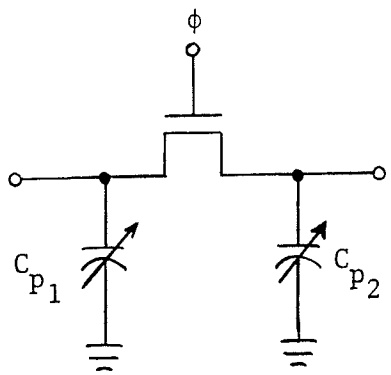

Fig. 2.8 The parasitic capacitances associated with an MOS switch.

2.5.2 MOS Capacitors

The passive precision elements in an SC filter are the MOS capacitors. The frequency response of the SC filter is determined by the capacitor ratios. With careful layout and process control, these capacitor ratios can be accurate within 0.1% of the nominal values [8]. The voltage and temperature coefficients are low enough to be insignificant for all applications [1].

Like the MOS switches, parasitic capacitances co-exist with MOS capacitors. An equivalent circuit for an MOS capacitor with parasitic capacitances is shown in Fig. 2.9 [1].

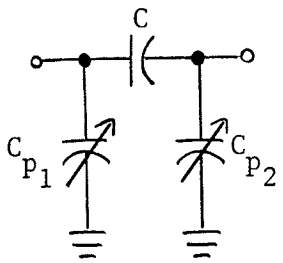

C_{p_1} = top-plate to substrate parasitic capacitance (.1% to 1% of C)

C_{p_2} = bottom-plate to substrate parasitic capacitance (5% to 20% of C)

Fig. 2.9 The parasitic capacitances associated with an MOS capacitor.

Usually, the top-plate parasitic capacitance is very small and can be ignored. However, the bottom-plate parasitic capacitance is relatively large and may cause the circuit to behave differently from theoretical predictions. In that case, the filter performance may be degraded considerably.

2.5.3 MOS Op Amps

Although stand-alone MOS op amps are not superior to their bipolar transistor counterparts (mainly due to the lower gain, higher offset voltage and larger RMS noise [22]), they are used as components in integrated SC filters. This is because MOS op amps are smaller, and more importantly, they are technologically compatible with other MOS circuit elements.

Since MOS op amps take up a lot of IC area, generate noise and consume most of the power, it is essential that the number of op amps be kept as small as possible. Factors that determine the highest possible sampling rate for the SC filters are such op amp non-idealities as finite gain-bandwidth product, slew rate and settling time [23,24].

2.6 SWITCHED CAPACITOR INTEGRATORS

In SC filters, the most important building block is the integrator. In this section, the simplest SC integrator will be described. This circuit will be analyzed to highlight the procedure involved in solving a simple SC circuit. Since this integrator is susceptible to parasitic capacitances, other useful integrators that are parasitic-insensitive will also be given.

2.6.1 Parasitic-Sensitive Inverting Integrator

The integrator shown in Fig. 2.10 is the simplest SC integrator. It has been analyzed with the continuous-time technique in Section 2.4. Here, the sampled-data technique will be used so that the restriction $f_s >> f$ is no longer necessary.

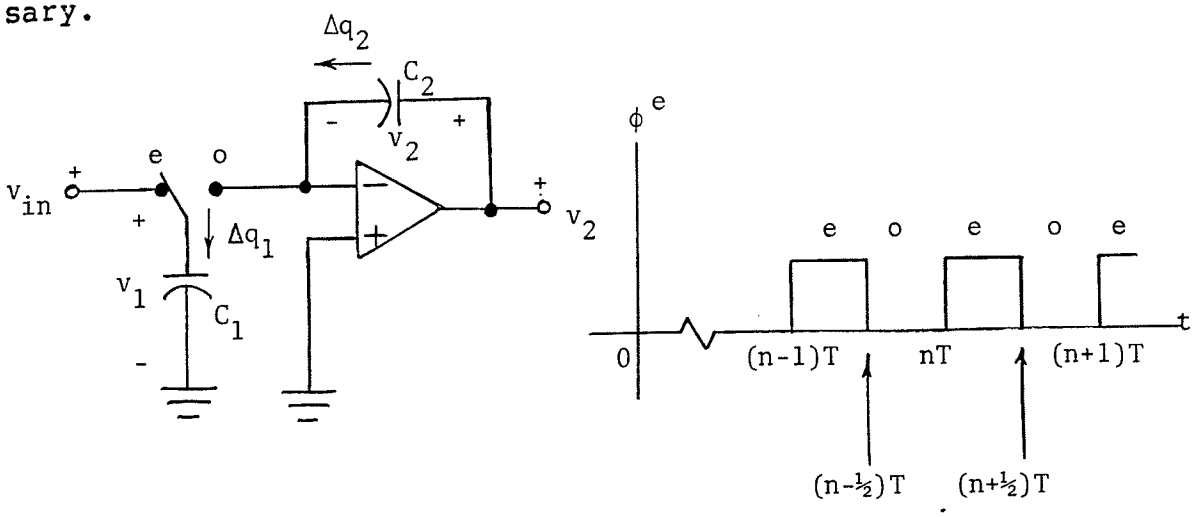

Fig. 2.10 A simple inverting SC integrator.

The analysis of an SC circuit usually involves three basic relations in circuit theory : Kirchhoff's Voltage Law, the principle of conservation of charge, and the equation of charge transfer. Throughout the analysis, all components will be assumed ideal.

Suppose at $t = nT$, ϕ^e becomes high and the switch is at position e. Thus,

$$v_1^e(nT) = v_{in}^e(nT) \tag{2.23}$$

where the superscript e indicates that the voltages are sampled during an even time interval.

At $t = (n+\frac{1}{2})T$, the switch is thrown to position o which is at the inverting terminal of the op amp. At this time instant, a transfer of charge occurs

$$\begin{aligned} \Delta q_1 &= q_1^o[(n+\tfrac{1}{2})T] - q_1^e(nT) \\ &= - q_1^e(nT) \end{aligned} \tag{2.24}$$

$$\Delta q_2 = q_2^o[(n+\tfrac{1}{2})T] - q_2^e(nT) \tag{2.25}$$

where Δq_1 and Δq_2 are the charge transfers with reference directions given in Fig. 2.10. Note that $q_1^o[(n+\frac{1}{2})T] = 0$ because the inverting terminal of the op amp is assumed to be at virtual ground.

The principle of conservation of charge requires that

$$\Delta q_1 + (-\Delta q_2) = 0 \tag{2.26}$$

Substituting (2.24) and (2.25) into (2.26), we obtain

$$q_2^o[(n+\tfrac{1}{2})T] = q_2^e(nT) - q_1^e(nT) \tag{2.27}$$

From the circuit, it can be seen that the charge on C_2 cannot change from $t = (n-\frac{1}{2})T$ to $t = nT$; therefore,

$$q_2^e(nT) = q_2^o[(n-\tfrac{1}{2})T] \tag{2.28}$$

Hence, (2.27) becomes

$$q_2^o[(n+\tfrac{1}{2})T] = q_2^o[(n-\tfrac{1}{2})T] - q_1^e(nT) \tag{2.29}$$

or

$$C_2\, v_2^o[(n+\tfrac{1}{2})T] = C_2\, v_2^o[(n-\tfrac{1}{2})T] - C_1\, v_{in}^e(nT) \tag{2.30}$$

Applying the z-transform to both sides of (2.30) and using the time-shifting property of (2.7) result in

$$C_2\, z^{\frac{1}{2}}\, V_2^o(z) = C_2\, z^{-\frac{1}{2}}\, V_2^o(z) - C_1\, V_{in}^e(z) \tag{2.31}$$

or

$$\frac{V_2^o(z)}{V_{in}^e(z)} = -\frac{C_1}{C_2}\,\frac{z^{\frac{1}{2}}}{z-1} \tag{2.32}$$

This transfer function corresponds to an inverting LDI integrator (see (2.11)). The gain constant is given by a capacitor ratio.

If the output v_2 is sampled during the even time interval, then we will rewrite (2.28) as

$$q_2^o[(n+\tfrac{1}{2})T] = q_2^e[(n+1)T] \tag{2.33}$$

Equation (2.27) becomes

$$q_2^e[(n+1)T] = q_2^e(nT) - q_1^e(nT) \tag{2.34}$$

Finally, we obtain the new transfer function

$$\frac{V_2^e(z)}{V_{in}^e(z)} = -\frac{C_1}{C_2}\,\frac{1}{z-1} \tag{2.35}$$

This corresponds to an inverting FD integrator. Comparing (2.32) and (2.35), we observe a very important fact : the characteristics of an SC filter depend on when the signals in it are sampled.

This simple SC integrator is, unfortunately, susceptible to parasitic capacitances. The parasitic capacitances (due to switches and capacitors as discussed earlier) are represented as C_a , C_b , C_c , C_d and C_e in Fig. 2.11.

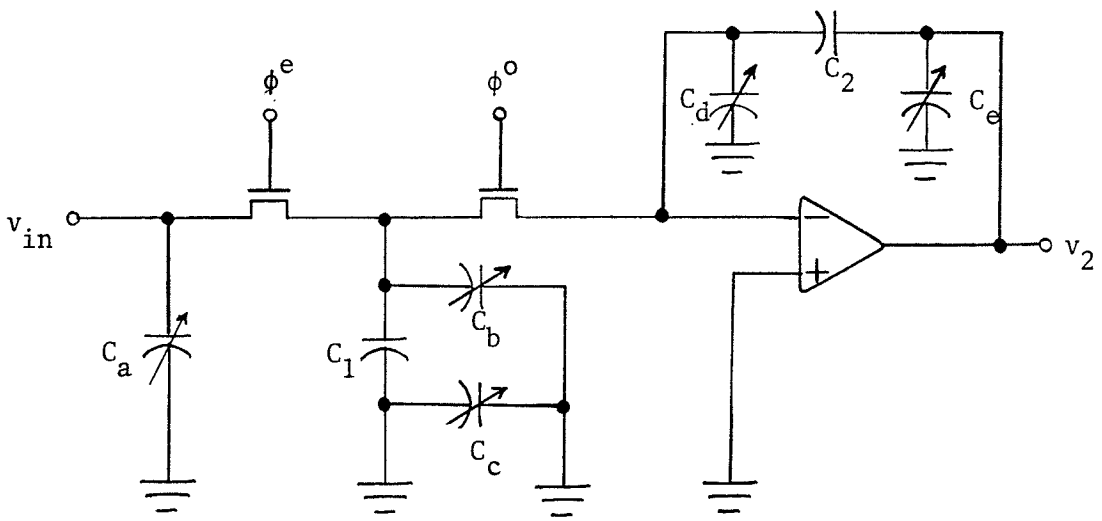

Fig. 2.11 The parasitic capacitances associated with the SC integrator shown in Fig. 2.10.

Since C_c and C_d have both their plates always connected to ground or virtual ground, they will not affect the circuit operation. Since C_a and C_e shunt the circuit input and output, respectively, they will not affect the transfer function either. Therefore, the only parasitic capacitance

of any significance is C_b. Consequently, the input capacitance of the integrator is not just C_1, but the parallel combination of C_1 and C_b. Specifically, the gain constants in (2.32) and (2.35) will be $-(C_1 + C_b)/C_2$ instead of $-C_1/C_2$. Since parasitic capacitances are nonlinear and process-dependent, their effect cannot be eliminated by predistorting the input capacitance value [15]. Hence, it is necessary to find new integrators that are insensitive to parasitic capacitances. Some important integrators [25] will be presented below. Their transfer functions will be stated without proof, as it is easy to derive them by following the procedure outlined in this section.

2.6.2 Parasitic-Insensitive Inverting Integrator

If v_2 of Fig. 2.12 is sampled during the odd time interval, then

$$\frac{V_2^o(z)}{V_1^e(z)} = -\frac{C_1}{C_2}\frac{z^{\frac{1}{2}}}{z-1} \qquad \text{(LDI)} \tag{2.36}$$

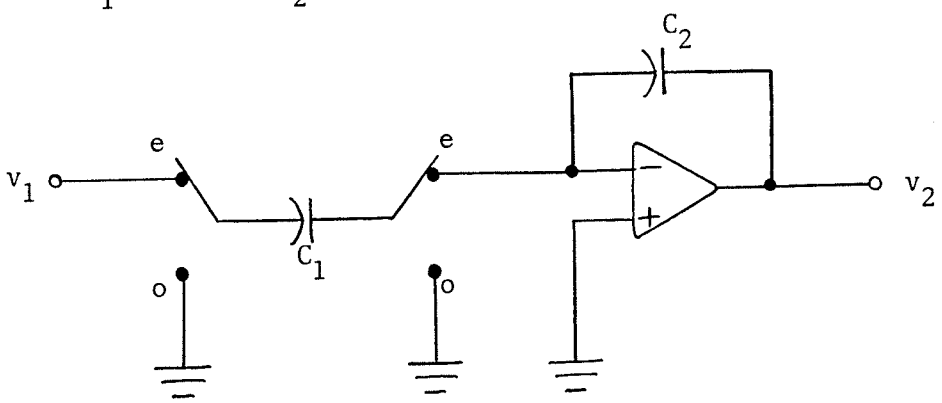

Fig. 2.12 A parasitic-insensitive inverting SC integrator.

2.6.3 Parasitic-Insensitive Non-Inverting Integrator

If v_2 of Fig. 2.13 is sampled during the even time interval, then

$$\frac{V_2^e(z)}{V_1^o(z)} = \frac{C_1}{C_2} \frac{z^{\frac{1}{2}}}{z - 1} \qquad \text{(LDI)} \qquad (2.37)$$

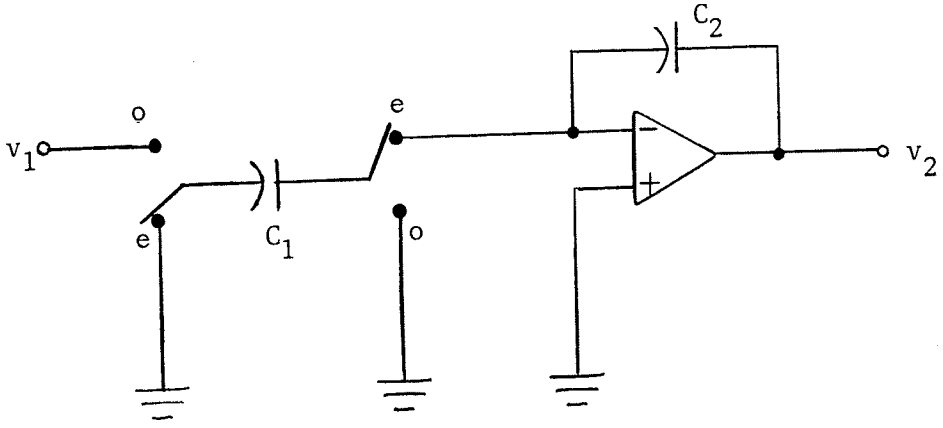

Fig. 2.13 A parasitic-insensitive non-inverting SC integrator.

2.6.4 Parasitic-Insensitive Inverting Damped Integrator

If v_2 of Fig. 2.14 is sampled during the odd time interval, then

$$\frac{V_2^o(z)}{V_1^e(z)} = -\frac{C_1}{C_2} \frac{z^{\frac{1}{2}}}{(1+\frac{C_3}{C_2})z - 1} \qquad (2.38)$$

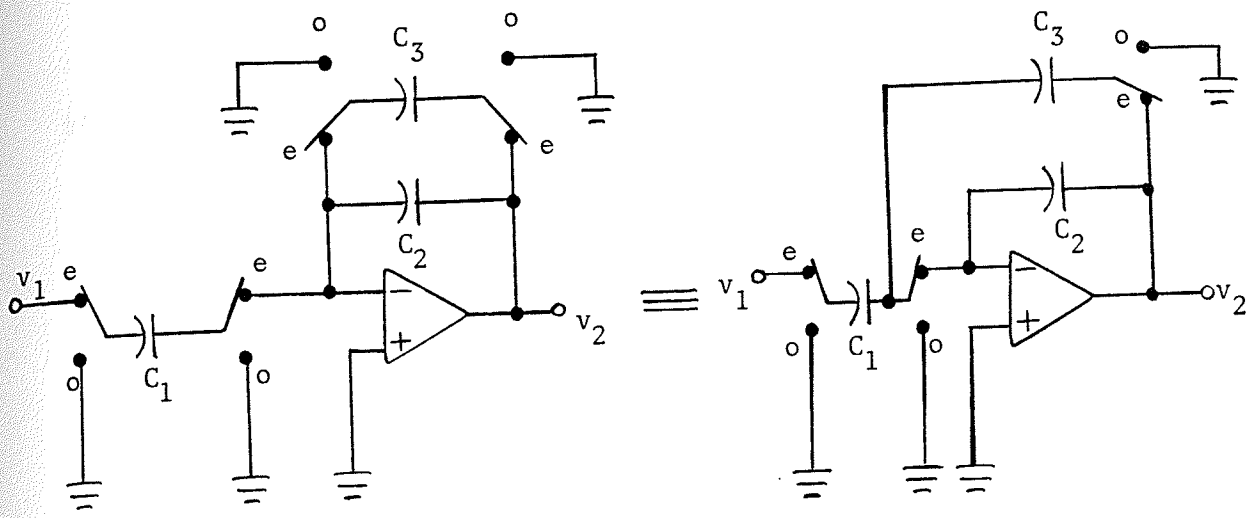

Fig. 2.14 A parasitic-insensitive inverting damped SC integrator and the switch-reduced version.

Note that this is not an exact LDI damped integrator. Consider the analog damped integrator shown in Fig. 2.15.

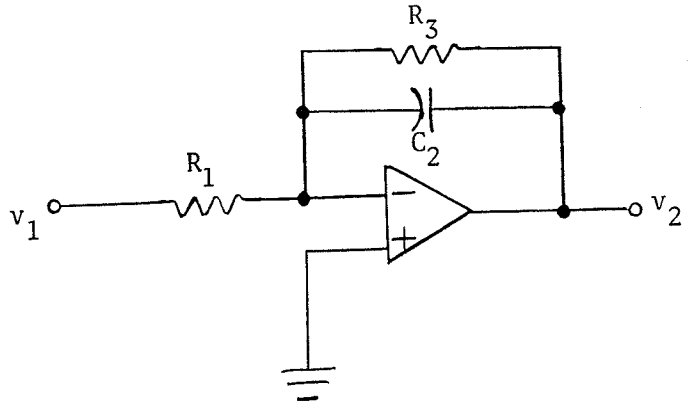

Fig. 2.15 An active-RC damped integrator.

The transfer function of this integrator is given by

$$\frac{V_2(s)}{V_1(s)} = -\frac{\frac{1}{R_1C_2}}{s + \frac{1}{R_3C_2}} \qquad (2.39)$$

If we define $R_1 \triangleq T/C_1$ and $R_3 \triangleq T/C_3$ for some C_1, C_3 and T, then the transfer function becomes

$$\frac{V_2(s)}{V_1(s)} = -\frac{C_1}{C_2} \frac{\frac{1}{T}}{s + \frac{C_3}{C_2}\frac{1}{T}} \tag{2.40}$$

Under the LDI, this transfer function should become

$$\frac{V_2(z)}{V_1(z)} = -\frac{C_1}{C_2} \frac{z^{\frac{1}{2}}}{z + \frac{C_3}{C_2} z^{\frac{1}{2}} - 1} \tag{2.41}$$

The $z^{\frac{1}{2}}$ term in the denominator makes the function unrealizable with SC components. One way to overcome this problem is to approximate $\frac{C_3}{C_2} z^{\frac{1}{2}}$ by $\frac{C_3}{C_2} z$; thus, (2.41) becomes

$$\frac{V_2(z)}{V_1(z)} = -\frac{C_1}{C_2} \frac{z^{\frac{1}{2}}}{(1+\frac{C_3}{C_2}) z - 1} \tag{2.42}$$

which is identical to (2.38). Thus the integrator in Fig. 2.14 which has a transfer function defined in (2.38) can be used to realize this modified transfer function in (2.42).

Equation (2.41) can be represented by the signal flowgraph shown in Fig. 2.16(a). Similarly, (2.42) defining the

approximate damped LDI integrator can be represented by the signal flowgraph shown in Fig. 2.16(b).

The difference between the exact and approximate damped LDI integrators is that the half-delay term $z^{-\frac{1}{2}}$ is absent in the feedback branch of the latter model. Thus, this approximation of a damped LDI integrator is called the minus-half-delay modification [26]. Note that after this modification, the termination loop gain $-\frac{C_3}{C_2}\frac{z}{z-1}$ has in fact become a BD integration.

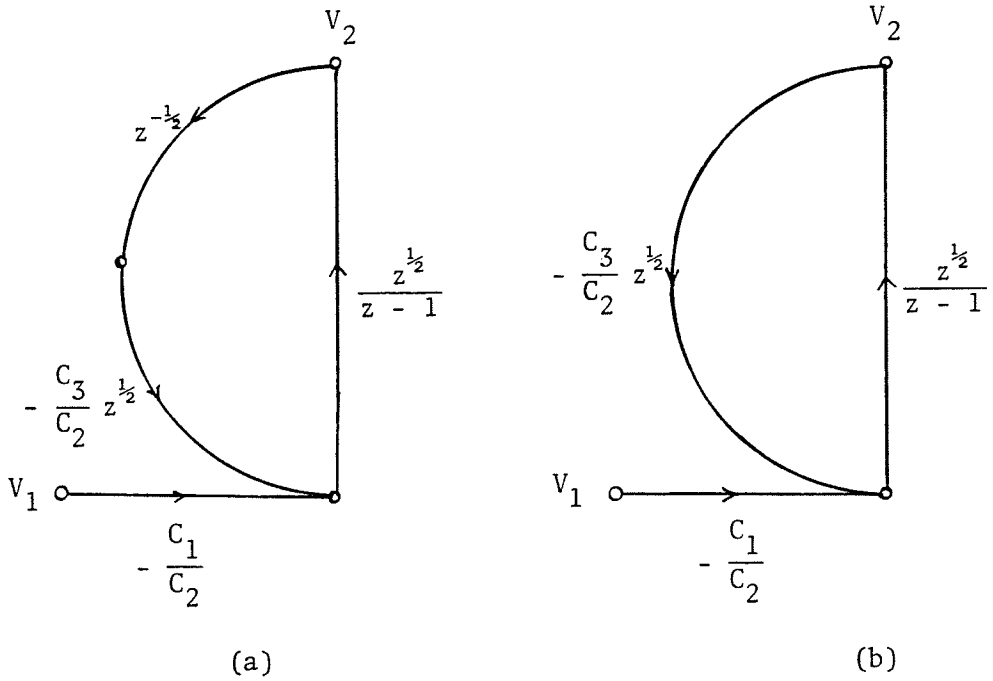

Fig. 2.16 The signal flowgraph representations for (a) an exact LDI damped integrator, and (b) a minus-half-delay modified LDI damped integrator.

2.6.5 Parasitic-Insensitive Non-Inverting Damped Integrator

If v_2 of Fig. 2.17 is sampled during the even time interval, then

$$\frac{V_2^e(z)}{V_1^o(z)} = \frac{C_1}{C_2} \frac{z^{\frac{1}{2}}}{(1 + C_3/C_2)z - 1} \tag{2.43}$$

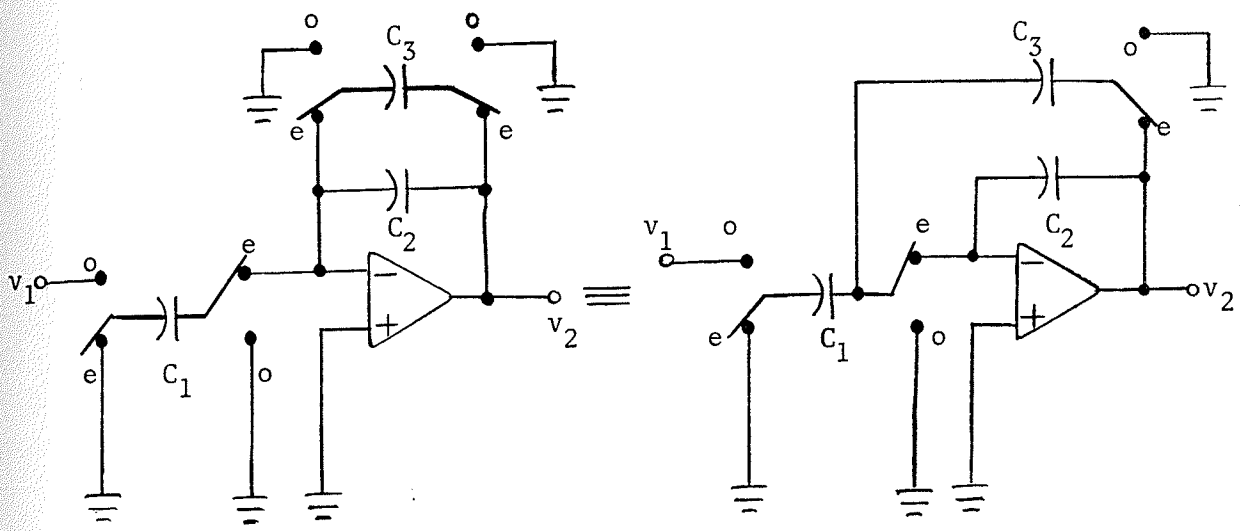

Fig. 2.17 A parasitic-insensitive non-inverting damped SC integrator and the switch-reduced version.

This non-inverting damped integrator is also a minus-half-delay modified LDI integrator.

2.6.6 Inverting Amplifier

If v_2 of Fig. 2.18 is sampled during either the odd or even time interval, then

$$\frac{V_2^o(z)}{V_1^o(z)} = \frac{V_2^e(z)}{V_1^e(z)} = -\frac{C_1}{C_2} \tag{2.44}$$

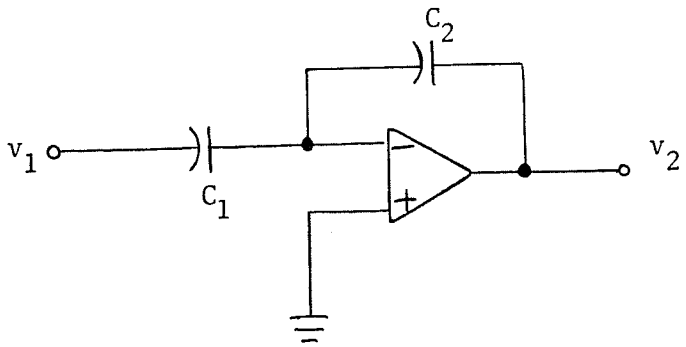

Fig. 2.18 An SC inverting amplifier.

Chapter III

LEAPFROG REALIZATION OF A SWITCHED-CAPACITOR FILTER

In this chapter, a brief survey of the various methods of realizing an SC filter will be presented. The SC leapfrog realization will be the only method used in this thesis. There are two major types of flowgraphs used in these leapfrog filters : one is based on the lossless-discrete-integrator transformation (LDI) and the other is based on the bilinear transformation (BT). We will discuss in detail the procedures of designing these filters.

3.1 METHODS OF REALIZING SC FILTERS

There are four main approaches to realizing an SC filter : signal-flow-graph (SFG) simulation, direct-form realization, component simulation and cascade synthesis. This section will provide a very brief description of each of these methods.

3.1.1 Signal-Flow-Graph Simulation

The SFG simulation includes the leapfrog [1,27], state-variable [4], multiple-feedback [1], and coupled biquad [28] structures. The building blocks are usually the SC integrators. The leapfrog simulation of a doubly-terminated LC lad-

der network is the most widely used method. One reason is that since the analog LC prototype is known to be very insensitive to element variations [16], its SC equivalent is expected to retain the same property. Another reason is that the dynamic range of the leapfrog filter can easily be maximized. The leapfrog realization will be discussed in detail later.

3.1.2 Component Simulation

This approach simulates the inductors and resistors [29,30,31,32] of a passive RLC ladder network using capacitors, switches and op amps. Although this method typically results in fewer op amps, the circuit usually requires a complex clocking scheme and very often it is susceptible to parasitic capacitances.

3.1.3 Direct-Form Realization

This approach to realizing an SC filter is analogous to the direct-form realization of a digital filter. The design starts with a discrete-time z-domain transfer function which is rewritten as a recursive difference equation. This difference equation is then implemented with such operations as addition, multiplication and delay [33]. A similar approach is to realize the transfer function in a state-space form [34]. These methods are not popular because the filter response is sensitive to the coefficients of the transfer

function, and the implementation generally requires a relatively large number of op amps.

3.1.4 Cascade Synthesis

This approach synthesizes a filter by cascading building blocks that are first-order, second-order or third-order sections [23,35,36,37,38]. The design is simple but the subsequent realization is usually sensitive to the capacitance values and requires careful tuning between sections.

In an overview paper [15], Martin concluded that the leapfrog simulation is the best method of realizing an SC filter. Hereafter, in this thesis, we will only consider the leapfrog SC filters.

3.2 DERIVATION OF A LEAPFROG FLOWGRAPH

A leapfrog filter is sometimes called an active ladder filter [39] because it uses active devices (e.g. op amps) to simulate a passive RLC ladder network. The leapfrog structure realizes the flowgraph representing the voltage and current relations of the passive network. If SC circuits are used as building blocks to implement the flowgraph, then the filter is called an SC leapfrog filter.

In this section, the procedure of deriving a leapfrog flowgraph for an analog network is reviewed. A fifth-order elliptic filter will be used as an example, and it is easy to generalize the results to an M-th order filter. Usually,

there are several valid flowgraph representations for a given analog prototype. The objective here is to choose the one that can be realized easily with SC integrators.

Consider the fifth-order lowpass elliptic filter shown in Fig. 3.1(a). The state variables chosen are V_1, I_2, V_3, I_4, and V_5 as indicated in the diagram. An equivalent circuit representation of the filter is shown in Fig. 3.1(b) [1].

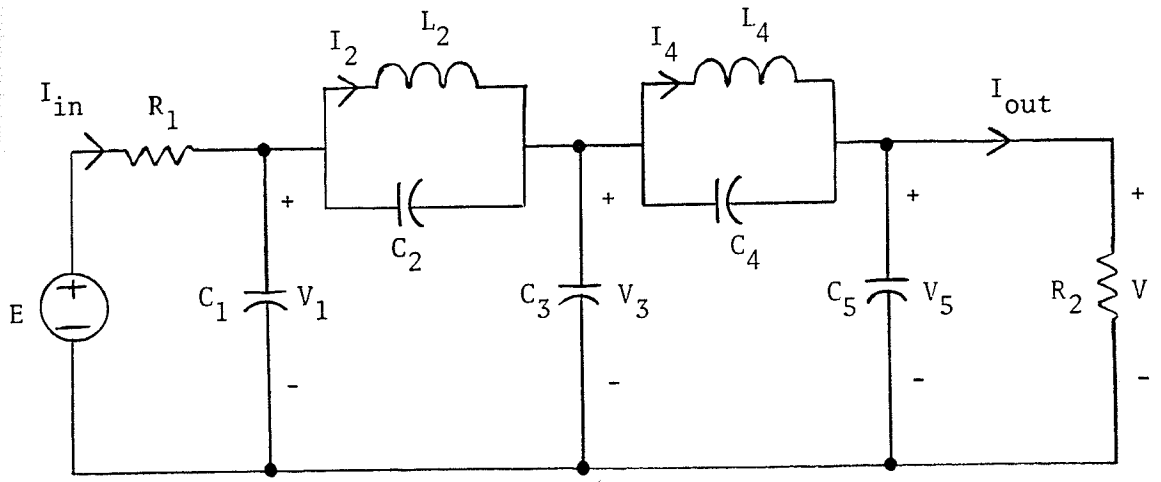

(a)

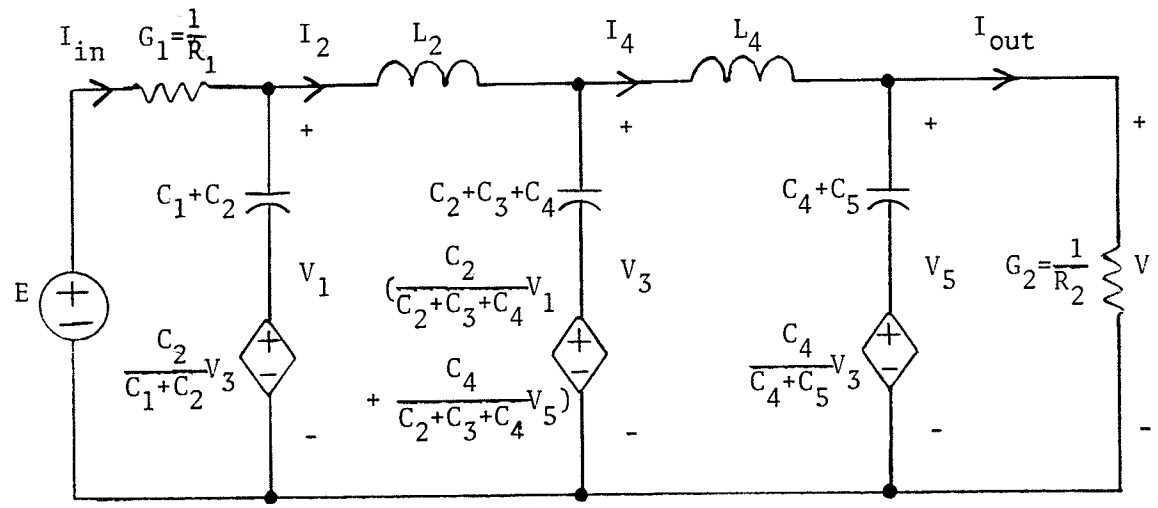

(b)

Fig. 3.1 (a) A fifth-order elliptic filter.
(b) The equivalent representation.

From Fig. 3.1(b), the following branch relations can be derived :

$$I_{in} = (E - V_1)G_1 \tag{3.1a}$$

$$V_1 = \frac{I_{in}-I_2}{s(C_1+C_2)} + \frac{C_2}{C_1+C_2} V_3 \tag{3.1b}$$

$$I_2 = \frac{V_1-V_3}{sL_2} \tag{3.1c}$$

$$V_3 = \frac{I_2 - I_4}{s(C_2+C_3+C_4)} + \frac{C_2}{C_2+C_3+C_4} V_1 + \frac{C_4}{C_2+C_3+C_4} V_5 \tag{3.1d}$$

$$I_4 = \frac{V_3-V_5}{sL_4} \tag{3.1e}$$

$$V_5 = \frac{I_4-I_{out}}{s(C_4+C_5)} + \frac{C_4}{C_4+C_5} V_3 \tag{3.1f}$$

$$I_{out} = G_2 V_5 \tag{3.1g}$$

$$V = V_5 \tag{3.1h}$$

Substituting (3.1a) into (3.1b), and (3.1g) into (3.1f), we obtain the following state and output equations :

$$V_1 = \frac{G_1E-G_1V_1-I_2}{s(C_1+C_2)} + \frac{C_2}{C_1+C_2} V_3 \tag{3.2a}$$

$$I_2 = \frac{V_1 - V_3}{sL_2} \tag{3.2b}$$

$$V_3 = \frac{I_2 - I_4}{s(C_2+C_3+C_4)} + \frac{C_2}{C_2+C_3+C_4} V_1 + \frac{C_4}{C_2+C_3+C_4} V_5 \tag{3.2c}$$

$$I_4 = \frac{V_3 - V_5}{sL_4} \tag{3.2d}$$

$$V_5 = \frac{I_4 - G_2 V_5}{s(C_4+C_5)} + \frac{C_4}{C_4+C_5} V_3 \tag{3.2e}$$

$$V = V_5 \tag{3.2f}$$

For convenience, define the following new set of state variables :

$$\hat{V}_1 = -V_1 \ , \ \hat{I}_2 = I_2 \ , \ \hat{V}_3 = V_3 \ , \ \hat{I}_4 = -I_4 \ , \ \hat{V}_5 = -V_5 \tag{3.3}$$

The corresponding state and output equations are

$$\hat{V}_1 = \frac{-G_1 E - G_1 \hat{V}_1 + \hat{I}_2}{s(C_1+C_2)} - \frac{C_2}{C_1+C_2} \hat{V}_3 \tag{3.4a}$$

$$\hat{I}_2 = \frac{-\hat{V}_1 - \hat{V}_3}{sL_2} \tag{3.4b}$$

$$\hat{V}_3 = \frac{\hat{I}_2 + \hat{I}_4}{s(C_2+C_3+C_4)} - \frac{C_2}{C_2+C_3+C_4} \hat{V}_1 - \frac{C_4}{C_2+C_3+C_4} \hat{V}_5 \tag{3.4c}$$

$$\hat{I}_4 = \frac{-\hat{V}_3 - \hat{V}_5}{sL_4} \tag{3.4d}$$

$$\hat{V}_5 = \frac{\hat{I}_4 - G_2\hat{V}_5}{s(C_4+C_5)} - \frac{C_4}{C_4+C_5}\hat{V}_3 \qquad (3.4e)$$

$$V = -\hat{V}_5 \qquad (3.4f)$$

The pictorial representation of the above equations yields the flowgraph shown in Fig. 3.2(a).

The flowgraph in Fig. 3.2(b) is obtained from Fig. 3.2(a) by choosing $G_1=G_2=1$, and defining

$$d_1 = \frac{1}{C_1 + C_2} \qquad d_6 = \frac{C_2}{C_1 + C_2}$$

$$d_2 = \frac{1}{L_2} \qquad d_7 = \frac{C_2}{C_2 + C_3 + C_4}$$

$$d_3 = \frac{1}{C_2 + C_3 + C_4} \qquad d_8 = \frac{C_4}{C_4 + C_5} \qquad (3.5)$$

$$d_4 = \frac{1}{L_4} \qquad d_9 = \frac{C_4}{C_2 + C_3 + C_4}$$

$$d_5 = \frac{1}{C_4 + C_5}$$

The transfer function V(s)/E(s) can be derived by using Mason's formula [40] (see Appendix A).

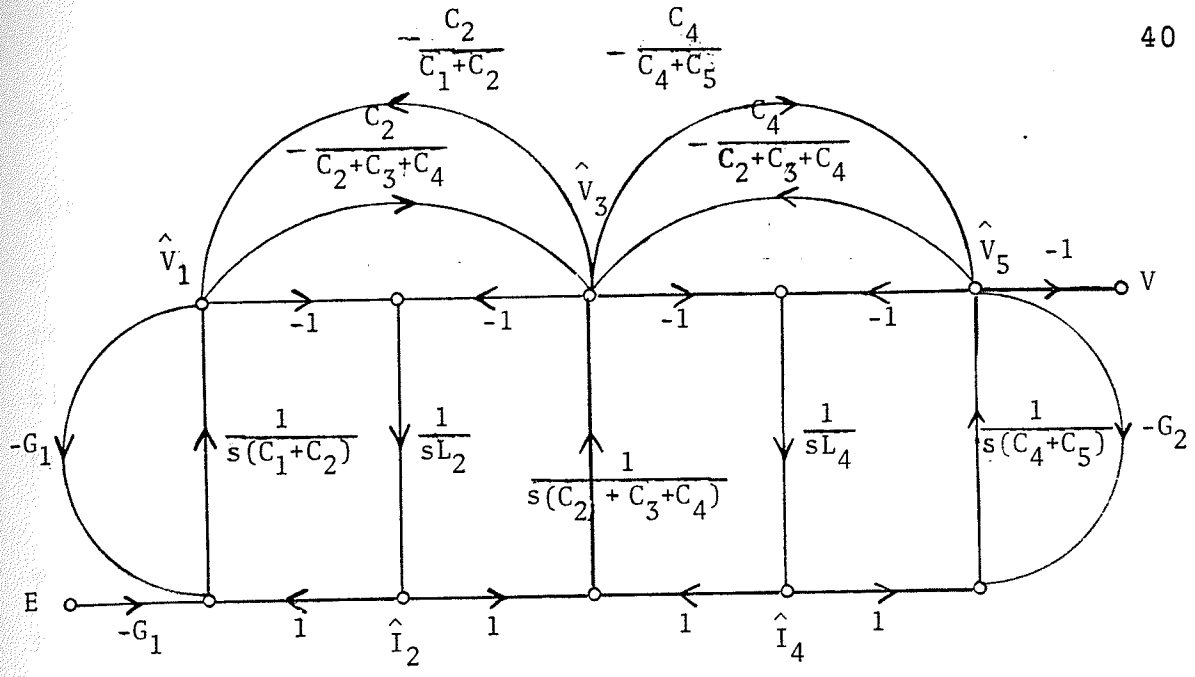

(a)

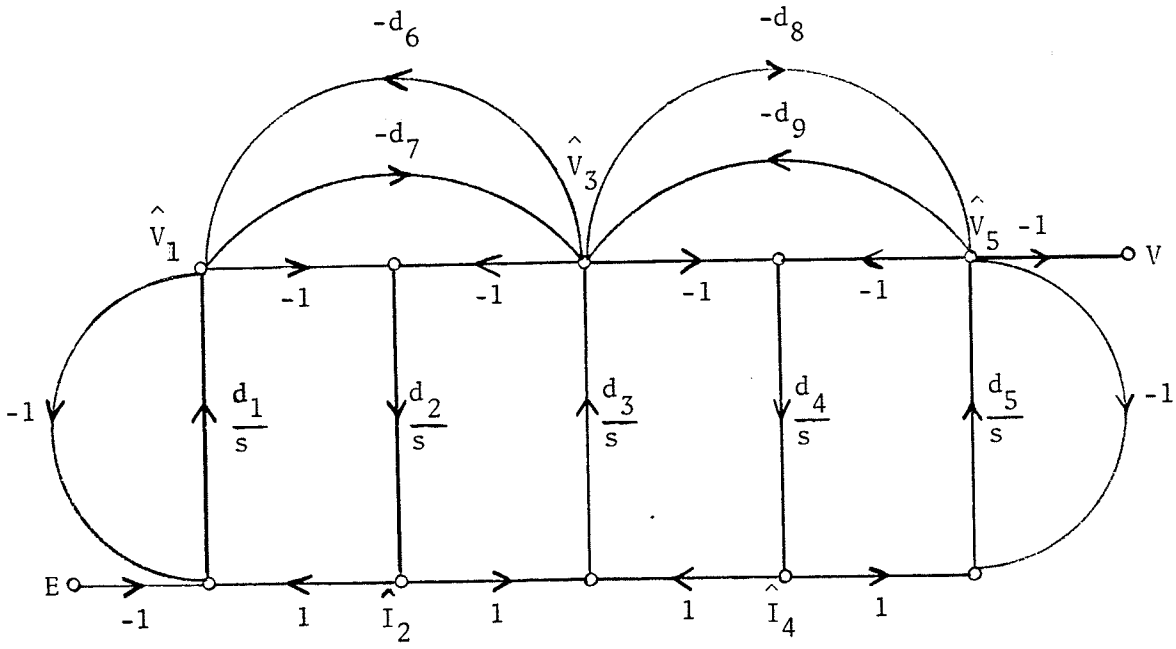

(b)

Fig. 3.2 The s-domain signal flowgraph for the fifth-order elliptic filter shown in Fig. 3.1.

3.3 REALIZATION OF AN SC LEAPFROG FILTER BASED ON LDI TRANSFORMATION

After an analog SFG is derived, the next step is to apply an s-to-z transformation to the analog integrators 1/s in order to obtain a z-domain SFG. The LDI and BT are the transformations commonly used; they will be discussed in this and the next sections, respectively.

We will consider the third-order all-pole filter shown in Fig. 3.3(a). The corresponding s-domain SFG is shown in Fig. 3.3(b). Applying the LDI transformation

$$\frac{1}{s} = T\,\frac{z^{\frac{1}{2}}}{z-1} \tag{2.11}$$

to the integrators of this SFG yields the z-domain SFG shown in Fig. 3.3(c).

Note that the input and output termination loops cannot be realized exactly (see Fig. 2.16). The transfer function of the flowgraph is of the form [41]

$$\frac{V}{E} = \frac{K_1\, z^{3/2}}{z^3 + \alpha_1 z^{5/2} + \alpha_2 z^2 + \cdots + \alpha_5 z^{\frac{1}{2}} + \alpha_6} \tag{3.6}$$

where K_1 and α_i's are real constants. Thus, the transfer function has three poles inside and three poles outside the unit circle [17,41]. This is obviously true because (2.11) remains unchanged when $z^{\frac{1}{2}}$ is replaced by $-z^{-\frac{1}{2}}$. This means

one s will map into two points, namely z and 1/z. An analog pole will thus map into two discrete-time poles — one inside and the other outside the unit circle. Consequently, the SC filter will be inherently unstable (even if the terminations were realizable).

A method to overcome both the realizability and stability problems is to modify the input and output termination feedback branches from -1 to $-z^{\frac{1}{2}}$ or $-z^{-\frac{1}{2}}$ or $-\frac{1}{2}(z^{\frac{1}{2}} + z^{-\frac{1}{2}})$ [26,41,42]. These modifications are equally valid. In this thesis, we will only consider the first modification (in fact, this has been introduced as the minus-half-delay modification in Section 2.6). The modified SFG is shown in Fig. 3.3(d). Note that each of the termination loop gains (i.e., $-b_1 z/(z-1)$ and $-b_3 z/(z-1)$) is a backward difference (BD) integration.

The new transfer function is of the form

$$\frac{V}{E} = \frac{K_2 \, z^{3/2}}{\beta_1 z^3 + \beta_2 z^2 + \beta_3 z - 1} \tag{3.7}$$

where K_2 and β_i's are real constants. The three poles obtained now, however, will not correspond to those that would be obtained by applying the LDI mapping to the original s-plane poles of the analog prototype. Hence, the SC filter frequency response will deviate from the nominal response. This distortion is negligible only when the sampling rate is much higher than the cutoff frequency of the filter [26].

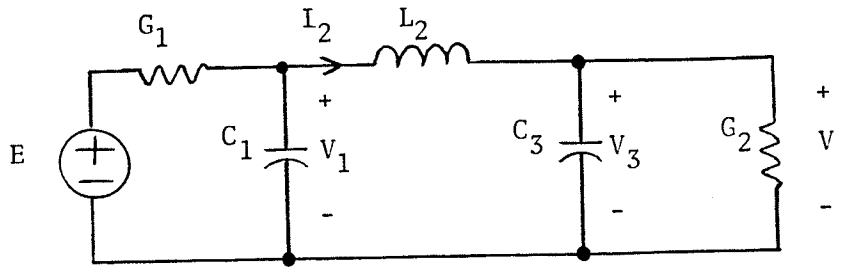

(a) The analog prototype.

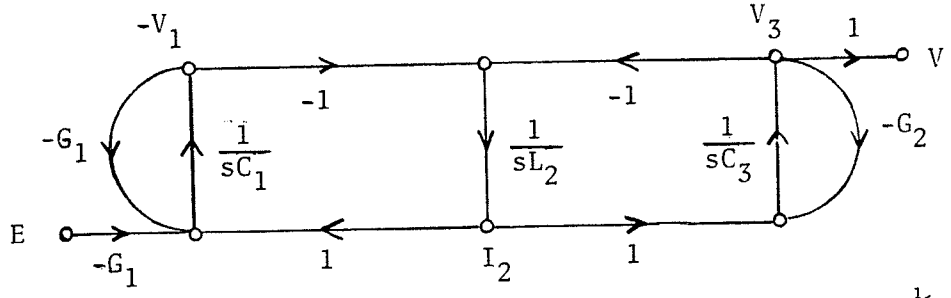

(b) The s-domain SFG.

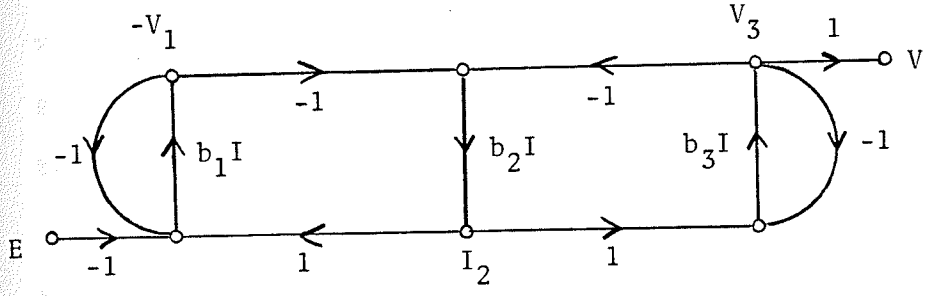

$I=\frac{z^{\frac{1}{2}}}{z-1}$

$G_1=G_2=1$

$b_1=T/C_1$

$b_2=T/L_2$

$b_3=T/C_3$

(c) The z-domain SFG.

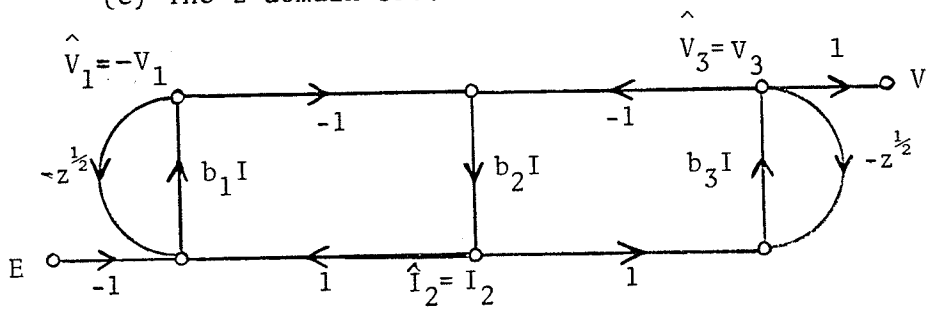

(d) The minus-half-delay modified SFG.

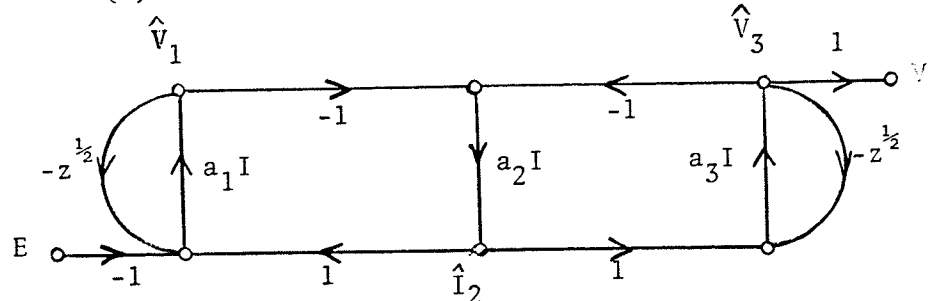

(e) The optimized minus-half-delay modified SFG.

Fig. 3.3 A third-order all-pole filter.

Davis and Trick [41] proposed that the poles of the modified filter should be moved back to their correct positions (i.e., those obtained by applying the LDI mapping directly to the s-plane poles) so that the SC filter will yield the correct response. Their method will be described below with an example.

3.3.1 Davis and Trick's Method

Consider the third-order all-pole filter shown in Fig. 3.3(a). The corresponding minus-half-delay modified z-domain flowgraph has been shown in Fig. 3.3(d). This SFG will not give the correct poles if the integrator gain constants assume those values defined in the diagram. In order to obtain the correct poles, we must have a correct set of integrator gain constants (i.e., a_i's in Fig. 3.3(e)). The values of these constants can be determined by the coefficient-matching technique described below.

The transfer function of the SFG in Fig. 3.3(e) is

$$\frac{V}{E} = \frac{a_1 a_2 a_3 \, z^{3/2}}{f_1 z^3 + f_2 z^2 + f_3 z - 1} \tag{3.8}$$

where

$$f_1 = (a_1 + 1)(a_3 + 1) \tag{3.9a}$$

$$f_2 = (a_1 + a_3)(a_2 - 2) + a_1 a_3 (2a_2 - 1) - 3 \tag{3.9b}$$

$$f_3 = (a_1 + a_3)(1 - a_2) + 3 \tag{3.9c}$$

Alternatively, this transfer function can be expressed in terms of the z-domain poles as

$$\frac{V}{E} = \frac{K\, z^{3/2}}{(z - p_1)\,(z - p_2)\,(z - p_3)} \tag{3.10a}$$

or

$$\frac{V}{E} = \frac{K\, z^{3/2}}{z^3 - z^2(p_1+p_2+p_3) + z(p_1p_2+p_1p_3+p_2p_3) - p_1p_2p_3} \tag{3.10b}$$

where K is a scaling factor, p_1, p_2 and p_3 are the z-plane poles (located inside the unit circle) that are obtained from their analog counterparts by the LDI formula

$$z = \tfrac{1}{2}\left[\, 2 + s^2T^2 \pm \sqrt{s^2T^2(\,4 + s^2T^2)}\,\right] \tag{3.11}$$

and

$$|z| < 1$$

Equating (3.8) and (3.10b), the transfer function coefficients can be computed by the following formulae :

$$f_1 = \frac{1}{p_1p_2p_3} \tag{3.12a}$$

$$f_2 = -\frac{p_1 + p_2 + p_3}{p_1p_2p_3} \tag{3.12b}$$

$$f_3 = \frac{1}{p_1} + \frac{1}{p_2} + \frac{1}{p_3} \qquad (3.12c)$$

Substituting these values into (3.9), we can solve for a_1, a_2 and a_3. Since (3.9) is a system of nonlinear equations, it is often necessary to solve it numerically on a digital computer. Davis and Trick [41] solved this equation using the Newton-Raphson method. However, for this simple example, there exists an analytic solution. We should solve for a_2 first, then a_3 and finally a_1 as follows :

$$a_2 = \frac{-B \pm \sqrt{B^2 - 4AC}}{2A} \qquad (3.13a)$$

$$a_3 = \frac{-D \pm \sqrt{D^2 - 4D - 2A}}{2} \qquad (3.13b)$$

$$a_1 = - D - a_3 \qquad (3.13c)$$

where

$$A = 2 (f_1 - 1) \qquad (3.14a)$$

$$B = f_3 - f_2 - 3(f_1 + 1) \qquad (3.14b)$$

$$C = f_1 + f_2 + f_3 - 1 \qquad (3.14c)$$

$$D = \frac{3 - f_3}{1 - a_2} \qquad (3.14d)$$

The + or - signs in (3.13a,b) must be appropriately chosen so that all of a_1, a_2 and a_3 will be real and positive.

3.3.2 Example 3.1

Consider the design of a third-order Chebyshev lowpass filter with a bandwidth of f_c=11 kHz, a passband ripple of 0.1 dB and a sampling frequency of f_s=100 kHz [41].

From tables [43], we obtain the normalized (Ω_c = 1 r/s) analog transfer function

$$H(s) = \frac{K}{s^3 + 1.93883\, s^2 + 2.62953\, s + 1.63809}$$

with poles located at

$$s_{1n} = -0.96942$$

$$s_{2,3n} = -0.48471 \pm j1.20616$$

The normalized circuit element values are C_{1n}=C_{3n}=1.4328 F and L_{2n}=1.5937 H where n indicates that the numbers are normalized values. The analog bandwidth is calculated using the frequency prewarping formula

$$\Omega_c = \frac{2}{T} \sin \omega_c T/2$$

$$= 2f_s \sin \pi f_c/f_s$$

$$= 67748 \text{ r/s}$$

The s-plane poles can be denormalized by multiplying each of them by Ω_c to yield

$$s_1 = -65676$$

$$s_{2,3} = -32838 \pm j81714$$

The corresponding z-plane poles are derived by applying (3.11) to the above s-plane poles :

$$p_1 = 0.52440$$

$$p_{2,3} = 0.47354 \pm j0.51544$$

Using (3.12), we compute the transfer function coefficients as

$$f_1 = 3.89237 \ , \quad f_2 = -5.72753 \quad \text{and} \quad f_3 = 3.84007$$

Finally, from (3.13) and (3.14), the correct integrator gain constants are evaluated as

$$a_1 = 0.5912 \ , \quad a_2 = 0.5877 \quad \text{and} \quad a_3 = 1.4462$$

The same result can be obtained by solving (3.9) numerically on a digital computer. The starting point for the iteration process is the set of nominal gain constants

$$b_1 = \frac{T}{C_{1n}/\Omega_c} = 0.47284$$

$$b_2 = \frac{T}{L_{2n}/\Omega_c} = 0.42510$$

$$b_3 = \frac{T}{C_{3n}/\Omega_c} = 0.47284$$

3.3.3 Analog Equivalent Circuit of an SC LDI Leapfrog Filter

Davis and Trick's method results in an optimized set of gain constants which is different from the original set. This optimized set of gain constants obviously corresponds to an analog circuit different from the original RLC prototype. The analog equivalent circuit of a third-order all-pole filter is presented in Fig. 3.4.

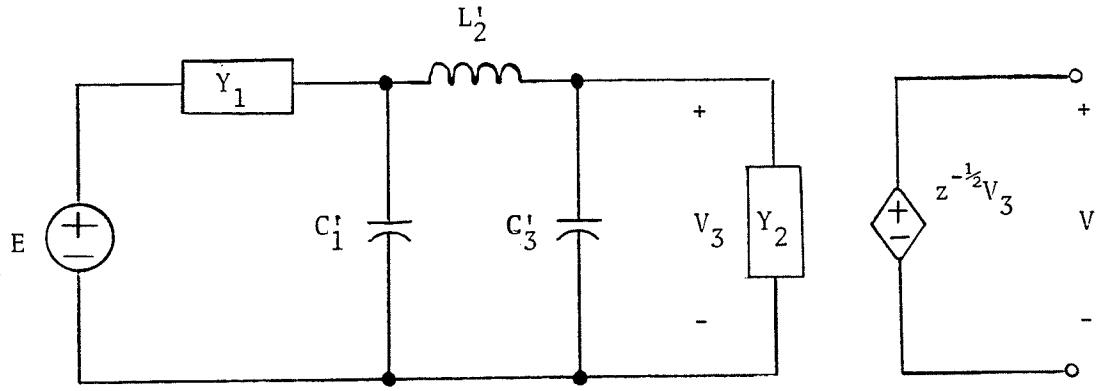

$$Y_1 = G_1 z^{\frac{1}{2}} = z^{\frac{1}{2}}$$

$$Y_2 = G_2 z^{\frac{1}{2}} = z^{\frac{1}{2}}$$

Fig. 3.4 The analog equivalent circuit of a third-order all-pole SC LDI leapfrog filter.

If the above circuit is LDI-transformed, it will lead to a flowgraph similar to that in Fig. 3.3(e). A slight difference exists however : the input branch gain is $-z^{\frac{1}{2}}$ instead of -1, and the output branch gain is $z^{-\frac{1}{2}}$ instead of 1. Since $z^{\frac{1}{2}}$ and $z^{-\frac{1}{2}}$ will cancel each other when the transfer function is derived using Mason's formula, the new SFG can be modified by changing the input branch gain to -1 and the output branch gain to 1. This operation will not affect the transfer function of the SFG. The modified SFG is now topologically identical to the LDI SFG shown in Fig. 3.3(e). The circuit will be the analog equivalent of this optimized SC LDI leapfrog filter if the circuit element values are related to the optimized gain constants by

$$C_1' = \frac{T}{a_1} \quad , \quad L_2' = \frac{T}{a_2} \quad , \quad C_3' = \frac{T}{a_3} \tag{3.15}$$

Note that the minus-half-delay modification has already been incorporated in the equivalent circuit by setting both terminating resistors to $z^{\frac{1}{2}}$.

It follows that a simpler design procedure would be possible if we could start with a nominal analog prototype such as the one shown in Fig. 3.3(a), and then obtain C_1', L_2' and C_3' from C_1, L_2 and C_3, and finally calculate the optimized gain constants a_1, a_2 and a_3 by means of (3.15). In this way, we would not need to solve any nonlinear equations for

the gain constants as suggested by Davis and Trick. Unfortunately, we have been unsuccessful in obtaining C'_1, L'_2 and C'_3 from C_1, L_2 and C_3. Thus far, these element values are obtainable only after the nonlinear equations have been solved numerically for the gain constants.

The equivalent circuit is introduced to help visualize the circuits involved in Davis and Trick's method. It does not simplify the design of SC LDI filters, but it is more useful in the design of BT leapfrog filters.

3.4 REALIZATION OF AN SC LEAPFROG FILTER BASED ON BILINEAR TRANSFORMATION

The design in the previous section is based on the LDI s-to-z transformation. However, it is more desirable to use the BT for the following reasons :

1. The frequency warping effect of the BT is a compression of the analog frequency axis. The corresponding discrete-time filter will have a narrower transition band.
2. The BT maps the entire analog $j\Omega$ -axis onto the unit circle. Thus, if the analog prototype has a transmission zero at $s=\infty$, then the discrete-time filter will maintain this zero at $z=-1$ or $\omega T=\pi$. This cannot occur under the LDI because only the range $-2/T \leq \Omega \leq 2/T$ is mapped onto the unit circle.

To realize an SFG based on the BT, we simply replace all the analog integrators in Fig. 3.2(b) by BT integrators. Un-

fortunately, all BT integrators are either sensitive to parasitic capacitances [44,45], or require extra switches and capacitors (usually equal-valued) [46,47]. From a practical design point of view, these undesirable conditions should be avoided. Hence, proposals have been made that the BT flowgraph be modified in such a way that the parasitic-insensitive LDI integrators be utilized as building blocks [48,49]. This kind of filter will be denoted as a BT/LDI filter. We will review one method[2] and introduce two other methods of designing such BT/LDI filters, and later show that they are in fact equivalent to each other.

3.4.1 Extension to Davis and Trick's Method

In this subsection, we suggest an extension to Davis and Trick's method (denoted as ED&T method) to derive a BT/LDI filter. The design procedure follows basically the same steps described in Subsection 3.3.1. The major difference is that all the frequency prewarping calculations and pole/zero determinations are now based on the BT instead of the LDI.

This method will be illustrated by the third-order elliptic filter shown in Fig. 3.5(a). The corresponding analog and minus-half-delay modified LDI SFGs are shown in Fig. 3.5(b) and (c), respectively. The branch gain constants a_i's are to be determined.

---

[2] Eriksson's method, to be discussed in Subsection 3.4.2.

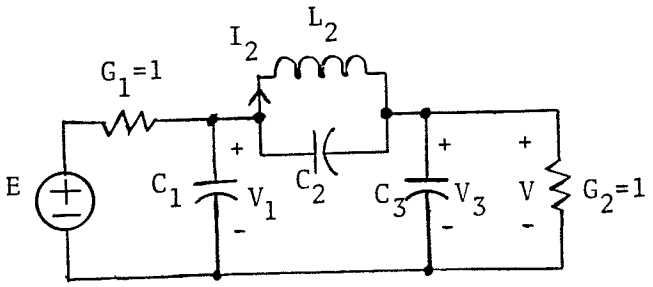

(a) The analog prototype.

$$d_1=\frac{1}{C_1+C_2}$$

$$d_2=\frac{1}{L_2}$$

$$d_3=\frac{1}{C_2+C_3}$$

$$d_4=\frac{C_2}{C_1+C_2}$$

$$d_5=\frac{C_2}{C_2+C_3}$$

Note : $d_5=\frac{d_3 d_4}{d_1}$

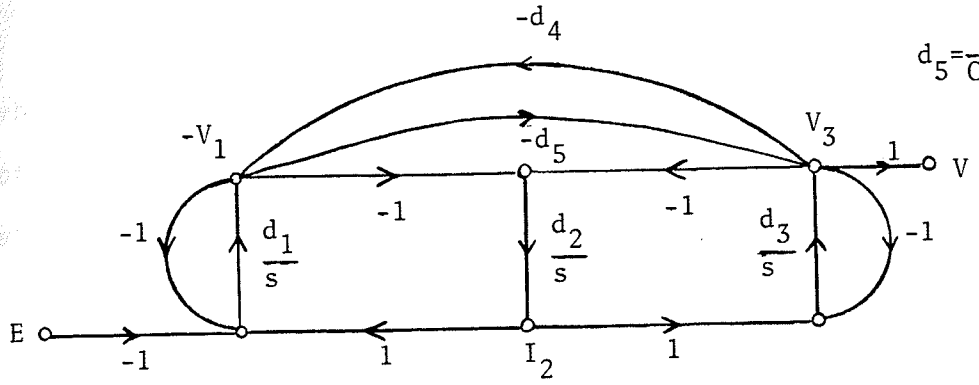

(b) The s-domain SFG.

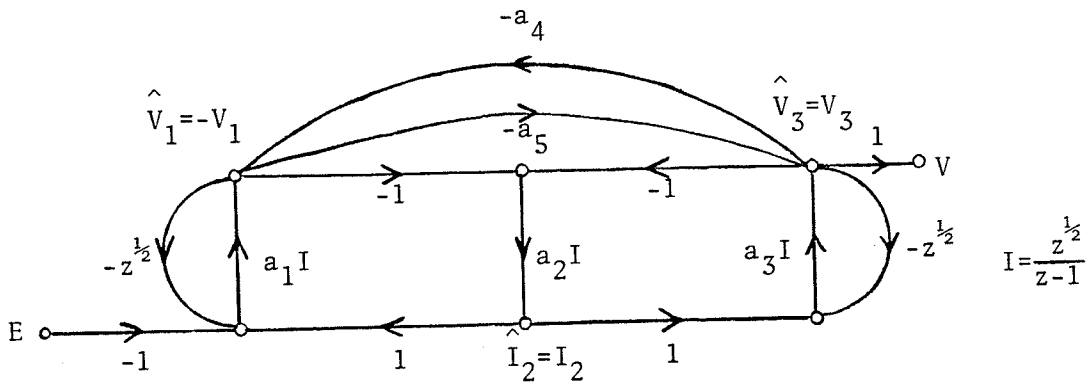

$$I=\frac{z^{\frac{1}{2}}}{z-1}$$

(c) The minus-half-delay modified LDI SFG.

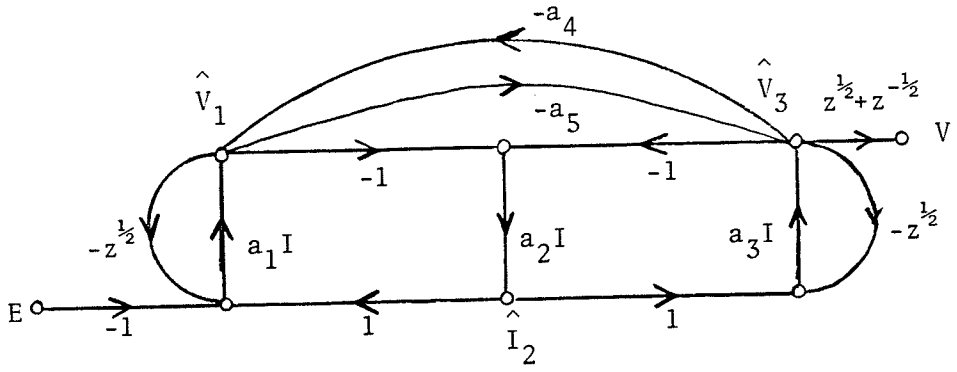

(d) The bilinearly-transformed SFG.

Fig. 3.5 A third-order elliptic filter used to illustrate the ED&T method.

The general transfer function of an analog third-order elliptic filter is

$$H(s) = \frac{K\,(s^2 + c_1)}{s^3 + c_2 s^2 + c_3 s + c_4} \tag{3.16}$$

where K is a scaling factor and c_i's are real positive constants. If the BT is applied to this H(s), then the corresponding discrete-time transfer function is of the form

$$H(z) = \frac{K_1 (z + 1)(z - z_1)(z - z_2)}{(z - p_1)(z - p_2)(z - p_3)} \tag{3.17a}$$

where K_1 is a scaling factor, z_1, z_2 (a complex conjugate pair) are the zeros on the unit circle and p_1, p_2, p_3 are the poles inside the unit circle. Equation (3.17a) can also be written as

$$H(z) = \frac{K_1 (z + 1)(z^2 + \gamma_1 z + 1)}{z^3 + \gamma_2 z^2 + \gamma_3 z + \gamma_4} \tag{3.17b}$$

where

$$\gamma_1 = - z_1 - z_2 \tag{3.18a}$$

$$\gamma_2 = - p_1 - p_2 - p_3 \tag{3.18b}$$

$$\gamma_3 = p_1 p_2 + p_1 p_3 + p_2 p_3 \tag{3.18c}$$

$$\gamma_4 = - p_1 p_2 p_3 \tag{3.18d}$$

Note that the z-domain zeros and poles are obtained from their analog counterparts using the BT formula

$$z = \frac{1 + \frac{sT}{2}}{1 - \frac{sT}{2}} \tag{3.19}$$

With Mason's formula, the transfer function of the flow-graph in Fig. 3.5(c) is determined to be

$$\frac{V}{E} = \frac{K_2 \, z^{\frac{1}{2}} \, (z^2 + \beta_1 z + 1)}{z^3 + \beta_2 z^2 + \beta_3 z + \beta_4} \tag{3.20}$$

where

$$\beta_1 = \frac{a_2 a_3}{a_5} - 2 \tag{3.21a}$$

$$\beta_2 = \frac{(a_2-2)(a_1+a_3+2a_1a_3) - a_2(a_1a_5+a_3a_4) + 3(a_1a_3+a_4a_5-1)}{(a_1+1)(a_3+1) - a_4a_5} \tag{3.21b}$$

$$\beta_3 = \frac{(a_1+a_3)(1-a_2) + a_2(a_1a_5+a_3a_4) - 3(a_4a_5-1)}{(a_1+1)(a_3+1) - a_4a_5} \tag{3.21c}$$

$$\beta_4 = \frac{a_4 a_5 - 1}{(a_1+1)(a_3+1) - a_4 a_5} \qquad (3.21d)$$

and

$$K_2 = \frac{a_1 a_5}{(a_1+1)(a_3+1) - a_4 a_5} \qquad (3.22)$$

K_2 is the scaling factor of the filter.

Comparing (3.17b) and (3.20), we notice that if $K_1 = K_2$ and $\gamma_i = \beta_i$, then H(z) can indeed be realized by V/E, provided that V/E is multiplied by a gain factor $(z^{\frac{1}{2}}+z^{-\frac{1}{2}})$. This multiplication is equivalent to multiplying the output branch of the flowgraph by the above gain factor. With this modification (shown in Fig. 3.5(d)), the analog filter is bilinearly-transformed but the building blocks of the SC filter are LDI integrators.

Note that there are five equations (i.e. (3.21a-d) and (3.22)) in five unknowns. Sometimes, we may decide not to let the integrator gain constants determine the scaling factor of the filter (see Appendix A). If this is the case, (3.22) is no longer a constraint equation and there will be one extra degree of freedom. This extra degree of freedom allows us to reduce the example to a 4-variable problem by

introducing a suitable constraint equation. We suggest the following constraint :

$$a_5 = \frac{a_3 a_4}{a_1} \tag{3.23}$$

because in the s-domain the equality $d_5 = d_3 d_4 / d_1$ must hold. A different argument will be given later. Substituting (3.23) into (3.21), we obtain the set of nonlinear equations which can be solved for the a_i's :

$$\beta_1 = \frac{a_1 a_2}{a_4} - 2 \tag{3.24a}$$

$$\beta_2 = \frac{(a_2-2)(a_1+a_3+2a_1a_3)-2a_2a_3a_4+3(a_1a_3-1+a_3a_4^2/a_1)}{(a_1+1)(a_3+1) - a_3a_4^2/a_1} \tag{3.24b}$$

$$\beta_3 = \frac{(a_1+a_3)(1-a_2)+2a_2a_3a_4+3(1-a_3a_4^2/a_1)}{(a_1+1)(a_3+1) - a_3a_4^2/a_1} \tag{3.24c}$$

$$\beta_4 = \frac{a_3a_4^2/a_1 - 1}{(a_1+1)(a_3+1) - a_3a_4^2/a_1} \tag{3.24d}$$

3.4.1.1 Example 3.2

Consider the analog network shown in Fig. 3.5(a) where the normalized element values are

$$C_{1n} = C_{3n} = 1.08546 \text{ F}$$

$$C_{2n} = .146580 \text{ F}$$

$$L_{2n} = 1.00896 \text{ H}$$

and the normalized zeros and poles are

zeros : $\pm j2.60032$

poles : $- 0.92127$

$- 0.36268 \pm j1.14294$

We want to realize an SC leapfrog filter based on this network and the BT. The cutoff frequency is to be 3.4 kHz, and the sampling rate is to be 128 kHz.

First, we compute the prewarped cutoff frequency

$$\Omega_c = \frac{2}{T} \tan \frac{\pi f_c}{f_s}$$

$$= 21412.56 \text{ r/s}$$

The denormalized s-plane zeros and poles are then

zeros : $\pm j55679$

poles : $- 19727$

$- 7765.9 \pm j24473$

The corresponding z-plane zeros and poles are

$$z_{1,2} = 0.90966 \pm j0.41535$$

$$p_1 = 0.85691$$

$$p_{2,3} = 0.92455 \pm j0.17857$$

The transfer function coefficients are computed as

$$\gamma_1 = -1.81932 \qquad \gamma_2 = -2.70600$$

$$\gamma_3 = 2.47118 \qquad \gamma_4 = -0.75980$$

Equating $\beta_i = \gamma_i$, we set up the nonlinear equations in (3.24). A user routine called ZSCNT (available from the University of Manitoba computer library) is used to solve this system of equations. The starting point is the set of original gain constants

$$b_1 = \frac{T}{(C_{1n}+C_{2n})/\Omega_c} = 0.13578$$

$$b_2 = \frac{T}{L_{2n}/\Omega_c} = 0.16580$$

$$b_3 = \frac{T}{(C_{2n}+C_{3n})/\Omega_c} = 0.13578$$

$$b_4 = \frac{C_{2n}}{(C_{1n}+C_{2n})} = 0.11897$$

$$b_5 = \frac{C_{2n}}{(C_{2n}+C_{3n})} = 0.11897$$

The solution is found to be

$$a_1 = 0.14480$$

$$a_2 = 0.16580$$

$$a_3 = 0.14479$$

$$a_4 = 0.13288$$

$$a_5 = 0.13287$$

If constraints other than the one in (3.23) are used, different answers can be expected. For example, if $a_4 = a_5$, then we obtain

$$a_1 = 0.14467$$

$$a_2 = 0.16583$$

$$a_3 = 0.14491$$

$$a_4 = 0.13300$$

$$a_5 = 0.13300$$

Or, if $a_1 = a_3$, we obtain

$$a_1 = 0.14478$$

$$a_2 = 0.16586$$

$$a_3 = 0.14478$$

$$a_4 = 0.13345$$

$$a_5 = 0.13291$$

3.4.2 Eriksson's Flowgraph Conversion Method

Eriksson [49] showed that by beginning with an SFG that uses bilinear integrators, it is possible to manipulate the flowgraph so that the building blocks will be LDI integrators. Since the derivation of Eriksson's method is more complicated than the ED&T method, a third-order filter may not provide enough insight into the procedure. Thus, a fifth-order elliptic filter is chosen as an example in reviewing Eriksson's method.

We start with the s-domain SFG in Fig. 3.2(a) or (b). Applying the BT to the integrators results in the z-domain BT SFG shown in Fig. 3.6(a). Note that there are no termination problems as in the LDI case. Using the identity

$$\frac{z+1}{z-1} = \frac{z+1}{2z}\,\frac{2z}{z-1} \tag{3.25}$$

we redraw Fig. 3.6(a) as Fig. 3.6(b).

Using the identities

$$\frac{z+1}{2z} = 1 - \frac{z-1}{2z} \tag{3.26}$$

and

$$\frac{(z+1)^2}{2z(z-1)} = \frac{2}{z-1} + \frac{z-1}{2z} \tag{3.27}$$

we redraw Fig. 3.6(b) as Fig. 3.6(c).

$b_i = d_i T/2$, $i=1,2,\ldots,5$; $b_i = d_i$, $i=6,7,8,9$ (for d_i, see Fig. 3.2)

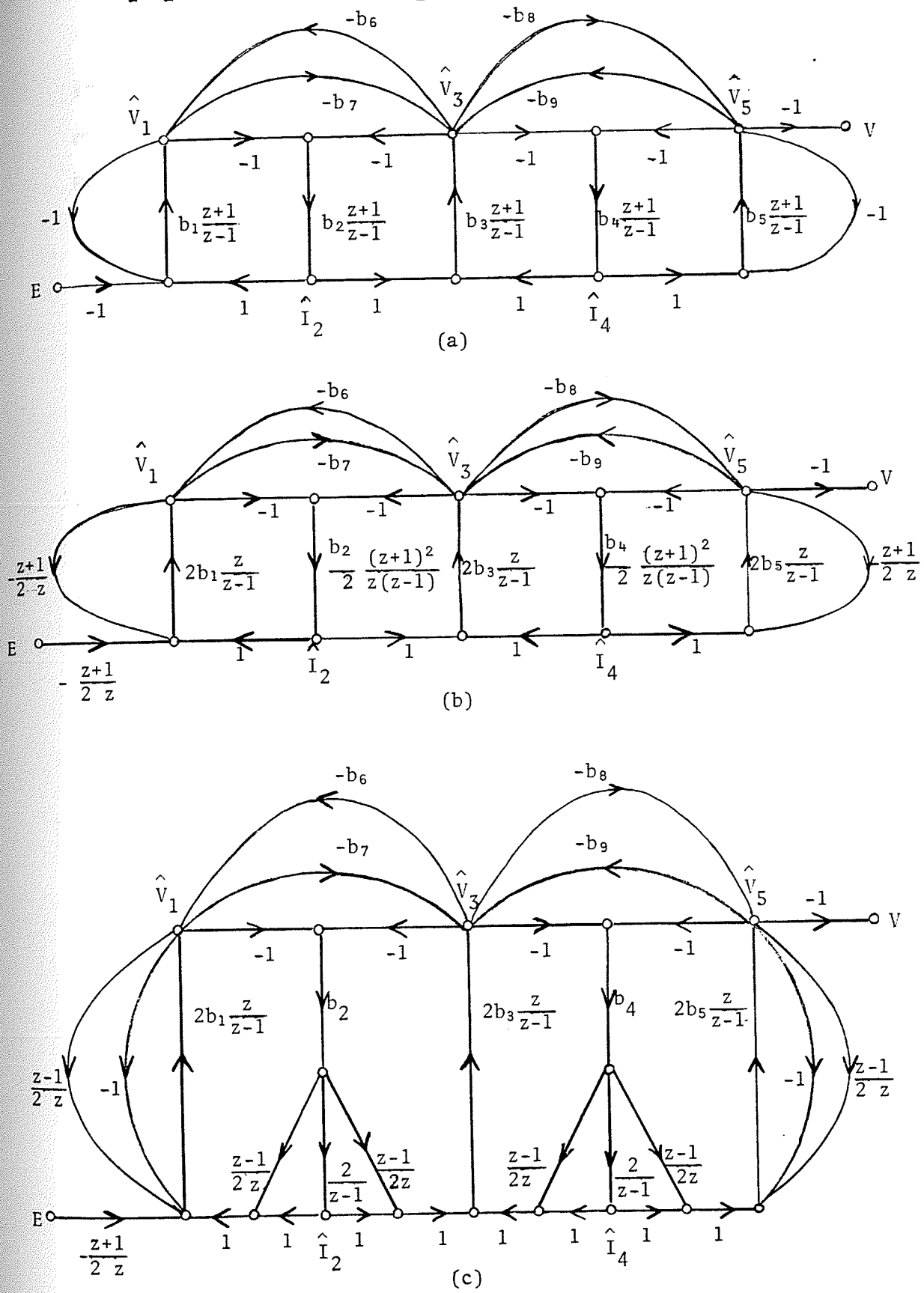

Fig. 3.6 Eriksson's flowgraph conversion steps.

With more manipulation, we simplify Fig. 3.6(c) as shown in Fig. 3.6(d). To further reduce the flowgraph, we write out the flow equations at nodes $\hat{V}_1$, $\hat{V}_3$ and $\hat{V}_5$, respectively. For instance, at node $\hat{V}_5$,

$$\begin{aligned}\hat{V}_5 &= 2b_5 \frac{z}{z-1}(\hat{I}_4 - \hat{V}_5 + \frac{1-b_4}{2}\frac{z-1}{z}\hat{V}_5) - (b_8+b_4b_5)\hat{V}_3 \\ &= \frac{2b_5}{1-b_5+b_4b_5}\frac{z}{z-1}(\hat{I}_4 - \hat{V}_5) - \frac{b_8+b_4b_5}{1-b_5+b_4b_5}\hat{V}_3\end{aligned} \tag{3.28}$$

There will be similar results for nodes $\hat{V}_1$ and $\hat{V}_3$. We use these simplified flow equations to redraw Fig. 3.6(d) as Fig. 3.6(e). The branch gain constants a_i's are defined as

$$a_1 = \frac{2b_1}{1 - b_1 + b_1b_2} \qquad a_6 = \frac{b_6 + b_1b_2}{1 - b_1 + b_1b_2}$$

$$a_2 = 2\ b_2 \qquad a_7 = \frac{b_7 + b_2b_3}{1 + b_2b_3 + b_3b_4}$$

$$a_3 = \frac{2b_3}{1 + b_2b_3 + b_3b_4} \qquad a_8 = \frac{b_8 + b_4b_5}{1 - b_5 + b_4b_5} \tag{3.29}$$

$$a_4 = 2\ b_4 \qquad a_9 = \frac{b_9 + b_3b_4}{1 + b_2b_3 + b_3b_4}$$

$$a_5 = \frac{2b_5}{1 - b_5 + b_4b_5}$$

Equivalently, the a_i's can be determined directly from the circuit element values by the following formulae :

$$a_1 = \frac{4L_2T}{4L_2(C_1+C_2) - 2L_2T + T^2}$$

$$a_2 = \frac{T}{L_2}$$

$$a_3 = \frac{4L_2L_4T}{4L_2L_4(C_2+C_3+C_4) + T^2(L_2+L_4)}$$

$$a_4 = \frac{T}{L_4} \qquad (3.30)$$

$$a_5 = \frac{4L_4T}{4L_4(C_4+C_5) - 2L_4T + T^2}$$

$$a_6 = \frac{4L_2C_2 + T^2}{4L_2(C_1+C_2) - 2L_2T + T^2}$$

$$a_7 = \frac{4L_2L_4C_2 + T^2L_4}{4L_2L_4(C_2+C_3+C_4) + T^2(L_2+L_4)}$$

$$a_8 = \frac{4L_4C_4 + T^2}{4L_4(C_4+C_5) - 2L_4T + T^2}$$

$$a_9 = \frac{4L_2L_4C_4 + T^2L_2}{4L_2L_4(C_2+C_3+C_4) + T^2(L_2+L_4)}$$

Note that the building blocks in the SFG are BD and FD integrators (see (2.9) and (2.10)). We now modify this Eriksson's SFG[3] and obtain a flowgraph with only LDI integrators by using the identity $\frac{z}{z-1} = \frac{z^{\frac{1}{2}}}{z-1} \cdot z^{\frac{1}{2}}$. The final flowgraph is shown in Fig. 3.6(f) where the input gain factor $\frac{1}{2}(z^{\frac{1}{2}} + z^{-\frac{1}{2}})$ has been moved to the output branch (this will not make any difference as far as the transfer function is concerned).

Note that for an all-pole filter, $C_2=C_4=0$ and $b_6=b_7=b_8=b_9=0$. Under the LDI, the SFG will not contain any direct paths between $\hat{V}_1$ and $\hat{V}_3$, as well as between $\hat{V}_3$ and $\hat{V}_5$. However, for a BT/LDI flowgraph, despite $b_6=b_7=b_8=b_9=0$, the gain constants a_6, a_7, a_8 and a_9 will not be zero; therefore, all the aforementioned paths exist. Thus, a BT/LDI all-pole filter has the same SFG topology as a BT/LDI elliptic filter of the same order. This property is very useful if the filter is intended to be programmable.

---

[3] The connection of one BD integrator and one FD integrator in a loop is equivalent to the connection of two LDI integrators in a loop. Thus Eriksson's SFG can be considered as composed of the LDI integrators too.

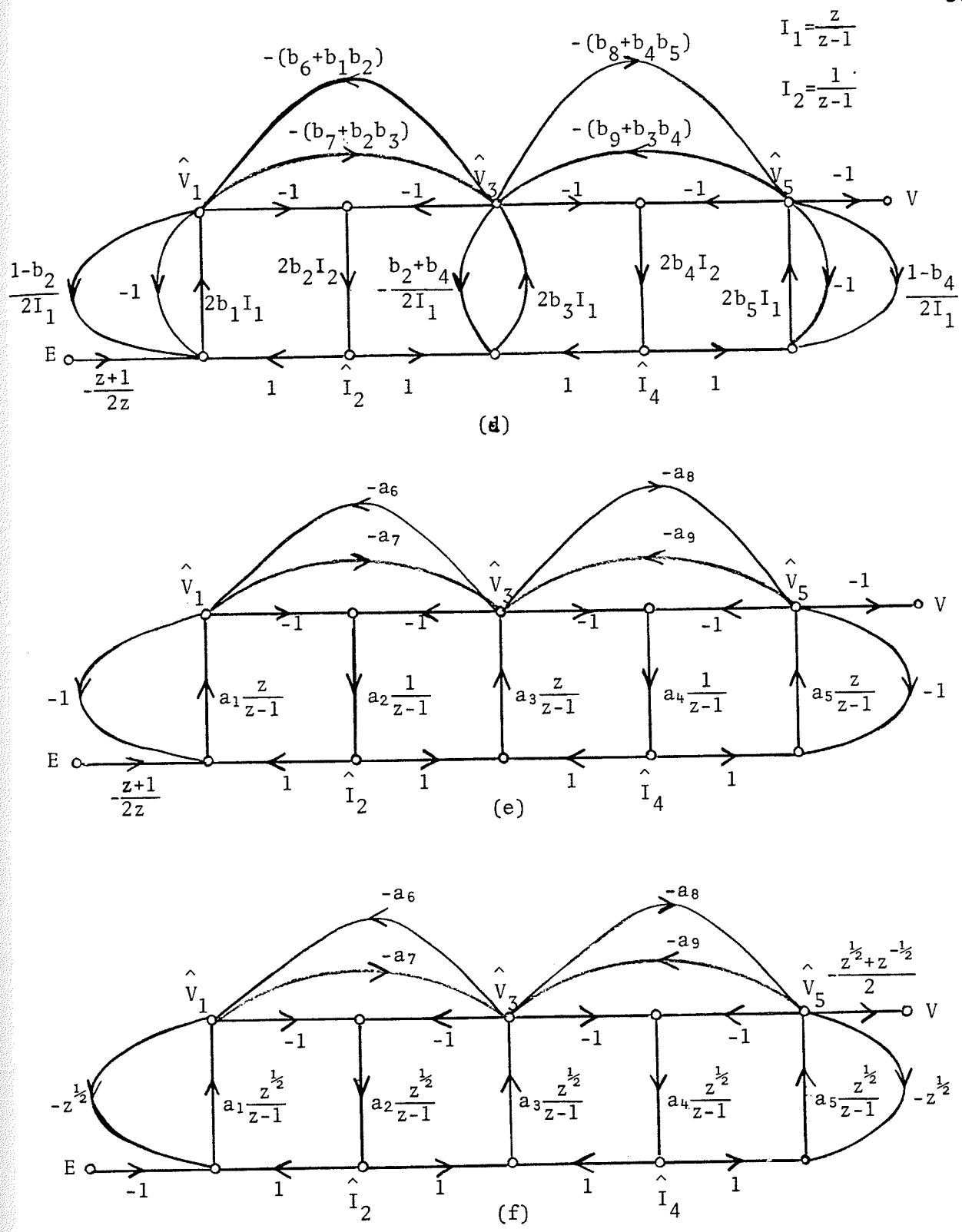

Fig. 3.6 (cont'd) Eriksson's flowgraph conversion steps.

3.4.3 Analog Equivalent Circuit Method

In Subsection 3.3.3, we derived the analog equivalent circuit of an SC LDI leapfrog filter designed with Davis and Trick's method. We will now present the analog equivalent circuit of an SC BT/LDI leapfrog filter based on the results of Eriksson's method. This equivalent circuit provides a new design procedure.

A fifth-order elliptic LDI SFG is shown in Fig. 3.7. The difference between this LDI SFG and the BT/LDI SFG shown in Fig. 3.6(f) is in the output branches which have different gains of -1 and $-\frac{1}{2}(z^{\frac{1}{2}} + z^{-\frac{1}{2}})$, respectively. Although the BT/LDI SFG is derived from a certain analog prototype N via the BT, its similarity to the LDI SFG suggests that it can indeed be obtained from some analog circuit N' that will be transformed via the LDI. The above concept is illustrated in Fig. 3.8(a). The circuit N, which will be bilinearly-transformed, is shown in Fig. 3.8(b). The circuit N', which will be LDI-transformed, is shown in Fig. 3.8(c).

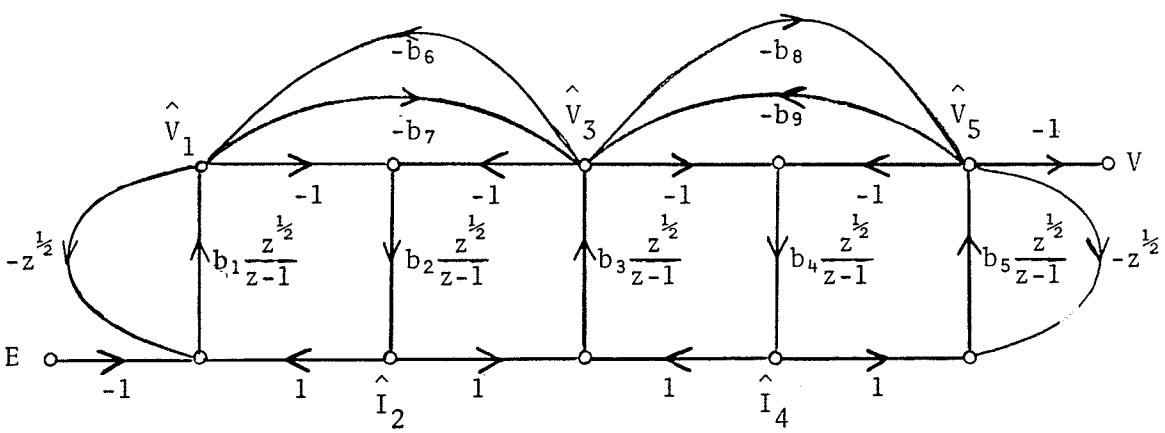

$b_i = d_i T$, $i=1,2,\ldots,5$; $b_i = d_i$, $i=6,7,8,9$

(for d_i , see Fig. 3.2)

Fig. 3.7 A fifth-order elliptic LDI SFG.

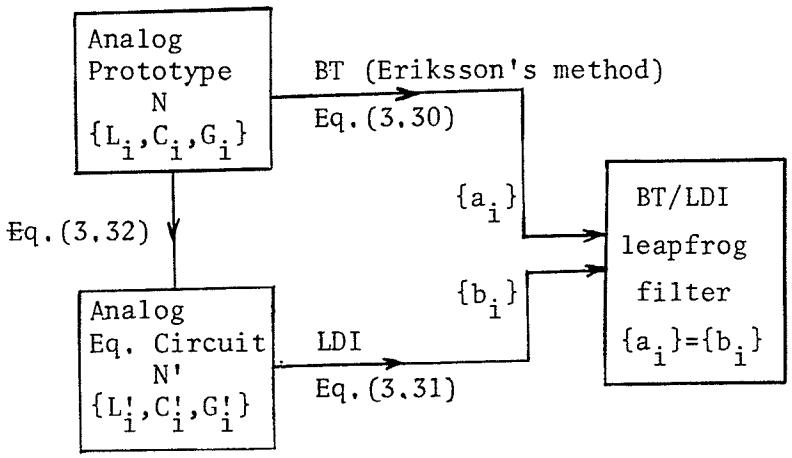

(a)

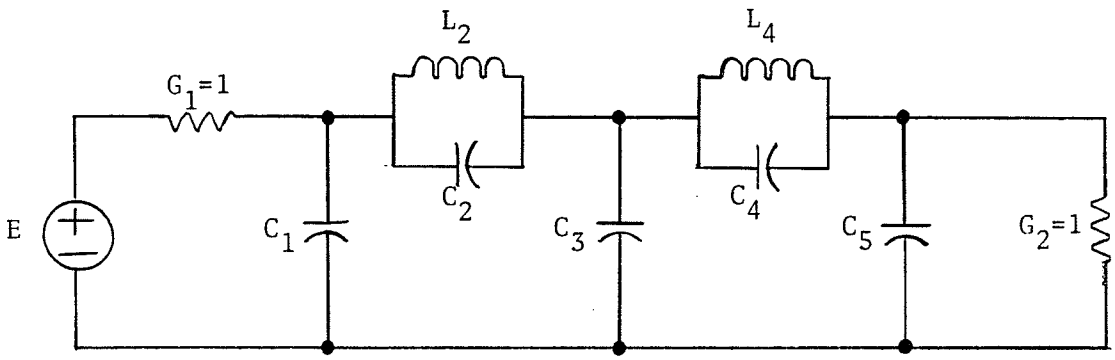

(b)

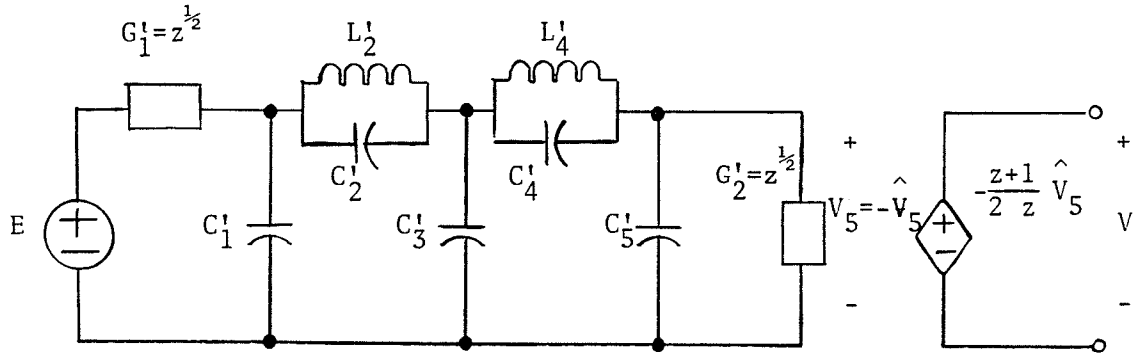

(c)

Fig. 3.8 (a) The relationship between Eriksson's method and the equivalent circuit method.

(b) The analog prototype N.

(c) The analog equivalent circuit N'.

With Eriksson's method, the first circuit leads to a BT/LDI SFG such as the one shown in Fig. 3.6(f). The gain constants are given by (3.29) or (3.30).

If the second circuit is transformed via the LDI, then the corresponding minus-half-delay SFG is shown in Fig. 3.9. The gain constants are given by

$$
\begin{aligned}
b_1 &= \frac{T}{C_1' + C_2'} & b_6 &= \frac{C_2'}{C_1' + C_2'} \\
b_2 &= \frac{T}{L_2'} & b_7 &= \frac{C_2'}{C_2' + C_3' + C_4'} \\
b_3 &= \frac{T}{C_2' + C_3' + C_4'} & b_8 &= \frac{C_4'}{C_4' + C_5'} \\
b_4 &= \frac{T}{L_4'} & b_9 &= \frac{C_4'}{C_2' + C_3' + C_4'} \qquad (3.31) \\
b_5 &= \frac{T}{C_4' + C_5'}
\end{aligned}
$$

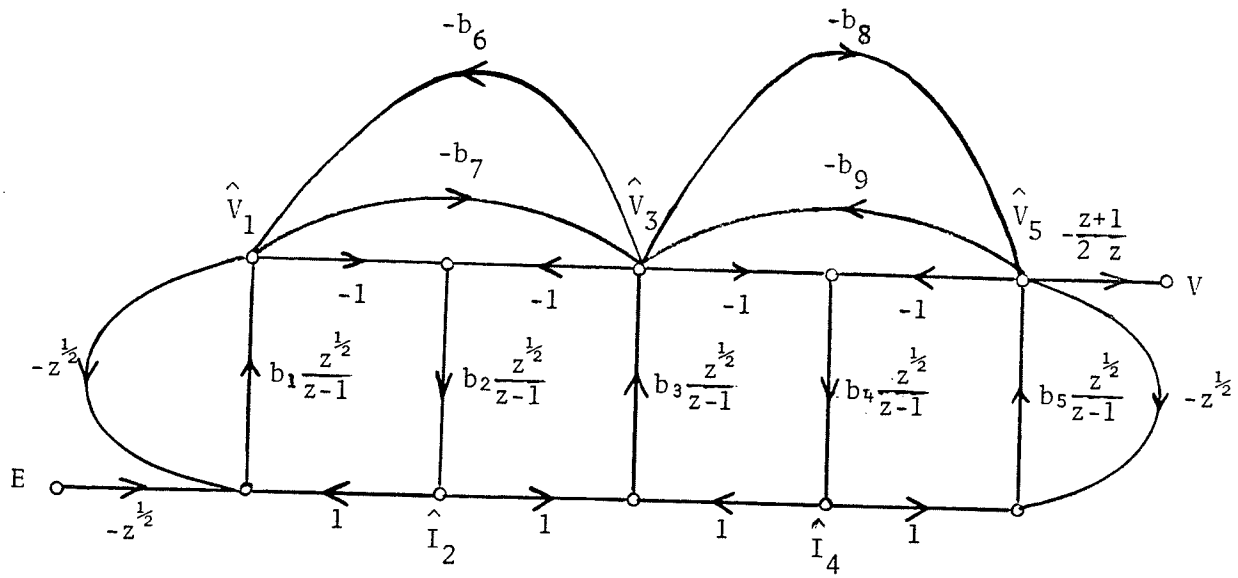

Fig. 3.9 The LDI SFG of the circuit N' in Fig. 3.8(c).

If the input branch gain $z^{\frac{1}{2}}$ of the SFG in Fig. 3.9 is shifted into the output branch, then the new input and output branches will be -1 and $-\frac{1}{2}(z^{\frac{1}{2}} + z^{-\frac{1}{2}})$, respectively. This new SFG will then be identical to that in Fig. 3.6(f). In other words, the two circuits in Fig. 3.8 will give the same SFGs (i.e. BT/LDI SFG) even though one is transformed via the BT and the other via the LDI. It follows that if the circuit in Fig. 3.8(b) is the analog prototype of the BT/LDI filter shown in Fig. 3.6(f), then the circuit in Fig. 3.8(c) will be the equivalent circuit of the BT/LDI filter.

Unlike the case for LDI filters in Subsection 3.3.3, we can now derive the relationships between the element values of the nominal prototype N and the equivalent circuit N'. Equating the gain constants a_i and b_i for i=1,2,...,9, we obtain

$$
\begin{aligned}
C_1' &= C_1 - \frac{T}{2} & L_2' &= L_2 \\
C_2' &= C_2 + \frac{T^2}{4L_2} & L_4' &= L_4 \\
C_3' &= C_3 \\
C_4' &= C_4 + \frac{T^2}{4L_4} \\
C_5' &= C_5 - \frac{T}{2}
\end{aligned}
\qquad (3.32)
$$

In summary, this design procedure starts with the nominal analog filter N, and next the equivalent circuit N' with the element values given by (3.32) is obtained. This equivalent

circuit is then transformed via the LDI into an SC filter. The resulting SC circuit is the desired BT/LDI SC filter for the original prototype. The gain constants of this BT/LDI SFG are given by the simple formulae in (3.31).

It is interesting to note that formulae similar to (3.32) have been obtained by Lee and Chang [48] and Lee et al.[50] using the concepts of discrete-time impedances and charge-voltage relationships for the RLC circuit elements.

The result of (3.32) can be generalized to an odd M-th order filter shown in Fig. 3.10(a). The corresponding analog equivalent circuit is shown in Fig. 3.10(b).

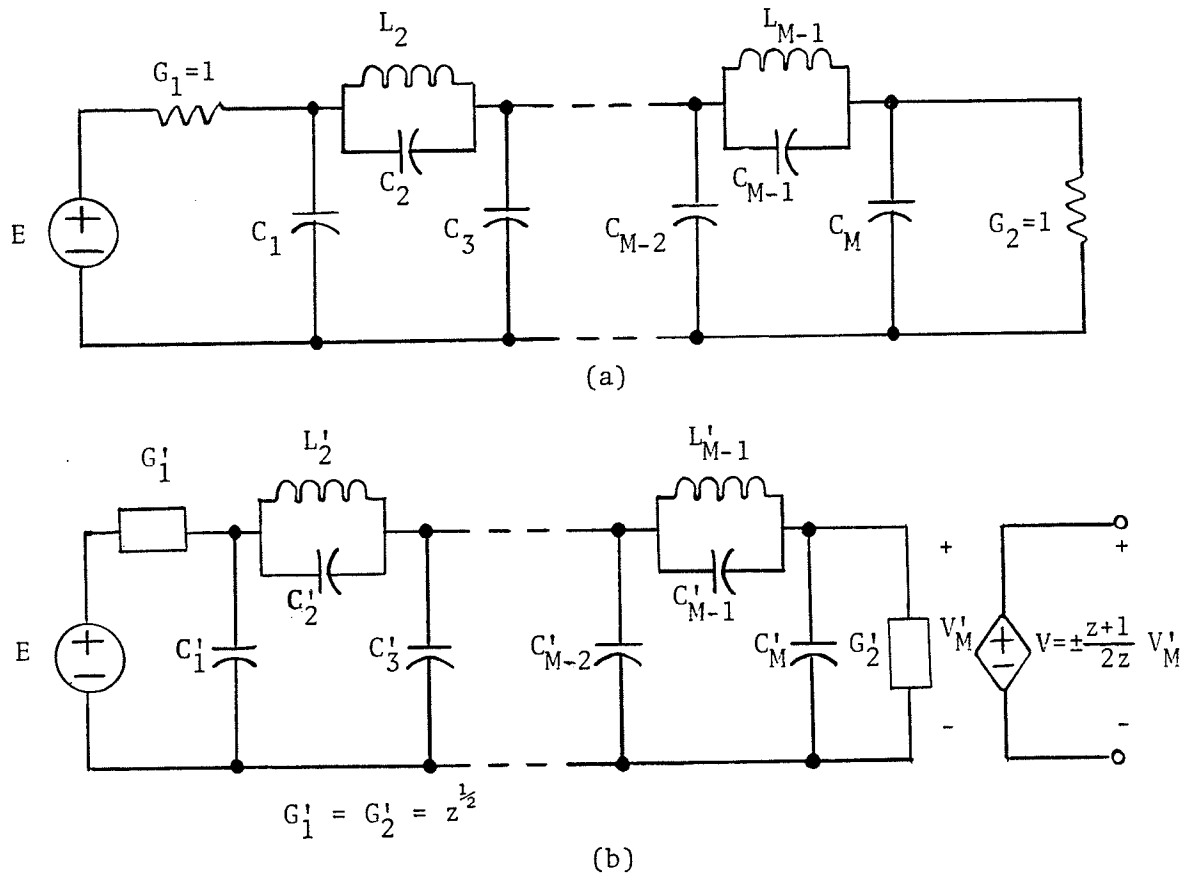

Fig. 3.10 (a) An odd M-th order elliptic filter.
(b) The corresponding analog equivalent circuit.

The modified reactive element values are given by

$$C_1' = C_1 - \frac{T}{2}$$

$$C_i' = C_i \qquad i = 3,5,\ldots,M-2$$

$$\left.\begin{aligned} L_i' &= L_i \\ C_i' &= C_i + \frac{T^2}{4L_i} \end{aligned}\right\} \qquad i = 2,4,\ldots,M-1 \qquad (3.33)$$

$$C_M' = C_M - \frac{T}{2}$$

The corresponding gain constants of the SFG are

$$b_i = \frac{T}{C_{i-1}' + C_i' + C_{i+1}'} \qquad i = 1,3,\ldots,M$$

$$b_i = \frac{T}{L_i'} \qquad i = 2,4,\ldots,M-1$$

$$\left.\begin{aligned} b_{M+2i-1} &= \frac{C_{2i}'}{C_{2i-2}' + C_{2i-1}' + C_{2i}'} \\ b_{M+2i} &= \frac{C_{2i}'}{C_{2i}' + C_{2i+1}' + C_{2i+2}'} \end{aligned}\right\} \qquad i = 1,3,\ldots,\frac{M-1}{2} \text{ or } \frac{M-3}{2} \qquad (3.34)$$

$$\left.\begin{aligned} b_{M+2i-1} &= \frac{C_{2i}'}{C_{2i}' + C_{2i+1}' + C_{2i+2}'} \\ b_{M+2i} &= \frac{C_{2i}'}{C_{2i-2}' + C_{2i-1}' + C_{2i}'} \end{aligned}\right\} \qquad i = 2,4,\ldots,\frac{M-1}{2} \text{ or } \frac{M-3}{2}$$

where

$$C_0' \triangleq 0 \quad \text{and} \quad C_{M+1}' \triangleq 0$$

3.4.4 Equivalence Among the Three Methods

In the previous subsection, we have shown the relationship between Eriksson's method and the equivalent circuit method. In this subsection, we will show the equivalence between the ED&T method and Eriksson's method.

The SFG in Fig. 3.5(d) can be extended to a fifth-order elliptic filter. The resulting SFG is similar to the one shown in Fig. 3.6(f), except that the output branch gains will differ by a constant of 1/2. Since an SFG filter can always be amplitude-scaled by varying the input branch gain constant, a difference of 1/2 is irrelevant. The similarity between the two configurations suggests that there must exist a solution common to both methods (viz the ED&T and Eriksson's methods). Recall that there are several valid sets of gain constants, under different constraints, for the ED&T method. However, there is only one set for Eriksson's method. Nevertheless, the two methods will produce the same results and thus will be equivalent if we choose the proper constraints for the ED&T method.

To conclude, we have shown the equivalence among the three methods of realizing a BT/LDI SC filter, i.e. all three methods will produce the same results. This fact can be observed in the following example.

3.4.4.1 Example 3.3

The specifications are the same as those given in Example 3.2, except Eriksson's and the equivalent circuit methods will be used this time.

Eriksson's Method

The normalized element values have been given in Example 3.2. After denormalization by Ω_c=21412.56 r/s, these element values become

$$C_1 = C_3 = 5.06924 \times 10^{-5} \text{ F}$$

$$C_2 = 6.84552 \times 10^{-6} \text{ F}$$

$$L_2 = 4.71198 \times 10^{-5} \text{ H}$$

The final gain constants a_i's are calculated as

$$a_1 = \frac{4L_2T}{4L_2(C_1+C_2) - 2L_2T + T^2} = 0.14480$$

$$a_2 = \frac{T}{L_2} = 0.16580$$

$$a_3 = \frac{4L_2T}{4L_2(C_2+C_3) - 2L_2T + T^2} = 0.14480$$

$$a_4 = \frac{4L_2C_2 + T^2}{4L_2(C_1+C_2) - 2L_2T + T^2} = 0.13287$$

$$a_5 = \frac{4L_2C_2 + T^2}{4L_2(C_2+C_3) - 2L_2T + T^2} = 0.13287$$

The result is exactly the same as that obtained in Example 3.2 by the ED&T method (under the constraint $a_1a_5=a_3a_4$).

Equivalent Circuit Method

Using (3.33), we modify the element values as

$$C_1' = C_1 - \frac{T}{2} = 4.67864 \times 10^{-5} \text{ F}$$

$$C_2' = C_2 + \frac{T^2}{4L_2} = 7.16934 \times 10^{-6} \text{ F}$$

$$C_3' = C_3 - \frac{T}{2} = 4.67864 \times 10^{-5} \text{ F}$$

$$L_2' = L_2 = 4.71198 \times 10^{-5} \text{ H}$$

The gain constants of the BT/LDI SFG are then evaluated as

$$b_1 = \frac{T}{C_1' + C_2'} = 0.14479$$

$$b_2 = \frac{T}{L_2'} = 0.16580$$

$$b_3 = \frac{T}{C_2' + C_3'} = 0.14479$$

$$b_4 = \frac{C_2'}{C_1' + C_2'} = 0.13287$$

$$b_5 = \frac{C_2'}{C_2' + C_3'} = 0.13287$$

These values are the same as those obtained by the ED&T method and Eriksson's method.

Eriksson's method and the equivalent circuit method allow us to use explicit formulae instead of nonlinear equations to obtain the correct gain constants, and it is easy to extend these formulae to higher-order filters. Therefore, from now on either one of these methods will be used for designing BT/LDI SC leapfrog filters. The physical implementation of the SFG with SC components will be discussed in Chapter V.

Chapter IV

PRACTICAL DESIGN CONSIDERATIONS

The design of an SC filter can be improved further with respect to the design vaules in the SFG in Fig. 3.6(f). There are some aspects that can be optimized : such as, minimizing the number of op amps, the total capacitance and the passband ripple; and maximizing the dynamic range and the minimum attenuation in the stopband. We should perform these optimizations under the assumption that the final design will satisfy the specifications. Moreover, before the design is implemented, a sensitivity study should be carried out to estimate the allowable tolerance of the filter components.

In this chapter, each of the aforementioned optimization criteria will be discussed. The objective function for an optimization program will be described. The single- and multi-parameter sensitivities of the SC filter will also be investigated.

4.1 NUMBER OF OP AMPS

The output branch of the SFG in Fig. 3.6(f) requires a gain function of $-\frac{1}{2}(z^{\frac{1}{2}} + z^{-\frac{1}{2}})$. This gain function is noncausal and thus unrealizable. However, we can multiply the function by half a delay period (i.e. $z^{-\frac{1}{2}}$) to obtain a new

gain function of $-\frac{1}{2}(1+z^{-1})$. Note that this replacement will not change the magnitude characteristic of the filter. The new gain function can be realized by the circuit [23,49] shown in Fig. 4.1.

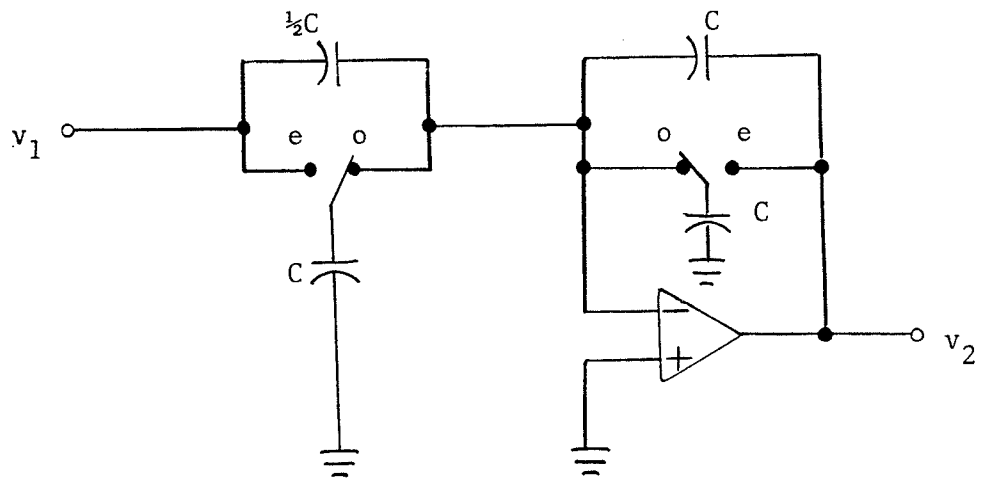

Fig. 4.1 An SC circuit that realizes a gain of $-\frac{1}{2}(1+z^{-1})$.

This circuit is sensitive to parasitic capacitances, and it requires a few capacitors and switches and an op amp that consumes power. We propose omitting the output branch of the SFG and taking $\hat{V}_5$ as the output so that the above circuit is not needed. The filter so realized is canonic in the number of op amps (i.e., an M-th order filter now requires only M op amps — one op amp for each integrator).

The removal of the output branch does not cause any significant change in the frequency response in the passband. However, there is typically a reduction in attenuation in the stopband; in fact, any transmission zero at $z=-1$ or $\omega T=\pi$ will vanish. Usually, the specifications are given in the form of a tolerance scheme such as the one shown in Fig. 4.2. Hence, if the new transfer function (i.e. $\hat{V}_5/E$) satisfies the specifications, then the output branch can simply be discarded; otherwise, an optimization is needed.

Note that the removal of the output branch eliminates the dependent source in Fig. 3.8(c) and the output voltage is now taken directly from the RLC network.

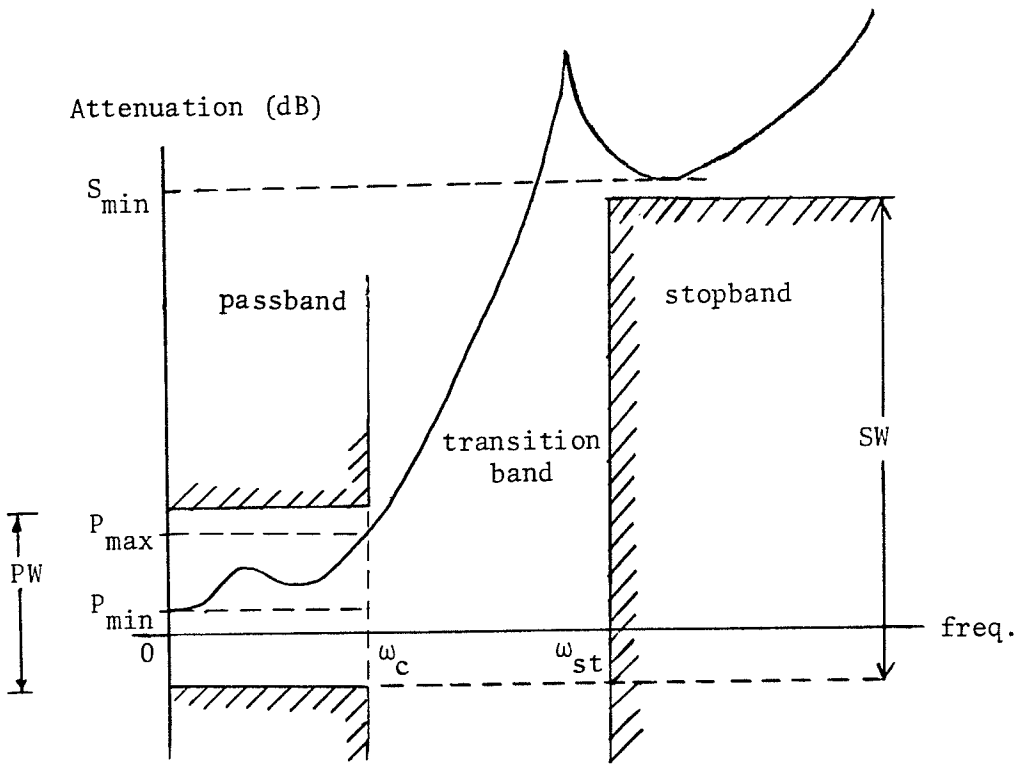

Fig. 4.2 A typical tolerance scheme, and a frequency response that satisfies the specifications.

4.2 DYNAMIC RANGE

By dynamic range is meant the range of input signal levels that the filter can accomodate without producing a distorted output [19]. The maximum signal levels in an SC filter are determined by the saturation levels and slew rates of the op amps. The minimum signal levels are limited by the system noise [19].

In an SC leapfrog filter, the signal levels of various nodes of the SFG may vary considerably. For example, Fig. 4.3(a) shows the responses of the three internal nodes of the SFG in Fig. 3.3(e) where the gain constants are $a_1=0.5912$, $a_2=0.5877$ and $a_3=1.4462$ (see Example 3.1). These magnitude responses are computed from their corresponding transfer functions with Mason's formula :

$$\frac{\hat{V}_1}{E} = \frac{-a_1 z^{\frac{1}{2}} [z^2(1+a_3) + z(a_2a_3-a_3-2) + 1]}{D} \tag{4.1}$$

$$\frac{\hat{I}_2}{E} = \frac{a_1a_2\, z\, [z(1+a_3) - 1]}{D} \tag{4.2}$$

$$\frac{\hat{V}_3}{E} = \frac{a_1a_2a_3\, z^{3/2}}{D} \tag{4.3}$$

where $$D = z^3[(a_1+1)(a_3+1)] + z^2[(a_1+a_3)(a_2-2)+a_1a_3(2a_2-1)-3] + z[(a_1+a_3)(1-a_2)+3] - 1$$

From Fig. 4.3(a), it can be seen that at a particular frequency, one op amp may have a very high gain whereas other op amps may have relatively small gains. Thus, it is pos-

sible for one op amp to saturate while other op amps have relatively small signal levels. Nevertheless, the maximum allowable input signal level is determined by the first mentioned op amp although the other op amps may not be required to accomodate signal levels that come even close to the saturation level. Hence, the dynamic range will not be optimum.

A simple solution to maximizing the dynamic range in a leapfrog filter is to scale each individual internal node response so that they all have the same peak gain value [51]. For convenience, we set this value to unity. The procedure thus becomes computing the maximum of each individual magnitude response, i.e.,

$$m_i = \max_{0 \leq \omega T \leq \pi} \left| \frac{\hat{V}_i(e^{j\omega T})}{E(e^{j\omega T})} \right| \quad \text{or} \quad m_i = \max_{0 \leq \omega T \leq \pi} \left| \frac{\hat{I}_i(e^{j\omega T})}{E(e^{j\omega T})} \right| \tag{4.4}$$

and then dividing the whole response by this factor. The resulting frequency responses for the example are shown in Fig. 4.3(b).

To implement the above procedure on a flowgraph, we divide the gain constants of all branches entering node $\hat{V}_i$ (or $\hat{I}_i$) by m_i, and multiply each branch leaving the node by m_i (see Fig. 4.4). In this way, the loop gains are kept constant and the overall transfer function remains unchanged (except the maximum output gain is now 1). If this maximum output gain is required to equal a certain value (say, K),

then the filter input branch constant should be multiplied by this factor K. All the node response maxima remain equal, namely K.

The dynamic-range-scaled SFG of a fifth-order elliptic BT/LDI filter is shown in Fig. 4.5. Note that the output branch $-\frac{1}{2}(z^{\frac{1}{2}} + z^{-\frac{1}{2}})$ has been removed and the new output is now given by $V=\hat{V}_5/m_5$. The a_i's are the pre-dynamic-range-scaling capacitor ratios and the α_i's are the post-dynamic-range-scaling capacitor ratios.

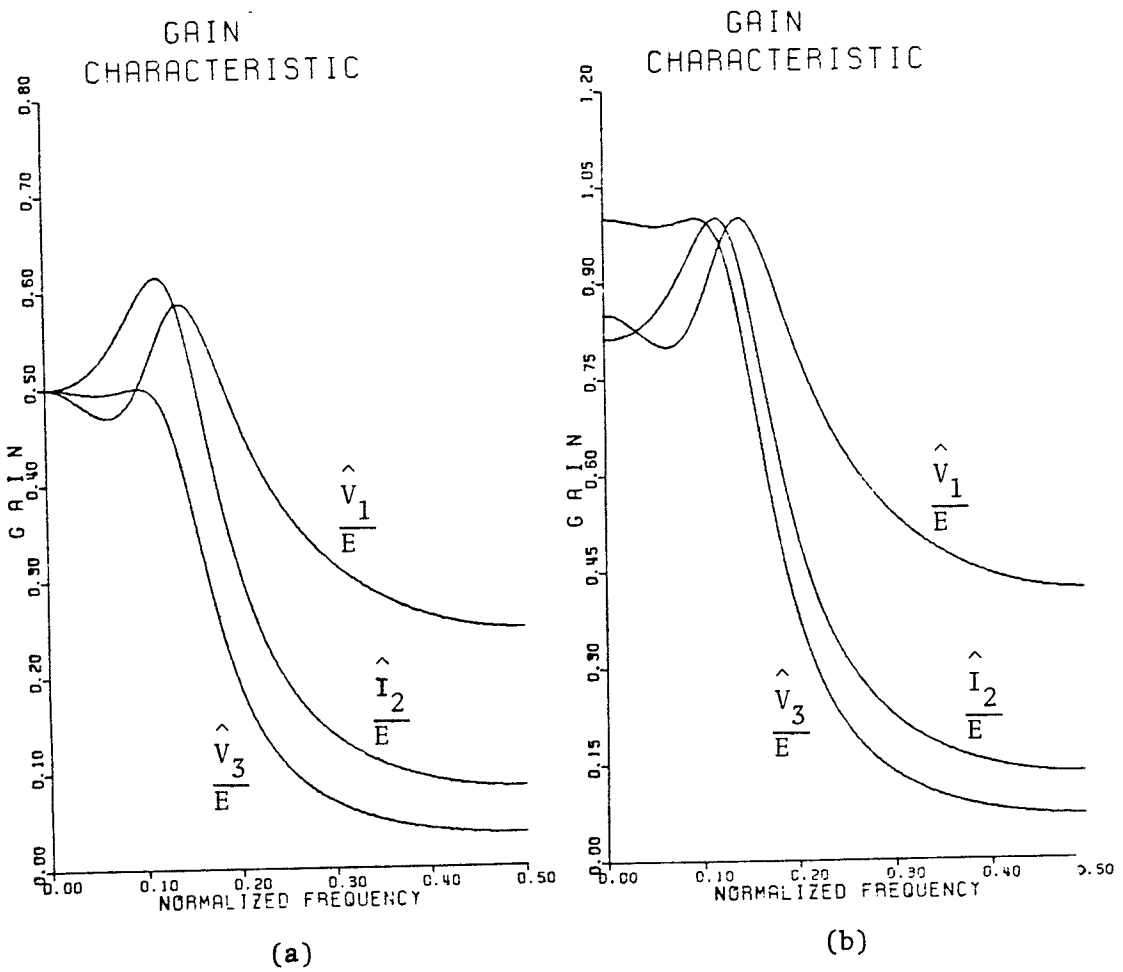

Fig. 4.3 The various node responses of the filter in Example 3.1 : (a) before and (b) after dynamic-range scaling.

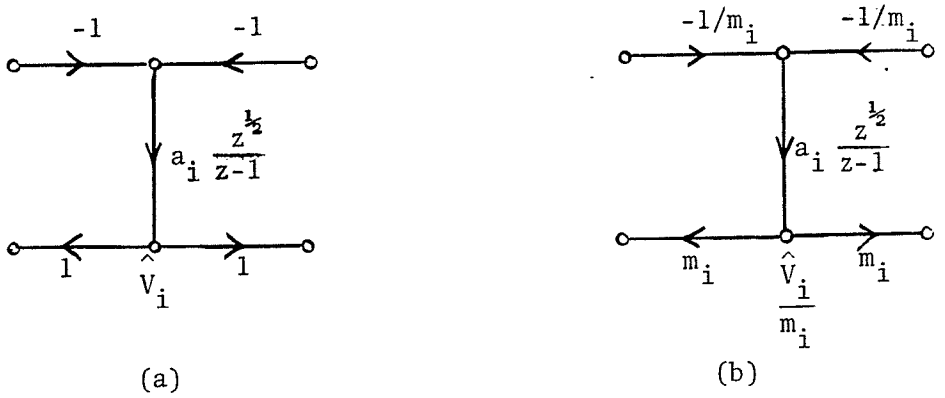

Fig. 4.4 Part of a signal-flow-graph (a) before and (b) after dynamic-range scaling.

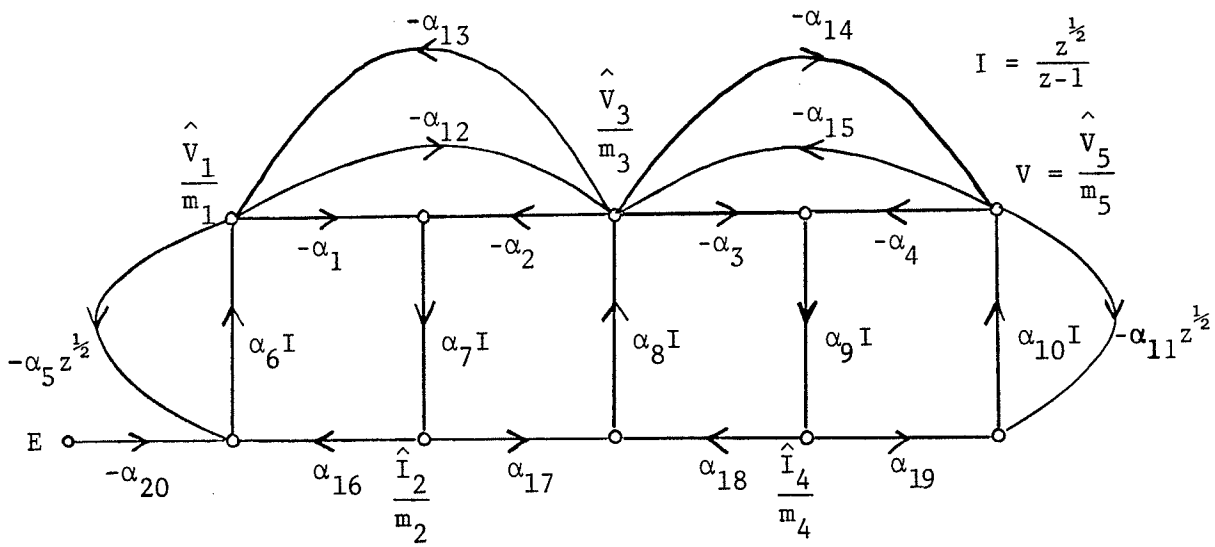

$$\alpha_1 = a_2 \frac{m_1}{m_2} \qquad \alpha_5 = a_1 \qquad \alpha_9 = 1 \qquad \alpha_{13} = a_6 \frac{m_3}{m_1} \qquad \alpha_{17} = a_3 \frac{m_2}{m_3}$$

$$\alpha_2 = a_2 \frac{m_3}{m_2} \qquad \alpha_6 = 1 \qquad \alpha_{10} = 1 \qquad \alpha_{14} = a_8 \frac{m_3}{m_5} \qquad \alpha_{18} = a_3 \frac{m_4}{m_3}$$

$$\alpha_3 = a_4 \frac{m_3}{m_4} \qquad \alpha_7 = 1 \qquad \alpha_{11} = a_5 \qquad \alpha_{15} = a_9 \frac{m_5}{m_3} \qquad \alpha_{19} = a_5 \frac{m_4}{m_5}$$

$$\alpha_4 = a_4 \frac{m_5}{m_4} \qquad \alpha_8 = 1 \qquad \alpha_{12} = a_7 \frac{m_1}{m_3} \qquad \alpha_{16} = a_1 \frac{m_2}{m_1} \qquad \alpha_{20} = \frac{a_1}{m_1}$$

Fig. 4.5 The dynamic-range-scaled SFG of a fifth-order elliptic SC filter.

4.3 TOTAL CAPACITANCE

The capacitance value of an MOS capacitor is proportional to the silicon area of the IC. It is therefore important to minimize the total capacitance value of an SC filter while still meeting the specifications.

It appears that not much work has been done on the minimization of the total capacitance of an SC filter after the initial design is completed. Mitra and Vaidyanathan [52] presented a method for minimizing the total capacitance in state-space SC filters. This thesis will discuss (in Section 4.5) an optimization technique to minimize the total capacitance in an SC leapfrog filter.

It can be readily shown that the total capacitance depends on the capacitor ratios. As an example, consider the following integrator with the capacitances expressed in terms of the unswitched feedback capacitor C.

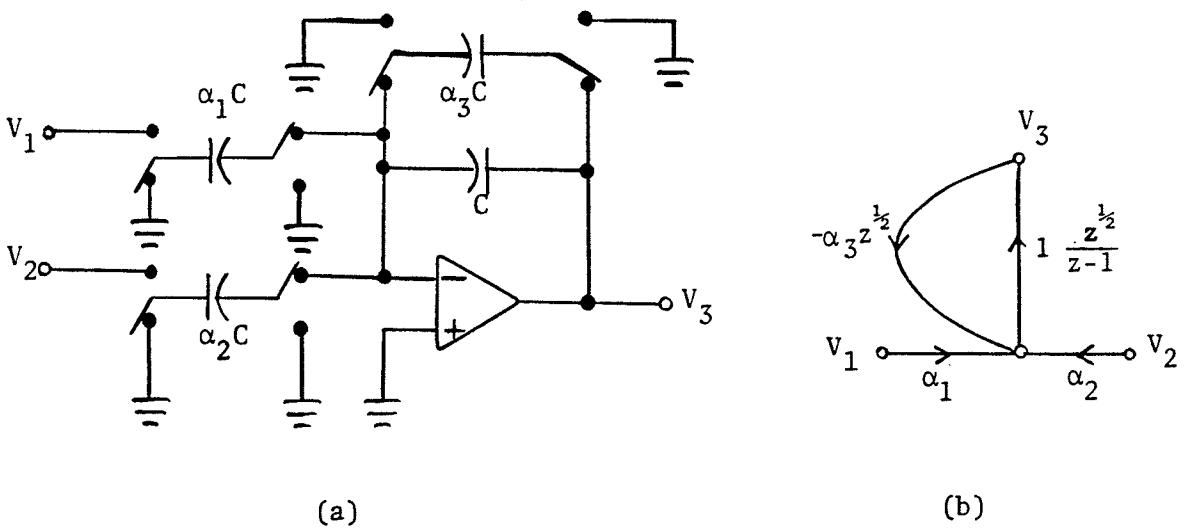

Fig. 4.6 An example used to illustrate the calculation of the total capacitance of an SC circuit.

The total capacitance associated with this integrator is

$$C_T = C(\alpha_1 + \alpha_2 + \alpha_3 + 1) \tag{4.5}$$

where α_1, α_2 and α_3 are the capacitor ratios. In view of practical limitations, there is a lower bound on the value of a capacitor that can be fabricated on an IC. Denote this smallest possible capacitance as C_{min}, then

$$\begin{aligned} C_{min} &= \min\ (\alpha_1 C\ ,\ \alpha_2 C\ ,\ \alpha_3 C\ ,\ C) \\ &= C\alpha_{min} \end{aligned} \tag{4.6}$$

where $\alpha_{min} = \min\ (\alpha_1\ ,\ \alpha_2\ ,\ \alpha_3\ ,\ \alpha_4)$ and $\alpha_4 = 1$.

Hence, the total capacitance can now be expressed as

$$\begin{aligned} C_T &= \frac{C_{min}}{\alpha_{min}} (\alpha_1 + \alpha_2 + \alpha_3 + \alpha_4) \\ &= C_{min}\ (\alpha_1' + \alpha_2' + \alpha_3' + \alpha_4') \end{aligned} \tag{4.7}$$

where

$$\alpha_i' = \frac{\alpha_i}{\alpha_{min}}\ ,\ i=1,2,3,4 \tag{4.8}$$

The total capacitance is minimized when the sum of the new capacitor ratios α_i' in (4.7) is minimized. Since these ratios must satisfy $\alpha_i' \geqslant 1$, minimizing their sum is equivalent to making each ratio approach unity as close as possible.

Note that for a leapfrog filter, α_{min} is not determined from among all of the capacitors in the filter. Instead, we divide the SFG into several sections (with each section defined by an integrator) and then determine a local α_{min} for

each section. The value α_{min_i} for the i-th section is chosen from among all the capacitors connected to the input terminal of the i-th op amp, or equivalently, from among all the branch gain constants associated with the input node of the i-th integrator in the SFG (see Fig. 4.6(b)).

For the dynamic-range-scaled SFG in Fig. 4.5, we can calculate the total capacitance of the filter by summing the total capacitance values of the five sections as follows :

$$C_T = C_{T_1} + C_{T_2} + C_{T_3} + C_{T_4} + C_{T_5} \tag{4.9}$$

where

$$C_{T_1} = \frac{C_{min}}{\alpha_{min_1}} (\alpha_5 + \alpha_6 + \alpha_{13} + \alpha_{16} + \alpha_{20}) \tag{4.10a}$$

$$\alpha_{min_1} = \min (\alpha_5 , \alpha_6 , \alpha_{13} , \alpha_{16} , \alpha_{20}) \tag{4.10b}$$

$$C_{T_2} = \frac{C_{min}}{\alpha_{min_2}} (\alpha_1 + \alpha_2 + \alpha_7) \tag{4.11a}$$

$$\alpha_{min_2} = \min (\alpha_1 , \alpha_2 , \alpha_7) \tag{4.11b}$$

$$C_{T_3} = \frac{C_{min}}{\alpha_{min_3}} (\alpha_8 + \alpha_{12} + \alpha_{15} + \alpha_{17} + \alpha_{18}) \tag{4.12a}$$

$$\alpha_{min_3} = \min (\alpha_8 , \alpha_{12} , \alpha_{15} , \alpha_{17} , \alpha_{18}) \tag{4.12b}$$

$$C_{T_4} = \frac{C_{min}}{\alpha_{min_4}} (\alpha_3 + \alpha_4 + \alpha_9) \tag{4.13a}$$

$$\alpha_{min_4} = \min (\alpha_3 , \alpha_4 , \alpha_9) \tag{4.13b}$$

$$C_{T_5} = \frac{C_{min}}{\alpha_{min_5}} (\alpha_{10} + \alpha_{11} + \alpha_{14} + \alpha_{19}) \tag{4.14a}$$

$$\alpha_{min_5} = \min (\alpha_{10} , \alpha_{11} , \alpha_{14} , \alpha_{19}) \tag{4.14b}$$

4.4 PASSBAND AND STOPBAND TOLERANCES

In general, it is desirable for a filter to have a passband ripple as small as possible, and a stopband attenuation as large as possible. This thesis proposes the following figure of merit :

$$\eta = \frac{P_{max} - P_{min}}{PW} + \frac{SW}{S_{min} - P_{min}} \tag{4.15}$$

where the symbols are defined in Fig. 4.2. The design will satisfy the tolerance specifications if each of the above ratios is equal to or less than 1 and then $\eta \leq 2$. For optimization purposes, we shall minimize η.

4.5 OPTIMIZATION

Of the four aspects described in the preceding section, the number of op amps and the dynamic range can be optimized easily; however, the minimization of the total capacitance and the passband/stopband deviations requires a computer-aided optimization program. Taking this into consideration, we define the objective function to be optimized (for the fifth-order elliptic SC leapfrog filter) as

$$f(\phi) = w_1 C_T + w_2 \eta \tag{4.16}$$

where ϕ is the set of gain constants $\{ a_1, \ldots, a_9 \}$, C_T is the total capacitance defined in (4.9)-(4.14), w_1 and w_2 are two different weighting factors and η is the figure of merit defined in (4.15).

The values of the weighting factors w_1 and w_2 are critical. A few runs of the optimization program are usually needed in order to establish the best values for them.

Note that in the original analog network (see Fig. 3.1), there are eight degrees of freedom (i.e., the number of circuit elements minus one). Since we set the resistances equal, there are seven degrees of freedom left. However, in the SC leapfrog filter, there are nine design parameters (i.e. a_1 to a_9). In order to reduce the 9-dimensional optimization problem to a 7-dimensional one, we shall introduce two constraints in the SC filter.

In (3.31), the branch gain constants are expressed in terms of the values of the reactive elements in the analog equivalent circuit. Conversely, if we obtain an optimum set of gain constants $\{ a_i \}$, we can express the reactive element values in terms of a_i's as follows :

$$C_1' = T\,\frac{1 - a_6}{a_1} \quad \text{or} \quad C_1' = T\left(\frac{1}{a_1} - \frac{a_7}{a_3}\right) \tag{4.17}$$

$$C_2' = T\,\frac{a_6}{a_1} \quad \text{or} \quad C_2' = T\,\frac{a_7}{a_3} \tag{4.18}$$

$$C_3' = T\left(\frac{1}{a_3} - \frac{a_6}{a_1} - \frac{a_8}{a_5}\right)$$

$$\text{or} \quad C_3' = T\left(\frac{a_6}{a_1 a_7} - \frac{a_6}{a_1} - \frac{a_8}{a_5}\right) \tag{4.19}$$

$$\text{or} \quad C_3' = T\left(\frac{a_8}{a_5 a_9} - \frac{a_6}{a_1} - \frac{a_8}{a_5}\right)$$

$$C_4' = T\,\frac{a_8}{a_5} \qquad \text{or} \qquad C_4' = T\,\frac{a_9}{a_3} \tag{4.20}$$

$$C_5' = T\,\frac{1 - a_8}{a_5} \qquad \text{or} \qquad C_5' = T\left(\frac{1}{a_5} - \frac{a_9}{a_3}\right) \tag{4.21}$$

$$L_2' = \frac{T}{a_2} \tag{4.22}$$

$$L_4' = \frac{T}{a_4} \tag{4.23}$$

The above equations show that the capacitance values are not unique. The reason is that there are two extra degrees of freedom in the SC domain. To ensure the uniqueness of the capacitance values, we introduce the following constraints :

$$a_1 = \frac{a_3 a_6}{a_7} \tag{4.24}$$

and

$$a_5 = \frac{a_3 a_8}{a_9} \tag{4.25}$$

With these two constraints, the capacitance values are uniquely given by

$$C_1' = T\left(\frac{a_7 - a_6 a_7}{a_3 a_6}\right)$$

$$C_2' = T\,\frac{a_7}{a_3}$$

$$C_3' = T\left(\frac{1 - a_7 - a_9}{a_3}\right) \tag{4.26}$$

$$C_4' = T \frac{a_9}{a_3}$$

$$C_5' = T \left(\frac{a_9 - a_8 a_9}{a_3 a_8} \right)$$

where the parameters a_1 and a_5 have been eliminated.

The optimization problem now becomes :

$$\text{Minimize} \qquad f(\psi) = w_1 C_T + w_2 \eta \tag{4.27}$$

subject to

$$\begin{aligned} & a_2 , a_3 , a_4 , a_7 , a_9 > 0 \\ 0 < \quad & a_6 \quad < 1 \\ 0 < \quad & a_8 \quad < 1 \\ 0 < \quad & a_7 + a_9 \quad < 1 \end{aligned} \tag{4.28}$$

where $\psi = \{ a_2, a_3, a_4, a_6, a_7, a_8, a_9 \}$

The above explicit constraints are derived from (4.22), (4.23) and (4.26) by requiring the L' and C' element values to be positive. We can transform this constrained problem into an unconstrained one by performing a parameter transformation.

Define the set of gain constants $\{a_i\}$ in terms of a new set of parameters $\{x_i\}$ as follows :

$$a_2 = e^{x_2}$$

$$a_3 = e^{x_3}$$

$$a_4 = e^{x_4}$$

$$a_6 = \frac{\cot^{-1} x_6}{\pi}$$

$$a_7 = \frac{\cot^{-1} x_7}{\pi} \qquad (4.29)$$

$$a_8 = \frac{\cot^{-1} x_8}{\pi}$$

$$a_9 = (1 - a_7) \frac{\cot^{-1} x_9}{\pi}$$

Thus, as x_i's vary from $-\infty$ to ∞, (4.28) will automatically be satisfied.

To summarize, we will minimize

$$f(\theta) = w_1 C_T + w_2 \eta \qquad (4.30)$$

where $$\theta = \{ x_2, x_3, x_4, x_6, x_7, x_8, x_9 \}$$

The optimization technique used is the simplex direct search method [53]. A simple flowchart of the optimization program is shown in Fig. 4.7. A FORTRAN subroutine for simplex written by Gole [54] is used in the program. As in any optimization problem, the location of the global minimum is never known for sure. However, if we begin with several different feasible designs as starting points and end up with the same final point, we can expect that the minimum achieved is a good one.

We will illustrate the above concepts in the next chapter with the aid of an example.

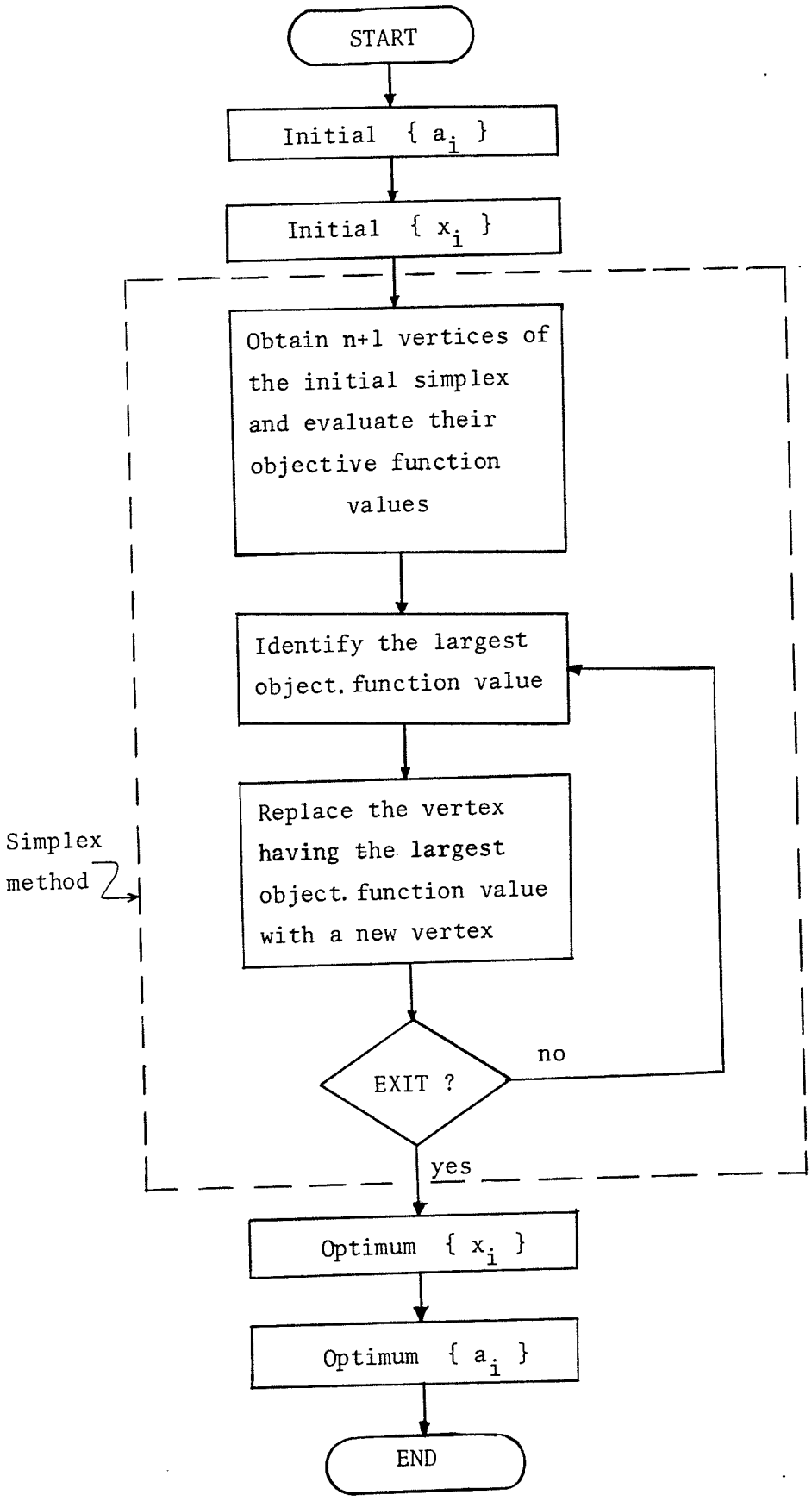

Fig. 4.7 A simple flowchart for the optimization program.

4.6 MAGNITUDE SENSITIVITY

After an SC filter design is finalized, it is important to evaluate the sensitivity of the magnitude response to changes in network parameters (i.e. the capacitor ratios).

It has been noted that a doubly-terminated LC ladder filter has very low sensitivity to element variations. Since an SC leapfrog filter originates from such an analog filter, it is expected to retain the same low-sensitivity property. This thesis will briefly examine this sensitivity property of an SC leapfrog filter.

In this section, we will first consider the single-parameter sensitivity as it is sometimes desirable to know how one specific capacitor ratio will affect the magnitude response. We will then consider the multi-parameter sensitivity as it provides a more realistic estimate of the sensitivity property of the SC filter.

4.6.1 Single-Parameter Sensitivity : Deterministic Approach

The transfer function H of an SC leapfrog filter (either LDI or BT/LDI) depends on all the capacitor ratios (i.e. a_i's). Since H is always a rational function, it can be expressed in terms of two polynomials N and D as follows :

$$H(z,a_1,a_2,\ldots) = \frac{N(z,a_1,a_2,\ldots)}{D(z,a_1,a_2,\ldots)} \qquad (4.31)$$

The sensitivity of H with respect to any capacitor ratio a_i is defined as

$$S^H_{a_i} = \frac{a_i}{H} \frac{\partial H}{\partial a_i} \tag{4.32}$$

It is possible to decompose each of N and D into two parts as follows :

$$N(z,a_1,a_2,\ldots) = N_1(z) + a_i\, N_2(z) \tag{4.33}$$

$$D(z,a_1,a_2,\ldots) = D_1(z) + a_i\, D_2(z) \tag{4.34}$$

where N_1, N_2, D_1 and D_2 are polynomials in z with coefficients that are not functions of a_i. Hence, H can be rewritten in the bilinear form [55]

$$H = \frac{N}{D} = \frac{N_1 + a_i N_2}{D_1 + a_i D_2} \tag{4.35}$$

Using (4.35), we can show that (4.32) becomes

$$\begin{aligned} S^H_{a_i} &= a_i \left(\frac{\partial N/\partial a_i}{N} - \frac{\partial D/\partial a_i}{D} \right) \\ &= a_i \left(\frac{N_2}{N} - \frac{D_2}{D} \right) \end{aligned} \tag{4.36}$$

If we are only interested in the magnitude characteristic $G(e^{j\omega T}) = |H(e^{j\omega T})|$, then it is well known from classical theory that the magnitude sensitivity is defined as [55]

$$S_{a_i}^{G(e^{j\omega T})} = \text{Re}\ [\ S_{a_i}^{H(e^{j\omega T})}\ ] = \text{Re}\ [\ S_{a_i}^{H(z)}\Big|_{z=e^{j\omega T}}\ ] \qquad (4.37)$$

Hence, the relative change in the magnitude response at a specific frequency due to a variation in a_i is given by

$$\frac{\Delta G(e^{j\omega T})}{G(e^{j\omega T})} = \frac{\Delta a_i}{a_i}\ S_{a_i}^{G(e^{j\omega T})} = \frac{\Delta a_i}{a_i}\ \text{Re}\ [\ S_{a_i}^{H(z)}\Big|_{z=e^{j\omega T}}\ ] \qquad (4.38)$$

where $\frac{\Delta a_i}{a_i}$ is the relative change in a_i.

4.6.1.1 Example 4.1

Consider the third-order Chebyshev filter shown in Fig. 3.3. The transfer function of the LDI SFG is given by (4.3) as

$$H = \frac{N}{D} = \frac{a_1 a_2 a_3\ z^{3/2}}{D}$$

where D has been defined in (4.3).

If $S_{a_1}^{H}$ is required, then

$$N_2 = a_2 a_3 z^{3/2}$$

$$D_2 = z^3(1+a_3) + z^2(a_2-2+2a_2a_3-a_3) + z(1-a_2)$$

and

$$S_{a_1}^{H} = a_1\left(\frac{N_2}{N} - \frac{D_2}{D}\right) = 1 - a_1\frac{D_2}{D}$$

Similarly,

$$S^{H}_{a_2} = 1 - \frac{a_2}{D} z \left[z(a_1+a_3+2a_1a_3) - (a_1+a_3) \right]$$

and

$$S^{H}_{a_3} = 1 - \frac{a_3}{D} z \left[z^2(1+a_1)+z(a_2-2+2a_1a_2-a_1)+(1-a_2) \right]$$

The magnitude sensitivities can then be evaluated using (4.37).

Note that this analytical method is useful only for low-order filters. For higher-order filters, the method may be very tedious. For those cases, we can change one capacitor ratio by a certain percentage at a time, and plot the corresponding magnitude response. From the diagram, we then make some observations about the sensitivity of the response with respect to that particular capacitor ratio. The same procedure is then repeated for every other capacitor ratio.

4.6.2 Multi-Parameter Sensitivity : Statistical Approach

In a practical circuit realization, all components are subject to simultaneous changes. To model a more realistic situation where all the components of the circuit deviate from their nominal values, we use a statistical method called the Monte Carlo method [19].

In a Monte Carlo simulation, the circuit is simply analyzed a statistically significant number of times, usually 100 to 10,000 times. In each analysis, each parameter (e.g. component value) of the circuit is varied randomly according to a prespecified probability distribution function. The variations are supposed to simulate the physical random processes of the problem under study. Meaningful statistical quantities are computed from all of these analyses and a conclusion about the sensitivity can be drawn. If the number of analyses is increased, then the model is of course more accurate.

In an SC leapfrog filter, the parameters that are subject to variations are the capacitor ratios. If the fifth-order elliptic filter is chosen as an example, then these parameters are the nine ratios a_1 to a_9 . In integrated circuits, all the components are on the same chip and thus the capacitors track each other to some extent. There is an even higher tracking (or correlation) factor for the capacitor ratios. This fact must be taken into consideration when random capacitor ratios are generated. Hence, in every analysis in the Monte Carlo simulation, a set of nine parameters is generated according to the following formula :

$$a_i = \tilde{a}_i [\, 1 + \rho n + (1-\rho) n_i \,] \quad , \quad i=1,2,\ldots 9 \qquad (4.39)$$

where $\tilde{a}_i$ is the i-th nominal capacitor ratio, ρ is the correlation factor of all the capacitor ratios, n is the

random number used to perturb all the capacitor ratios, and n_i is the random number used to perturb the i-th ratio. The above formula was described in [56] except that the resistance values instead of the capacitor ratios were used there. The correlation factor can vary from $\rho=0$ for no correlation to $\rho=1$ for complete correlation. The random numbers n and n_i are generated according to a prespecified probability distribution function such as a uniform or a Gaussian distribution function. These random number generators are usually available from computer-routine libraries.

For each set of a_i's, the attenuation $A(e^{j\omega T})$ is evaluated. After N samples, we can calculate the first moment (or mean) m and second moment m_2 of the attenuation at each frequency point $\omega_i T$ by the following formulae :

$$m(\omega_i T) = \frac{1}{N} \sum_{k=1}^{N} A_k(e^{j\omega_i T}) \tag{4.40}$$

$$m_2(\omega_i T) = \frac{1}{N} \sum_{k=1}^{N} [A_k(e^{j\omega_i T})]^2 \tag{4.41}$$

where A_k is the k-th sample of the attenuation evaluated at $\omega_i T$. The standard deviation of the attenuation at that frequency is calculated by

$$\sigma(\omega_i T) = \sqrt{m_2(\omega_i T) - m^2(\omega_i T)} \tag{4.42}$$

Three different attenuation functions m, $m-\sigma$ and $m+\sigma$ should be plotted. If these all fall inside the tolerance scheme of the specifications, then the design is acceptable. Otherwise, we may have to restart the design with more stringent requirements, and see if the final design will satisfy the original specifications. We will apply the Monte Carlo method to the design example discussed in the next chapter.

Chapter V

DESIGN EXAMPLE OF A FIFTH-ORDER ELLIPTIC SC FILTER

In this chapter, we will demonstrate the procedure of designing an SC BT/LDI leapfrog filter. The filter will be implemented with discrete components to verify the design.

5.1 DESIGN PROCEDURE

Consider the design of an SC BT leapfrog filter with the specifications given in Fig. 5.1(a) : the sampling frequency is f_s=128 kHz, the cutoff frequency is f_c=3.4 kHz and the stopband-edge frequency is f_{st}=4.6 kHz.

The normalized cutoff and stopband-edge frequencies are 0.02656 and 0.03594, respectively. The corresponding analog frequencies are calculated from the BT prewarping formula as

$$\Omega_c = 2 f_s \tan \left(\frac{\pi f_c}{f_s} \right) = 21412.56 \text{ r/s}$$

and

$$\Omega_{st} = 2 f_s \tan \left(\frac{\pi f_{st}}{f_s} \right) = 29026.09 \text{ r/s}$$

Since the filter tables always list circuits with a cutoff frequency of 1 r/s, it is convenient to normalize the specifications. The resulting normalized cutoff and stopband-edge frequencies are 1 and 1.35556 r/s, respectively.

The normalized analog-frequency tolerance scheme is given in Fig. 5.1(b).

From tables [43], we find that the frequency response of the fifth-order elliptic filter C052058 will satisfy the specifications. The nominal frequency response of this filter is sketched in Fig. 5.1(c) where Ω_{st}=1.17918 r/s, P=.1773 dB, and S=29.4 dB. The normalized element values are given as (see Fig. 3.1(a))

C_{1n} = 1.046363 F C_{4n} = 1.165607 F R_2 = 1 Ω

C_{2n} = 0.344225 F C_{5n} = 0.643438 F L_{2n} = 1.034563 H

C_{3n} = 1.453789 F R_1 = 1 Ω L_{4n} = 0.585543 H

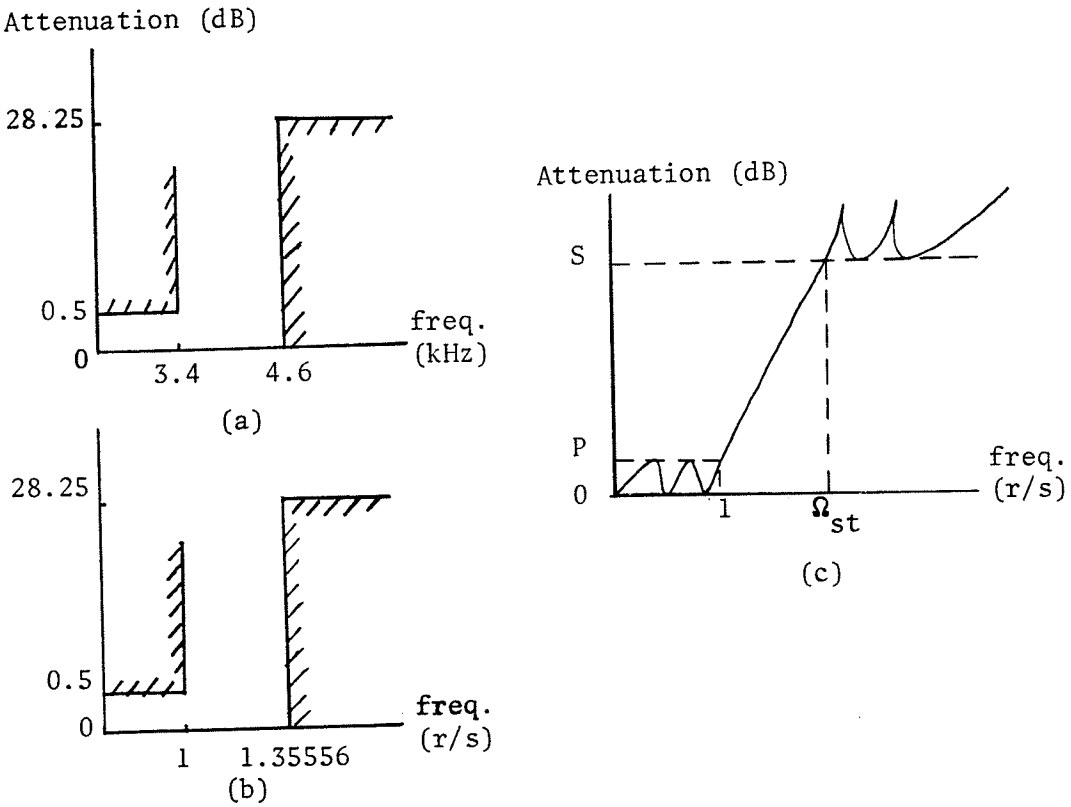

Fig. 5.1 The design specifications in (a) digital domain and (b) analog domain. The nominal response of the analog prototype : (c).

The next step is to frequency-denormalize these element values, i.e.,

$$C_i = \frac{C_{i,n}}{\Omega_c} \qquad \text{and} \qquad L_i = \frac{L_{i,n}}{\Omega_c}$$

Since Ω_c=21412.56, the nominal reactive element values are given by

$C_1 = 4.88667\times10^{-5}$ F $L_2 = 4.83156\times10^{-5}$ H

$C_2 = 1.60758\times10^{-5}$ F $L_4 = 2.73457\times10^{-5}$ H

$C_3 = 6.78941\times10^{-5}$ F

$C_4 = 5.44355\times10^{-5}$ F

$C_5 = 3.00495\times10^{-5}$ F

With these values, the branch gain constants of the BT/LDI SFG are given by (3.30)

$a_1 = 0.12734$ $a_6 = 0.26717$

$a_2 = 0.16170$ $a_7 = 0.11769$

$a_3 = 0.05609$ $a_8 = 0.67779$

$a_4 = 0.28569$ $a_9 = 0.39484$

$a_5 = 0.09629$

This completes the initial design of the SC leapfrog filter. The next step of the design procedure is the optimization.

We should use the canonic number (i.e. five) of op amps and take $\hat{V}_5$ (see Fig. 3.6(f)) as the output. The theoretical frequency response at this node is shown in Fig. 5.2. It shows that the specifications are still met and thus the removal of the output branch $-\frac{1}{2}(z^{\frac{1}{2}} + z^{-\frac{1}{2}})$ is justified.

We now proceed with the computer-aided optimization program described in the previous chapter. After a number of trials, we choose the weighting factors w_1 to be $1/C_{min}$ and w_2 to be 2, the side-length of the initial simplex to be .05 and the exit criterion to be .001. Before optimization, the total capacitance is $C_T = 87.15 \times C_{min}$, $\eta = 1.33$ and $f(\theta) = 89.81$. In this thesis, we use $C_{min} = 1$ nF.

The final result is a set of optimum gain constants which reduces the total capacitance value quite significantly (a saving of about 30%) :

$A_1 = 0.28875$ $\quad$ $C_T = 61.11$ nF

$A_2 = 0.11711$ $\quad$ $\eta = 1.75$

$A_3 = 0.09078$ $\quad$ $f(\theta) = 64.61$

$A_4 = 0.17001$

$A_5 = 0.21108$

$A_6 = 0.34156$

$A_7 = 0.10739$

$A_8 = 0.60963$

$A_9 = 0.26219$

where A_i is the optimum value of a_i.

The frequency response due to this set of parameters is also shown in Fig. 5.2 and it meets the specifications. The corresponding dynamic-range-scaled SFG is the one shown in Fig. 4.5 where the pre-scaled internal node response maxima m_i's are :

$m_1 = 0.9911$ $\quad$ $m_4 = 0.9562$

$m_2 = 0.9911$ $\quad$ $m_5 = 0.5$

$m_3 = 0.9020$

and the branch gain constants (after the minimum-capacitance scaling) are

$\alpha'_1 = 1.0987$ $\quad$ $\alpha'_{11} = 1$

$\alpha'_2 = 1$ $\quad$ $\alpha'_{12} = 1.2260$

$\alpha'_3 = 1.8040$ $\quad$ $\alpha'_{13} = 1.0766$

$\alpha'_4 = 1$ $\quad$ $\alpha'_{14} = 5.2103$

$\alpha'_5 = 1$ $\quad$ $\alpha'_{15} = 1.5102$

$\alpha'_6 = 3.4632$ $\quad$ $\alpha'_{16} = 1$

$\alpha'_7 = 9.3819$ $\quad$ $\alpha'_{17} = 1.0365$

$\alpha'_8 = 10.3908$ $\quad$ $\alpha'_{18} = 1$

$\alpha'_9 = 11.2488$ $\quad$ $\alpha'_{19} = 1.9124$

$\alpha'_{10} = 4.7375$ $\quad$ $\alpha'_{20} = 1.0090$

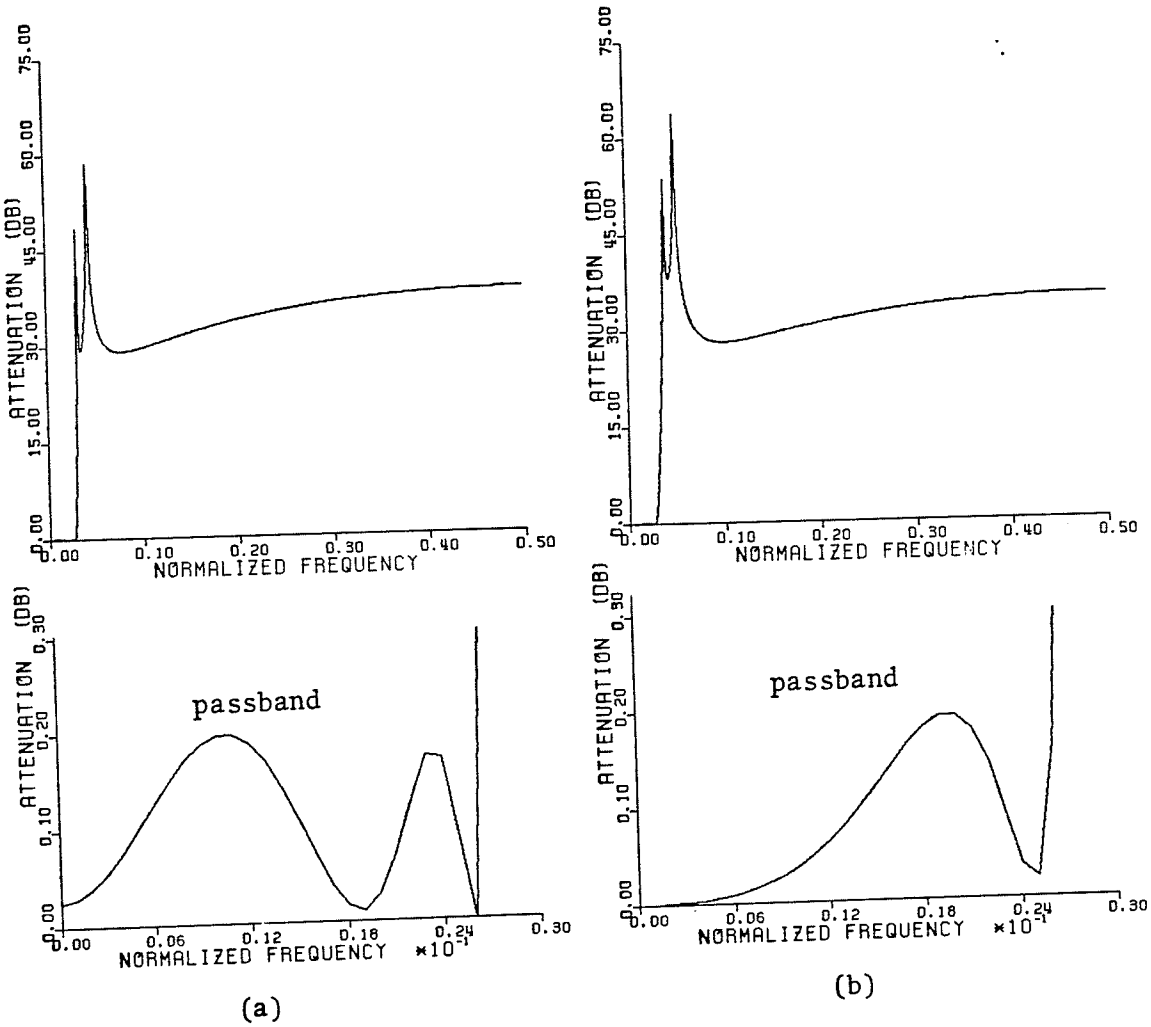

Fig. 5.2 (a) The theoretical response of the fifth-order elliptic filter without the output branch.

(b) The theoretical response of the optimized filter.

As mentioned earlier, we should repeat the optimization with several different starting points. Since the filters C051545 and C052548 (and several others) also satisfy the specifications, they were chosen as the initial points for two more runs. Following the same procedure used earlier for C052058, we summarize the results below:

	C051545	C052548
Ω_{st}	1.41421 r/s	1.34563 r/s
P	0.0988 dB	0.2803 dB
S	39.8 dB	41.2 dB

Normalized analog prototype circuit elements :

C_{1n} ; C_{4n}	1.00463; 0.53610	1.28329; 0.64069 F
C_{2n} ; C_{5n}	0.17934; 0.75913	0.21771; 0.99833 F
C_{3n}	1.57870	1.77253 F
L_{2n} ; L_{4n}	1.18849; 0.86860	1.11477; 0.80597 H
R_1 ; R_2	1 ; 1	1 ; 1 Ω

Final gain constants (or capacitor ratios) :

α'_1 ; α'_{11}	1.0828 ; 1	1.1280 ; 1
α'_2 ; α'_{12}	1 ; 1	1 ; 1
α'_3 ; α'_{13}	1.7867 ; 1	1.7472 ; 1
α'_4 ; α'_{14}	1 ; 6.2227	1 ; 5.8798
α'_5 ; α'_{15}	1.0797 ; 1.7949	1.1945 ; 1.8080
α'_6 ; α'_{16}	4.5571 ; 1.1194	4.3541 ; 1.1678
α'_7 ; α'_{17}	9.6248 ; 1.0338	9.7046 ; 1.0353
α'_8 ; α'_{18}	10.6396 ; 1	10.7550 ; 1.0026
α'_9 ; α'_{19}	9.8586 ; 1.9403	9.7988 ; 1.8661
α'_{10} ; α'_{20}	3.9806 ; 1.1153	3.9938 ; 1.2121

Before optimization :

C_T ; η ; $f(\theta)$ 70.70; 1.16; 73.02 79.12; 1.26; 81.65

After optimization :

C_T ; η ; $f(\theta)$ 61.84; 1.53; 64.89 61.65; 1.95; 65.55

Note that all three designs give practically the same minimum value of the objective function. However, the sets of A_i's are not the same in values. A conjecture is that there can be more than one set of parameters that will yield the same (local) minimum value of the objective function. Also note that while C_T decreases after the optimization, η increases — this is a trade-off that should not be ignored.

We arbitrarily select C052058 as the filter to implement. But first, we should study the sensitivity property of the filter by the Monte Carlo method. We will use N=300 samples, a correlation factor of ρ=0.8 and a uniform probability distribution function of ±5% (which is a very pessimistic assumption). The functions m, m+σ and m-σ are shown in Fig. 5.3. They demonstrate that the design is indeed insensitive to changes in capacitor ratios.

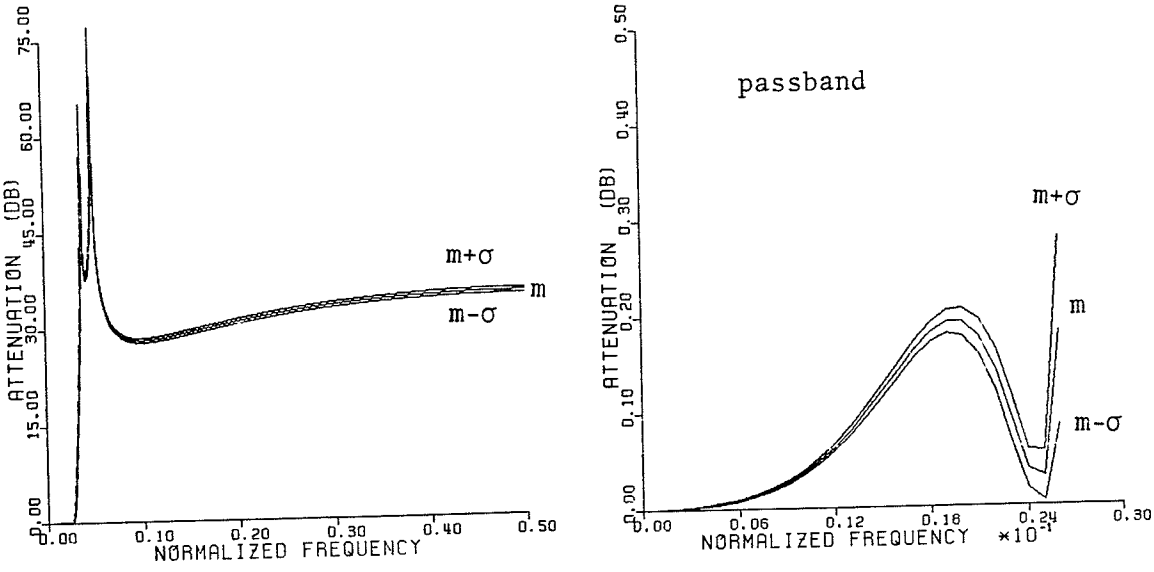

Fig. 5.3 Attenuation characteristics obtained from the Monte Carlo simulation.

5.2 IMPLEMENTATION AND EXPERIMENTAL RESULTS

The optimized BT/LDI SC filter for the network C052058 has been implemented with discrete components by realizing the SFG shown in Fig. 4.5. The implementation of this SFG with SC components is shown in Fig. 5.4. The building blocks are the parasitic-insensitive LDI integrators given in Section 2.6. The set of capacitor ratios realized is $\{ \alpha_i' \}$. Each capacitor in the circuit is given by $C_i = \alpha_i' \times C_{min}$, i=1,2,...20. Note that because of the sign inversion in the input branch gain constant, the output is in fact -V, but this will not affect the magnitude response.

The discrete components used are μA741 op amps, MC14053 single-pole-double-throw CMOS switches and ceramic/metallized-film capacitors. The power supply voltages for the op amps are ±7.5 V. The power supply voltages for the switches are V_{DD} =7.5 V, V_{SS} =0 V and V_{EE} =-7.5 V. The clock is a square wave of amplitude 0-7.5 V. The MC14053 chip itself produces the required complementary clock. To suppress noise, capacitors of 0.1 μF are added across V_{DD} and V_{SS} as well as across V_{SS} and V_{EE}. The smallest capacitor used (i.e. C_{min}) is 1 nF. The capacitor ratios used are accurate within 5% of the nominal values.

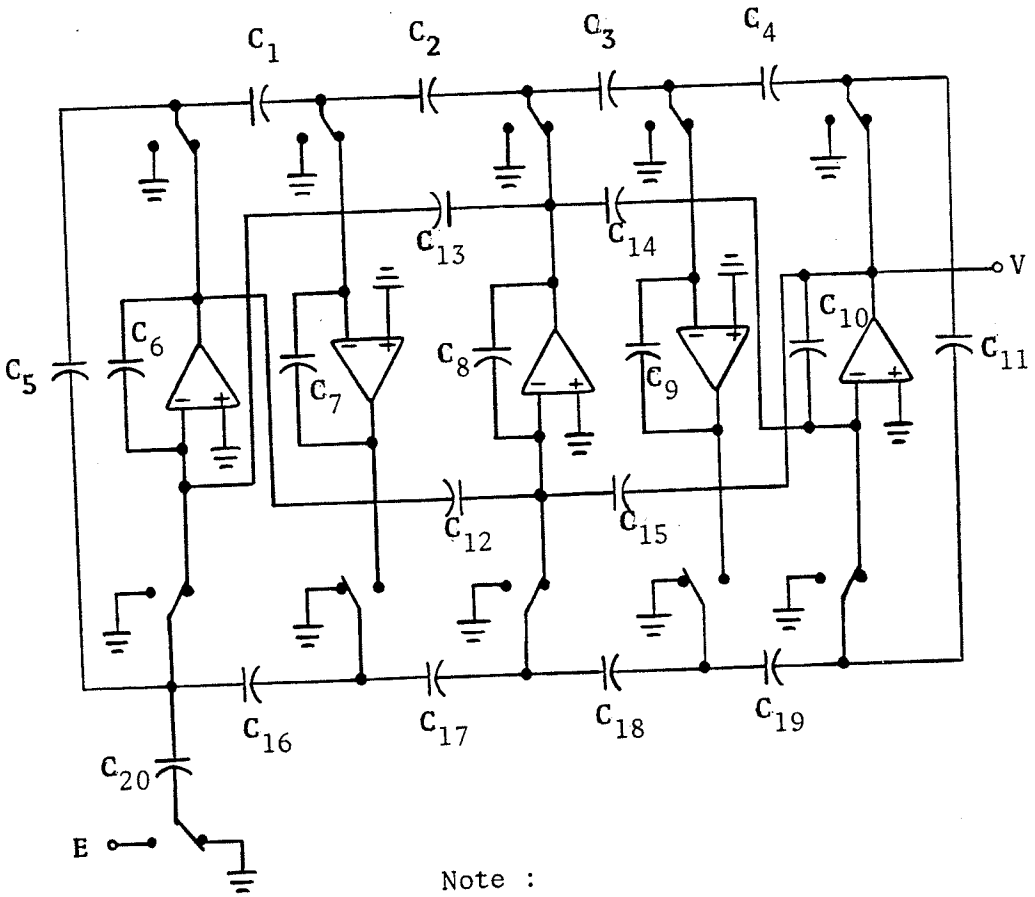

Note :

$C_i = \alpha'_i \times C_{min}$ $\quad i=1,2,\ldots 20$

Typically, C_{min} = 1 pF with integrated components

C_{min} = 1 nF with discrete components

Fig. 5.4 The physical implementation of a fifth-order elliptic SC leapfrog filter.

The filter response is shown in Fig. 5.5, and apparently it satisfies the specifications. The performance in the passband is, however, less satisfactory.

To show the effect of omitting the output branch $-\frac{1}{2}(z^{\frac{1}{2}} + z^{-\frac{1}{2}})$ on the magnitude response, we connect the circuit in Fig. 4.1 to the output of Fig. 5.4. The subsequent response is shown in Fig. 5.6. It shows that there is no noticeable difference in the passband, but clearly a larger attenuation in the stopband. However, as mentioned in the previous chapter, it is really not necessary to have this extra section in the filter.

To show that the bandwidth can be varied by adjusting the sampling frequency, we change the sampling rate from 128 kHz to 100 kHz. The resulting frequency response is shown in Fig. 5.7.

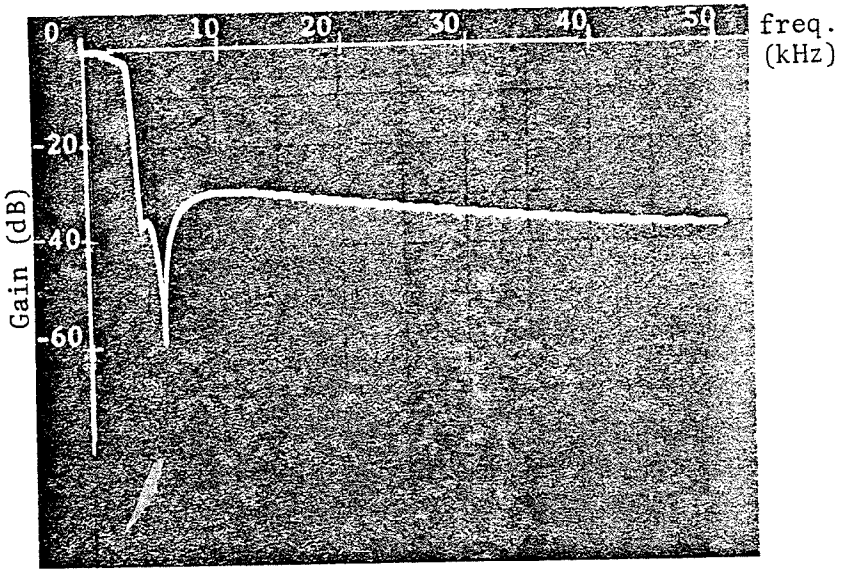

Fig. 5.5 The experimental magnitude response.

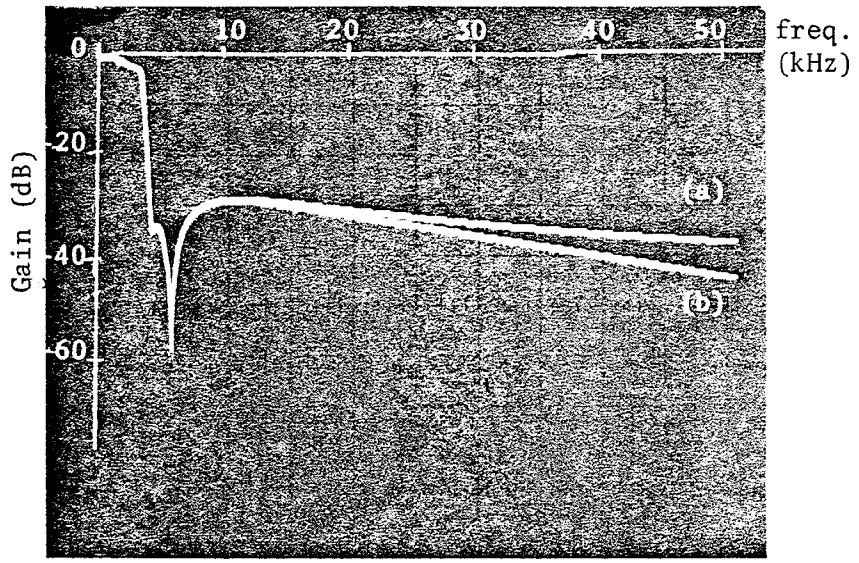

Fig. 5.6 The magnitude response of the filter (a) without and (b) with the output branch.

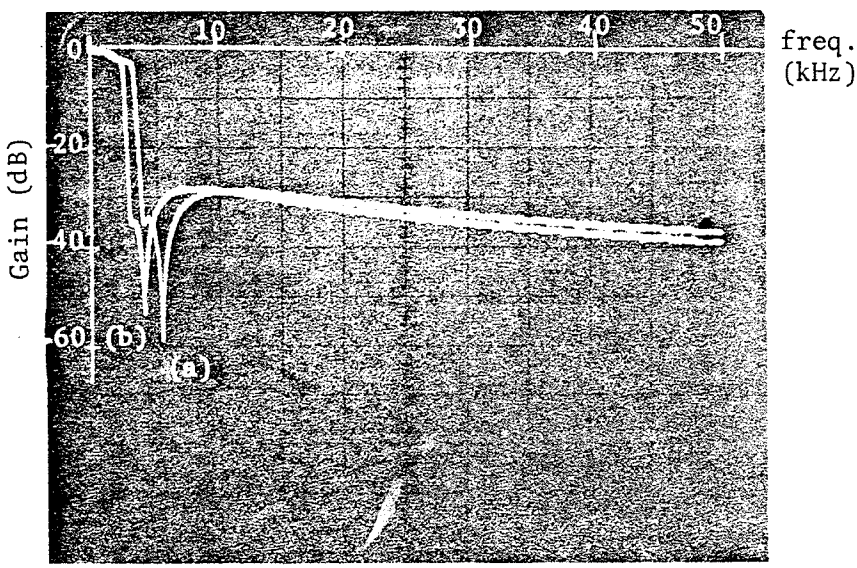

Fig. 5.7 The magnitude response of the filter operated at a sampling frequency of (a) 128 and (b) 100 kHz.

Chapter VI

SUMMARY AND CONCLUSIONS

The most widely used approach in designing a switched-capacitor filter is the leapfrog simulation of a passive doubly-terminated LC ladder network. The procedure is to obtain a leapfrog signal flowgraph for the RLC network first, and then apply an analog-to-digital transformation to the integrators in the flowgraph. The subsequent discrete-time z-domain flowgraph is then realized by the switched-capacitor circuits.

This thesis has reviewed the derivation of an analog signal flowgraph and has shown that the branch gain constants of the z-domain flowgraph are the capacitor ratios to be realized in the SC building blocks. The thesis has also discussed Davis and Trick's method of designing an LDI-transformed SC filter. Although the bilinear transformation is always preferred, the bilinear SC integrators are unfortunately either parasitic-sensitive or inefficient in hardware. This trade-off can be avoided if the parasitic-insensitive LDI integrators are used as the building blocks in realizing a bilinearly-transformed signal flowgraph (this kind of filter is denoted as the BT/LDI filter). The above technique has been devised by Lee and Chang [48] using the

concepts of discrete-time impedances and charge-voltage relationships for the RLC elements. Eriksson achieved the same goal using a flowgraph conversion method. While Lee and Chang's method requires the bilinear termination integrations, Eriksson's method results in the backward difference integrations in the termination loops as a natural result of the flowgraph conversion procedure. This thesis has adopted the backward difference termination integrations, and has presented two new methods of designing the BT/LDI filters : 1) an extension to Davis and Trick's method, and 2) an analog equivalent circuit method. The first method requires the formulation of the transfer function of the filter using Mason's formula and the solution of a system of nonlinear equations derived from the transfer function. However, Eriksson's method and the equivalent circuit method provide explicit design formulae and can readily be extended to higher-order filters. Thus, the latter two methods are preferred. All of the above methods use M+1 op amps for an odd M-th order filter.

This thesis, however, has shown that it is possible to use M op amps for an odd M-th order SC leapfrog filter, and to optimize the filter with respect to the dynamic range, the total capacitance and the passband/stopband tolerance. The dynamic range can easily be optimized by scaling the branch gain constants of the signal flowgraph properly, but the latter two criteria require a computer-aided optimiza-

tion program. The objective of the optimization in this thesis is thus to minimize the total capacitance and the passband/stopband deviations of the canonic, dynamic-range-scaled SC filter. We have imposed constraints on some parameters of optimization in order to reduce the dimension of the parameter set, and have introduced a parameter transformation to the remaining parameters so that the optimization becomes an unconstrained problem. This thesis has used the simplex direct search method to minimize the objective function of a fifth-order elliptic filter. If a higher-order filter is optimized, then the simplex method will not be efficient and other methods must be used.

Furthermore, the thesis has discussed the single- and multi-parameter sensitivities of an SC leapfrog filter. The single-parameter case is investigated analytically whereas the multi-parameter case is examined statistically by the Monte Carlo method.

The complete design procedure for a BT/LDI filter is summarized as follows :

1. Obtain an analog network that meets the specifications.
2. Use either Eriksson's method or the equivalent circuit method to derive the values of branch gain constants of the BT/LDI signal flowgraph.
3. With the set of initial gain constants as the starting point, perform the optimization to obtain the optimum set of gain constants $\{A_i\}$.

4. Perform the dynamic-range scaling to obtain a new set of gain constants $\{\alpha_i\}$.
5. Perform the minimum-capacitance scaling to obtain the final set of gain constants $\{\alpha_i'\}$.
6. Implement the flowgraph with $\{\alpha_i'\}$ realized as the capacitor ratios in the SC integrators.
7. Apply the Monte Carlo method to examine the sensitivity behaviour of the filter.

A fifth-order elliptic low-pass filter has been designed and optimized to demonstrate the procedure outlined above. The optimization results in a saving of 30% of the capacitance value of the filter. Before an SC filter is realized in an integrated circuit, it is a common practice to test the design by building a prototype with discrete op amps, switches and capacitors. A discrete prototype for the optimized fifth-order elliptic filter has been constructed. The network satisfies the specifications and is found to be insensitive to variations in the capacitor ratios. The performance of this discrete-component filter warrants the implementation of the design in an integrated circuit.

Although this thesis has discussed only the low-pass filters, the concepts presented also apply to the high-pass, band-pass and band-reject filters. Furthermore, this thesis has not considered even-order filters. Research on deriving the corresponding BT/LDI signal flowgraphs is suggested.

Appendix A

MASON'S FORMULA

Mason's formula is used to derive the relationship between any two node variables of a flowgraph. Usually, we are interested in the input-output relationship of the flowgraph.

We will demonstrate the procedure of applying Mason's rule by considering the third-order elliptic filter shown in Fig. 3.5(a). The corresponding s-domain flowgraph is shown in Fig. 3.5(b).

Assume that the transfer function from the source node E to the sink node V is required. There are two forward paths from E to V, i.e.,

$$P_1 = \frac{d_1}{s} d_5 \qquad \text{and} \qquad P_2 = \frac{d_1}{s}\frac{d_2}{s}\frac{d_3}{s}$$

There are seven self-loops :

$$L_1 = -\frac{d_1}{s} \qquad L_4 = -\frac{d_3}{s} \qquad L_6 = \frac{d_2}{s}\frac{d_3}{s} d_4$$

$$L_2 = -\frac{d_1}{s}\frac{d_2}{s} \qquad L_5 = \frac{d_1}{s} d_5 \frac{d_2}{s} \qquad L_7 = d_4 d_5$$

$$L_3 = -\frac{d_2}{s}\frac{d_3}{s}$$

There are three pairs of 2-nontouching-loops[4] :

$$L_1L_3 \ , \ L_1L_4 \ \text{ and } \ L_2L_4$$

There are no groups of 3-nontouching-loops.

Mason's formula [40] states that the transfer function is given by the following :

$$\frac{V}{E} = \frac{P_1\Delta_1 + P_2\Delta_2 + \cdots}{\Delta} \qquad \text{(A.1)}$$

where P_i is the i-th path from node E to node V,

Δ = 1 - (sum of self-loop loop gains) + (sum of 2-nontouching-loops loop gains) - (sum of 3-nontouching-loops loop gains) + - ...

Δ_i = Δ minus any loop gains with loops touching P_i

In this example, we have

$$\Delta = 1 - (L_1 + L_2 + \ldots + L_7) + (L_1L_3 + L_1L_4 + L_2L_4) \qquad \text{(A.2)}$$

and

$$\Delta_1 = \Delta_2 = 1$$

Hence, the transfer function is

$$\frac{V}{E} = \frac{P_1 + P_2}{\Delta} \qquad \text{(A.3a)}$$

$$= \frac{d_1\,(d_5s^2 + d_2d_3)}{s^3(1-d_4d_5) + s^2(d_1+d_3) + s[d_1d_2(1-d_5)+d_2d_3(1-d_4)+d_1d_3] + 2d_1d_2d_3} \qquad \text{(A.3b)}$$

---

[4] Two (or more) loops are nontouching if they do not have any common nodes.

$$= \frac{s^2LC_2 + 1}{s^3L(C_1C_2 + C_1C_3 + C_2C_3) + s^2L(C_1 + 2C_2 + C_3) + s(L + C_1 + C_3) + 2} \qquad \text{(A.3c)}$$

Similar results can be obtained by applying conventional network analysis techniques to the circuit in Fig. 3.5(a). Note that Mason's formula applies to any two nodes in the flowgraph (not just the source and sink nodes). Furthermore, the transfer function can easily be amplitude-scaled by changing the input branch of the flowgraph from -1 to -K, where K is any real constant.

REFERENCES

1. R.W. Brodersen, P.R. Gray, and D.A. Hodges, "MOS switched-capacitor filters," Proc. IEEE, vol. 67, pp. 61-75, Jan. 1979.

2. D.J. Allstot, R.W. Brodersen, and P.R. Gray, "MOS switched-capacitor ladder filters," IEEE J. Solid-State Circuits, vol. SC-13, pp. 806-814, Dec. 1978.

3. G.M. Jacobs, D.J. Allstot, R.W. Brodersen, and P.R. Gray, "Design techniques for MOS switched capacitor ladder filters," IEEE Trans. Circuits Syst., vol. CAS-25, pp. 1014-1021, Dec. 1978.

4. B.J. Hosticka, R.W. Brodersen, and P.R. Gray, "MOS sampled data recursive filters using switched capacitor integrators," IEEE J. Solid-State Circuits, vol. SC-12, pp. 600-608, Dec. 1977.

5. T.A.C.M. Classen, W.F.G. Mecklenbräuker, and J.B.H. Peek, "Effects of quantization and overflow in recursive digital filters," IEEE Trans. Acoust., Speech, Signal Processing, vol. ASSP-24, pp. 517-529, Dec. 1976.

6. C.W. Barnes and A.T. Fam, "Minimum norm recursive digital filters that are free of overflow limit cycles," IEEE Trans. Circuits Syst., vol. CAS-24, pp. 569-574, Oct. 1977.

7. C.T. Mullis and R.A. Roberts, "Synthesis of minimum roundoff noise fixed point digital filters," IEEE Trans. Circuits Syst., vol. CAS-23, pp. 551-562, Sept. 1976.

8. J.L. McCreary and P.R. Gray, "All-MOS charge redistribution analog-to-digital conversion techniques - Part I," IEEE J. Solid-State Circuits, vol. SC-10, pp. 371-379, Dec. 1975.

9. P.R. Gray, D. Senderowicz, H. Ohara, and B.M. Warren, "A single-chip NMOS dual channel filter for PCM telephony applications," IEEE J. Solid-State Circuits, vol. SC-14, pp. 294-303, Dec. 1979.

10. R. Gregorian and W. Nicholson, "CMOS switched-capacitor filters for a PCM voice CODEC," IEEE J. Solid-State Circuits, vol. SC-14, pp. 970-980, Dec. 1979.

11. B.J. White, G.M. Jacobs, and G.F. Landsburg, "A monolithic dual tone multifrequency receiver," IEEE J. Solid-State Circuits, vol. SC-14, pp. 991-997, Dec. 1979.

12. D.L. Fried, "Analog sample-data filters," IEEE J. Solid-State Circuits, vol. SC-7, pp. 302-304, Aug. 1972.

13. J.T. Caves, M.A. Copeland, C.F. Rahim, and S.D. Rosenbaum, "Sampled analog filtering using switched capacitors as resistor equivalents," IEEE J. Solid-State Circuits, vol. SC-12, pp. 592-599, Dec. 1977.

14. G.C. Temes, "The derivation of switched-capacitor filters from active RC prototypes," Electron. Lett., vol. 14, pp. 361-362, June 8, 1978.

15. K. Martin, "An overview of switched-capacitor networks," Conf. Rec. 14th Asilomar Conf. on Circuits, Systems and Computers, pp. 10-14, Nov. 1980.

16. H.J. Orchard, "Inductorless filters," Electron. Lett., vol. 2, pp. 224-225, June 1966.

17. L.T. Bruton, "Low-sensitivity digital ladder filters," IEEE Trans. Circuits Syst., vol. CAS-22, pp. 168-176, Mar. 1975.

18. A.V. Oppenheim and R.W. Schafer, Digital Signal Processing. New Jersey : Prentice-Hall, 1975.

19. M.S. Ghausi and K.R. Laker, Modern Filter Design : Active RC and Switched Capacitor. New Jersey : Prentice-Hall, 1981.

20. M. Ismail, Y.K. Co, and G.O. Martens, "On mixed s to z transforms for discrete-time biquadratic filter design," Proc. ISCAS 1983, Newport Beach, U.S.A., pp. 308-311.

21. R. Gregorian and W.E. Nicholson, "Switched-capacitor decimation and interpolation circuits," IEEE Trans. Circuits Syst., vol. CAS-27, pp. 509-514, June 1980.

22. B.J. Hosticka and G.S. Moschytz, "Practical design of switched-capacitor networks for integrated circuit implementation," IEE Electronic Circuits and Systems, vol. 3, pp. 76-88, March 1979.

23. G. Szentirmai and G.C. Temes, "Switched-capacitor building blocks," IEEE Trans. Circuits Syst., vol. CAS-27, pp. 492-501, June 1980.

24. K. Martin and A. Sedra, "Effects of the op amp finite gain and bandwidth on the performance of switched-capacitor filters," IEEE Trans. Circuits Syst., vol. CAS-28, pp. 822-829, Aug. 1981.

25. K. Martin, "Improved circuits for the realization of switched-capacitor filters," IEEE Trans. Circuits Syst., vol. CAS-27, pp. 237-244, Apr. 1980.

26. T.C. Choi and R.W. Brodersen, "Consideration for high-frequency switched-capacitor ladder filters," IEEE Trans. Circuits Syst., vol. CAS-27, pp. 545-552, June 1980.

27. S.O. Scalan, "Analysis and synthesis of switched-capacitor state-variable filters," IEEE Trans. Circuits Syst., vol. CAS-28, pp. 85-93, Feb. 1981.

28. K. Martin and A. Sedra, "Exact design of switched-capacitor bandpass filters using coupled-biquad structures," IEEE Trans. Circuits Syst., vol. CAS-27, pp. 469-475, June 1980.

29. A. Fettweis, "Basic principles of switched-capacitor filters using voltage inverter switches," Arch. Elek. Übertragung., vol. 33, pp. 13-19, Jan. 1979.

30. G.C. Temes, H.J. Orchard, and M. Jahanbegloo, "Switched-capacitor filter design using the bilinear z-transform," IEEE Trans. Circuits Syst., vol. CAS-25, pp. 1039-1044, Dec. 1978.

31. J.A. Nossek and G.C. Temes, "Switched-capacitor filter design using bilinear element modelling," IEEE Trans. Circuits Syst., vol. CAS-27, pp. 481-491, June 1980.

32. M.S. Lee and C. Chang, "Low-sensitivity switched-capacitor ladder filters," IEEE Trans. Circuits Syst., vol. CAS-27, pp. 475-480, June 1980.

33. I.A. Young and D.A. Hodges, "MOS switched-capacitor analog sampled-data direct-form recursive filters," IEEE J. Solid-State Circuits, vol. SC-14, pp. 1020-1033, Dec. 1979.

34. E.I. El-Masry, "State-space switched-capacitor filter structures," Conf. Rec. 14th Asilomar Conf. on Circuits, Systems and Computers, pp. 5-9, Nov. 1980.

35. P.E. Fleischer and K.R. Laker, "A family of active switched capacitor biquad building blocks," Bell Syst. Tech. J., vol. 58, pp. 2235-2269, Dec. 1979.

36. R. Gregorian, "Switched-capacitor filter design using cascaded sections," IEEE Trans. Circuits Syst., vol. CAS-27, pp. 515-521, June 1980.

37. A.W.T. Ismail, "The triquad : A third order low sensitivity - programmable switched capacitor filter," Master of Eng. Report, Texas A&M University, May 1981.

38. U.W. Brugger, D.C. von Grünigen, and G.S. Moschytz, "A comprehensive procedure for the design of cascaded switched-capacitor filters," IEEE Trans. Circuits Syst., vol. CAS-28, pp. 803-810, Aug. 1981.

39. F.E.J. Girling and E.F. Good, "Active filters : Part 12. The leapfrog or active-ladder synthesis," Wireless World, pp. 341-345, July 1970.

40. S.J. Mason, "Feedback theory : Further properties of signal flow graphs," Proc. IRE, vol. 44, pp. 920-926, July, 1956.

41. R.D. Davis and T.N. Trick, "Optimum design of low-pass switched-capacitor ladder filters," IEEE Trans. Circuits Syst., vol. CAS-27, pp. 522-527, June 1980.

42. K. Haug, "Design, analysis and optimization of switched-capacitor filters derived from lumped analog models," Arch. Elek. Übertragung., vol. 35, pp. 279-287, July/Aug. 1981.

43. R. Saal, Handbook of Filter Design. Berlin, West Germany : AEG-Telefunken, 1979.

44. G.C. Temes and I.A. Young, "An improved switched-capacitor integrator," Electron. Lett., vol. 14, pp. 287-288, Apr. 27, 1978.

45. C.F. Rahim, M.A. Copeland, and C.H. Chan, "A functional MOS circuit for achieving the bilinear transformation in switched capacitor filter," IEEE J. Solid-State Circuits, vol. SC-13, pp. 906-909, Dec. 1978.

46. A. Knob, "Novel strays-insensitive switched-capacitor integrator realising the bilinear z-transform," Electron. Lett., vol. 16, pp. 173-174, Feb. 28, 1980.

47. D.C. von Grünigen, U.W. Brugger, and B.J. Hosticka, "Bottom-plate stray-insensitive bilinear switched-capacitor integrators," Electron. Lett., vol. 16, pp. 25-26, Jan. 3, 1980.

48. M.S. Lee and C. Chang, "Switched-capacitor filters using the LDI and bilinear transformations," IEEE Trans. Circuits Syst., vol. CAS-28, pp.267-270, Apr. 1981.

49. S. Eriksson, "Design of parasitics-insensitive bilinear switched-capacitor filters - a flowgraph conversion method," Proc. ISCAS 1982, Rome, Italy, pp. 443-446.

50. M.S. Lee, G.C. Temes, C. Chang and M.B. Ghaderi, "Bilinear switched-capacitor ladder filters, IEEE Trans. Circuits Syst., vol. CAS-28, pp. 811-822, Aug. 1981.

51. K. Martin and A. Sedra, "Designing leap-frog and SFG filters with optimum dynamic range," Proc. IEEE, pp. 1210-1211, Aug. 1977.

52. S.K. Mitra and P.P. Vaidyanathan, "Design of switched-capacitor filter networks with minimum capacitor ratio and total capacitance," Proc. ISCAS 1981, Chicago, U.S.A., pp. 326-329.

53. J.A. Nelder and R. Mead, "A simplex method for function minimization," The Computer Journal, vol. 7, pp. 308-313, Jan. 1965.

54. A.M. Gole, private communication.

55. L.P. Huelsman and P.E. Allen, Introduction to the Theory and Design of Active Filters. New York : McGraw-Hill, 1980.

56. C.L. Semmelman, E.D. Walsh, and G.T. Daryanani, "Linear circuits and statistical design," Bell Syst. Tech. J., vol. 50, pp. 1149-1171, Apr. 1971.